DNA 4115F

AIR BLAST MEASUREMENT TECHNOLOGY

Kaman Sciences Corporation
P.O. Box 7463
Colorado Springs, Colorado 80933

September 1976

Final Report for Period October 1975—September 1976

CONTRACT No. DNA 001-76-C-0088

> APPROVED FOR PUBLIC RELEASE;
> DISTRIBUTION UNLIMITED.

Prepared for

Director

DEFENSE NUCLEAR AGENCY

Washington, D. C. 20305

REPORT DOCUMENTATION PAGE		READ INSTRUCTIONS BEFORE COMPLETING FORM
1. REPORT NUMBER DNA 4115F	2. GOVT ACCESSION NO.	3. RECIPIENT'S CATALOG NUMBER
4. TITLE (and Subtitle) AIR BLAST MEASUREMENT TECHNOLOGY		5. TYPE OF REPORT & PERIOD COVERED Final Report for Period Oct 75—Sep 76
		6. PERFORMING ORG. REPORT NUMBER K-76-38U(R)
7. AUTHOR(s) Donald C. Sachs, Project Leader Eldine Cole		8. CONTRACT OR GRANT NUMBER(s) DNA 001-76-C-0088
9. PERFORMING ORGANIZATION NAME AND ADDRESS Kaman Sciences Corporation P.O. Box 7463 Colorado Springs, Colorado 80933		10. PROGRAM ELEMENT PROJECT. TASK AREA & WORK UNIT NUMBERS Subtask J11AAXSX352-34
11. CONTROLLING OFFICE NAME AND ADDRESS Director Defense Nuclear Agency Washington, D.C. 20305		12. REPORT DATE September 1976
		13. NUMBER OF PAGES 218
14. MONITORING AGENCY NAME & ADDRESS(if different from Controlling Office)		15. SECURITY CLASS (of this report) UNCLASSIFIED
		15a. DECLASSIFICATION DOWNGRADING SCHEDULE

16. DISTRIBUTION STATEMENT (of this Report)

Approved for public release; distribution unlimited.

17. DISTRIBUTION STATEMENT (of the abstract entered in Block 20, if different from Report)

18. SUPPLEMENTARY NOTES

This work sponsored by the Defense Nuclear Agency under RDT&E RMSS Code B344076462 J11AAXSX35234 H2590D.

19. KEY WORDS (Continue on reverse side if necessary and identify by block number)

Air Blast Measurement	Gas Particle Velocity
Transducers	Gas Density
Static Overpressure	Gas Temperature
Total Pressure	Dynamic Pressure
Shock Front Velocity	

20. ABSTRACT (Continue on reverse side if necessary and identify by block number)

Primary objectives of the project are to establish a baseline regarding currently available transducers and measurement technology for the study of air blast phenomena. This project represents an effort toward improvements in existing sensors and measurement practices through understanding and dissemination of information as well as a search for techniques to

DD FORM 1473 EDITION OF 1 NOV 65 IS OBSOLETE
1 JAN 73

18. SUPPLEMENTARY NOTES (Continued)

Reference to specific products and companies by name in this report is not to be construed as endorsement or criticism either by the authors or the U.S. Government.

20. ABSTRACT (Continued)

measure parameters that are being measured with limited success or not at all.

The study is focused on measurements of air blast parameters associated with peak overpressures above 140 N/cm^2 (200 psi) that are related to HE tests and large-scale explosively-driven shock tubes designed to simulate the air blast effects and environment from a nuclear explosion.

The parameters of special concern for this study are pressure, density, velocity and temperature. Specific definitions regarding the type of measurement (e.g. static overpressure) are given as each is discussed.

Consideration of several significant areas of related interest has been placed outside of the scope of this project. Problems unique to measurements in a nuclear blast environment, transducer signal conditioning and recording systems as well as calibration of the measuring system are all excluded from consideration in this report.

PREFACE

State-of-the-art for measurement of air blast parameters
is not determined by isolated study. This report represents
an interpretation by the authors of the information exchanged
during personal interviews with many friends and colleagues
who are involved with air blast measurements. It is not
surprising to discover a certain amount of disagreement among
the experts regarding the best method for some measurements.
An honest effort has been made to sort fact from opinion and
bias in order to present a meaningful document that outlines
the existing boundaries of free-field air blast measurement
technology in the high overpressure regime.

With a sincere feeling of appreciation for their coopera-
tive spirit shown and unqualified support given, we gratefully
acknowledge and recognize the following persons who contributed
from their technical expertise and knowledge to this report.

BRL - John H. Keefer
        George D. Teel
        Noel H. Ethridge
        George Coulter
        Rodney Abrahams
        William Schuman

AFWL - Major Fred Walter
        Joseph Renick
        Joseph Quintana

UNM/
CERF - Neal P. Baum
        Kenneth Simmons

NSWC - Joe Petes

1

TABLE OF CONTENTS

TABLE OF CONTENTS (CONT'D)

1. INTRODUCTION

1.1 Objectives

This report contains results of a survey conducted by Kaman Sciences Corporation in an effort to establish the status of current technology for measurement of the various physical properties of an air blast environment.

Primary objectives of the project are to establish a base-line regarding currently available transducers and the status of measurement technology for the study of air blast phenomena. This project represents an effort toward improvements in existing sensors and measurement practices through understanding and dissemination of information as well as a search for techniques to measure parameters that are being measured with limited success or not at all.

1.2 Scope

The study is focused on measurements of air blast parameters associated with peak overpressures above 140 N/cm^2 (200 psi) that are related to HE tests and large-scale explosively-driven shock tubes designed to simulate the air blast effects and environment from a nuclear explosion. The upper bound on the measurements represents the current state-of-the-art and an effort has been made to identify this limit for each parameter considered.

The parameters of special concern for this study are pressure, density, gas particle and shock wave front velocities, and temperature. Specific definitions regarding the type of measurement (e.g. static overpressure) are given as each is discussed in Chapter 3.

Preceding page blank

Considerations of several significant areas of related interest have been placed outside of the scope of this project. Problems unique to measurements in a nuclear blast environment, transducer signal conditioning and recording systems as well as calibration of the measuring system are all excluded from consideration in this report.

While numerous measurement techniques are cited, their detailed descriptions are not included. References to applicable reports are provided for the reader who seeks more complete information on any given topic.

During the course of the survey, personal visits were made to several laboratories and facilities considered by the technical community to be among the leaders in the field of air blast measurements. A review of contemporary literature has complemented the survey. Numerous transducer manufacturers were also contacted for revised technical data on their products that have been found to be in preferred usage by experimenters.

1.3 Report Contents

Results and conclusions are presented in summary statements in Chapter 2, followed by a detailed discussion of the present state-of-the-art for measurement of each of the important air blast parameters including recent experimental transducer developments in Chapter 3. A special chapter has been dedicated to photographic techniques and methods that are used for quantitative measurements of the air blast parameters. Promising extensions of present measurement capabilities and several advanced concepts for future development consideration are presented in Chapters 5 and 6 respectively.

While the detailed discussions of air blast theory are left for others, useful equations that give relationships between the parameters for the case of an ideal gas are presented in Appendix A.

Certain transducers have come to be known as preferred types within the technical community of air blast experimenters. Manufacturer's specification data sheets for these transducers are included as Appendix B to this report.

A glossary of terms commonly used is found in Appendix C to clarify the meaning and connotation and to provide definitions of words common to air blast work. Symbols used in the report and metric conversion tables are included as appendices for the conveience of the reader.

2. SUMMARY OF AIR BLAST MEASUREMENT TECHNOLOGY

The substance of this report is an assessment of the current technological status for the measurement of air blast parameters in the high overpressure regime. Particular attention is given to measurements in regions where the peak overpressure may be from 140 N/cm^2 (200 psi) up to the existing boundaries for measurements as an upper limit. In many instances, the measurement does not approach the lower limit of 140 N/cm^2 (200 psi). For these cases, the maximum capability is cited even though it is otherwise below the lower limit of peak overpressures under consideration.

In the high overpressure regime, the measurements are not only difficult from a viewpoint of available instrumentation but also the meaning and correct interpretation of the data is sometimes obscure.

Sources of major complications stem from:

1. The destructive effects of the hostile environment on the measurement system;

2. The existence of dust and debris as a mixture with the air;

3. The non-ideal character of the gas due to dissociation with high temperature and contamination with products of combustion from the charge detonation; and

4. Perturbation of the measured quantity by the measurement process or device.

Two distinct classes of problems are identified. The first deals with the accurate measurement of the air blast properties (e.g. pressure, temperature, etc.). A second set of problems relates to interpretation of the measured data and construction or definition of the blast field from local measurements of some of its properties. This report is primarily concerned with the first class of problems, namely the ability to make the desired measurements. The remainder of Chapter 2 is a summary of these air blast measurement capabilities. Detailed discussions of the measurement techniques and capabilities are presented along with many pertinent references in Chapters 3 and 4.

The major physical properties of the air blast that one would like to measure are pressure, density, velocity and temperature. These terms all require additional qualification prior to meaningful discussion of their measurement. Definitions found in the Glossary (Appendix C) are given to remove ambiguity and clarify the meaning of terms. More detailed discussions regarding measurement techniques and implications of each measurement are given in Chapters 3 and 4.

2.1 Pressure

A discussion of pressure measurement needs to include identification of which type of pressure is under consideration. Commonly one is concerned with static, total, reflected and dynamic pressures. These may be expressed as overpressures relative to the pre-blast ambient pressure or they may be given in absolute terms. Orientation and design of the pressure sensor, probe geometry and placement relative to the flow are factors that determine which pressure is to be measured.

11

Static overpressure and normally reflected overpressure measurements are consistently reported in the region of 1400 to 2800 N/cm^2 (2000 to 4000 psi). Less frequently, and yet not uncommonly, measurements are noted above 7000 N/cm^2 (10,000 psi) and perhaps as high as 14,000 N/cm^2 (20,000 psi). Higher level measurements are rare and are generally viewed with great skepticism. Total pressure measurement is complicated by considerations of local flow conditions around the probe that is necessarily inserted in the flow. Corrections to the indicated measurement are necessary for flow velocities above Mach 1 due to the influence on the measurement of the bow shock from the probe. This correction requires a knowledge of local static overpressure and gamma (γ) the ratio of specific heats of the gas. Since static overpressure is measured in proximity to the total pressure and γ is assumed, the validity of the measurement becomes more questionable as the pressure increases. For these reasons, total pressure is only measured with confidence up to about 210 N/cm^2 (300 psi).

The capability for measurement of dynamic pressure is closely allied to that for measurement of total pressure. This is because dynamic pressure is a derived quantity and is not directly measured. Generally, the dynamic pressure is computed using measured values of static and total pressures. An alternative procedure involves measurement of the loading force on a calibrated target and computation of dynamic pressure using the drag coefficient of the target and the measured force data.

Peak values for stagnation and dynamic pressures are sometimes calculated from measurements of shock wave front Mach number and static overpressures by using Rankine-Hugoniot relationships. Again, assumed values for γ are used in these calculations and as the overpressure increases, the sensitivity to γ is greater.

12

2.2 Density

The direct measurement of gas density is desirable because, coupled with gas particle velocity, a direct and unambiguous calculation of dynamic pressure would be possible.

Density in a relatively clean subsonic flow environment is directly measured using a beta densitometer that measures absorption of energy from a beta radiation source by a known volume of air. This method has been used at peak overpressures up to 31 N/cm^2 (45 psi) to record peak density ratios of 1.9 or less.

Indirect methods have been applied to measurement in higher pressure environments. Photographic techniques show promise for mapping the position-time histories of smoke puffs in a grid. The trajectories thus determined are then used to calculate the density profile behind the shock wave front. Results of such density measurements at overpressures up to 250 N/cm^2 (360 psi) have not yet been published for the DIPOLE WEST test series.

Like the beta densitometer, this optical method is only applicable in the clean flow ahead of the debris and fireball.

The presence of particulate matter in the air blast brings up questions regarding the definition, meaning, and interpretation of density measurement. The particle size, density, shape and size distribution can be expected to be highly dependent on the composition of the surface at each particular test site.

2.3 Velocity

Measurement of shock wave front velocity and gas particle velocity are both considered to be of interest to this report.

Shock wave velocity is one of the more readily measured parameters of the air blast environment. Available methods range from very inexpensive measurements of shock front arrival time at discrete locations to costly radar and laser systems that provide continuous measurement along a radial line emanating from the blast source.

Gas particle velocity behind the shock wave front has been measured in the subsonic region quite successfuly with a vortex shedding anemometer. In high pressure regions above Mach 1 the smoke puff grid and high-speed photography is used in clean air flow.

In general practice, gas particle velocity has been calculated from other parameters. A radar doppler system utilizing a low mass aluminum foil target has been utilized by the Air Force Weapons Laboratory (AFWL) in the Dynamic Air Blast Simulator (DABS) shock tube to effect a brief Lagrangian-type measurement of particle velocities on the order of 1400 m/sec.

Photographic and optical techniques lend themselves to measurement of shock front and gas particle velocity measurement. These techniques have been widely exploited in shock tube and HE experiments.

2.4 Temperature

Present day instrumentation for temperature measurements in the free-field air blast environment is severely limited. Direct measurements are not made and indirect methods, such as hot film anemometry, are limited to blast overpressures of about 100 N/cm^2 (150 psi) by considerations of the thin film maximum temperature range. A total temperature measurement

has been reported at 50 N/cm^2 (72 psi) peak overpressure showing
a maximum temperature slightly above 600 degrees Celsius ($^{\circ}$C).
Reduction of the data measured with hot film anemometer probes
is quite complex and involves considerations of heat transfer,
knowledge of static and total pressure and flow Mach number.

At the higher overpressures often the interpretation of
the measurement is further complicated by the presence of dust
and combustion of detonation products that continue to burn in
the fireball that engulfs the measurement station.

2.5 Conclusions

Some general comments and observations are in order regard-
ing the current state-of-the-art for measurement of air blast
parameters. One asks the questions: where do we stand?, and
what is needed in terms of development? These are not totally
objective questions and the answers are dependent upon
perspective and the frame of reference. The answers given here
are then based on facts learned and opinions formed by the author
while pursuing the study reported herein.

In the subsonic flow regime where peak overpressures are
35 N/cm^2 (50 psi) or less, most needed measurements are made
acceptably well. This is not to say the measurements do not
require very careful consideration and planning. As the over-
pressure decreases, the environment becomes friendlier and
response time requirements less stringent. While this is
happening, a new class of problems are developing that have not
been addressed by this study; namely, that of often measuring
low-level phenomena in the presence of higher level natural
meteorological influnces.

15

In the higher level pressure regime that is the principal subject of this study (above 140 N/cm^2 (200 psi)) there is considerable room for improvement in virtually every free-field measurement the experimenter would like to make. No doubt that pressure is measured better than density, particle velocity and temperature. Pressure sensing elements are available for measurements above 80,000 N/cm^2 (116,000 psi). Major deficiencies lie in probe and mounting design, dynamic calibration methods and in interpretation of the data.

Because of the interrelationships between the parameters, it is difficult to assign higher importance or value to one than the other. For one who is primarily concerned with blast effects, the dynamic pressure may be singled out as most important while knowledge of the other parameters is equally important for the one who is concerned with prediction of the air blast environment.

3. MEASUREMENT METHODS AND CAPABILITIES

3.1 The Air Blast Environment

It will be convenient to consider three spatial regions
or zones in the unconfined free air blast environment. It
should be recognized that physical dimensions associated with
these regions will depend upon the charge yield, type, and
geometry. An intermediate range will be identified as the
region wherein the blast wave is well behaved and closely
follows the relationships given in Appendix A that characterize
an ideal or classical blast wave.

Let us refer to Zone 1 as being the close-in region extend-
ing from the blast origin toward Zone 2 which is in the
intermediate range. Zone 3 is the far-out region where peak
overpressures are not significantly above ambient levels.
These zones are mentioned for perspective and to emphasize that
this report deals primarily with measurements in or approaching
Zone 1. These regions are identified graphically in Figure 1
for a 100-ton TNT surface tangent sphere.

Measurements in Zone 3 are often difficult to interpret
because of perturbation from meteorological conditions.
Atmospheric effects such as focusing, local wind vector and
temperature gradients exert significant influence on the blast
propagation in the outer reaches of an air blast wave which
finally degenerates to a sonic disturbance. Terrain will
also have a measurable effect in Zone 3. While this study is
not concerned with measurement of parameters in this region, it
is mentioned as a matter of perspective. The problems and
measurement techniques for low-level air blast parameters are
largely separate from those addressed in this report.
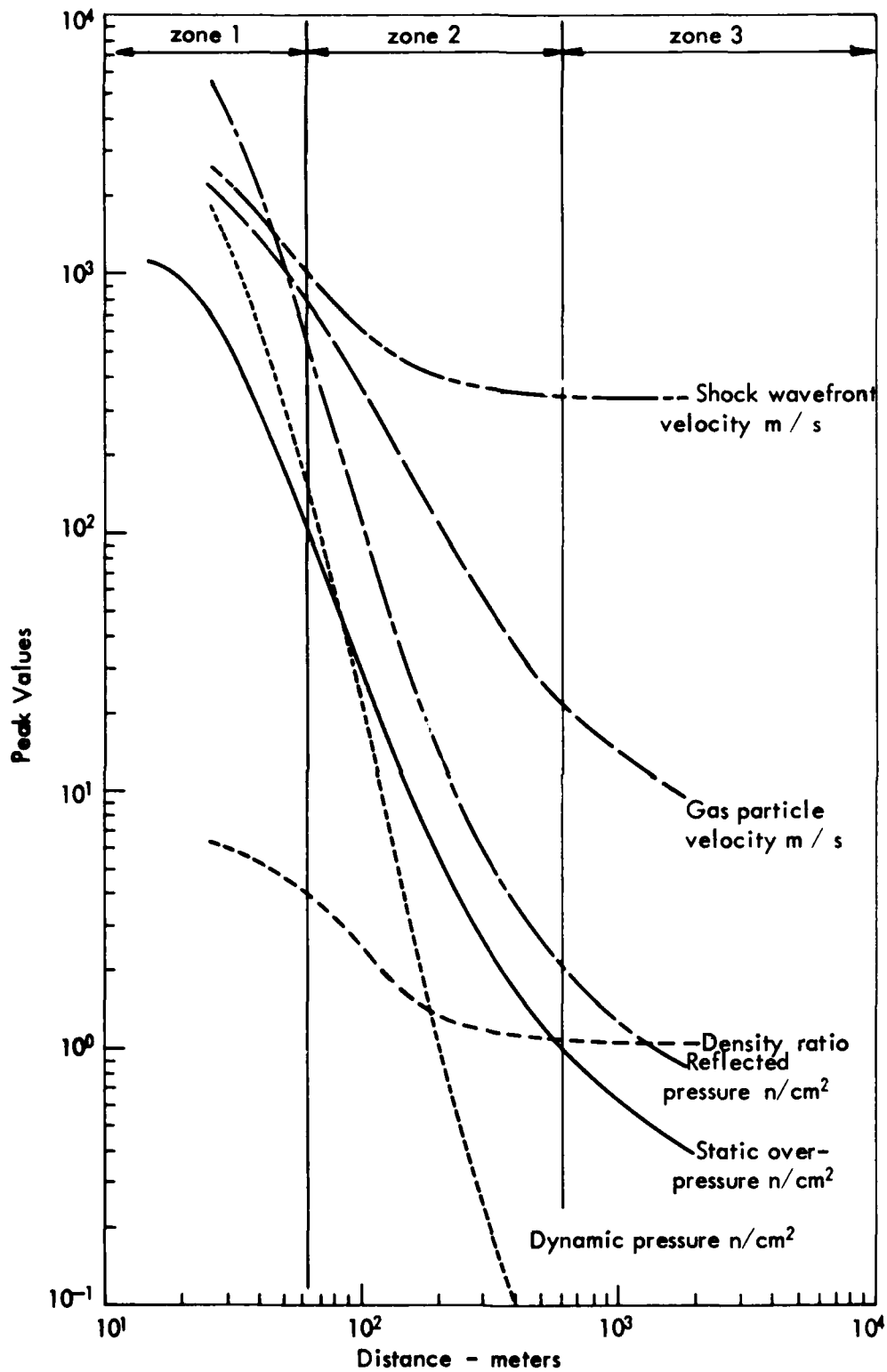
FIGURE 1   BLAST CHARACTERISTICS AT SHOCK FRONT FROM 100 TON
TNT SURFACE TANGENT SPHERE

The intermediate range (Zone 2) is, generally speaking, the easiest location for measuring properties of an air blast. Here anomalies in the blast wave have healed and the shock front is expanding radially in a regular pattern according to theory. As one moves in closer toward ground zero, the measurement is confounded by various elements, and interpretation of the data is increasingly more ambiguous.

3.1.1 The High Overpressure Regime

The major emphasis in this report is concentrated on measurements in the close-in region (Zone 1) where the static overpressure is above 140 N/cm^2 (200 psi). Many factors complicate measurements in this region. Transducers are subject to physical damage by the extreme thermal environment, ejecta from the crater, and debris that is picked up and swept along by the blast. Detonation products and ionized gases cast a large uncertainty on determining gas properties, such as the value of gamma (γ) to use as the ratio of specific heats.

It is emphasized that whereas the detonation products, dust, and debris are a complication both to measurement and to interpretation of that measurement, they must be considered a part of the blast wave which should be measured to the extent they are considered of importance; some can be very important. In addition to the environmental hazards mentioned, there is the EMP generated by the HE charge. This can be quite perturbing to some systems, particularly high impedance ones such as those using quartz gages. In fact, some "pressure" signals from dummy glass gages have in truth turned out to be EMP signals.

The blast wave in Zone 1 is non-ideal in every sense of the word. Irregularities in the detonation give rise to anomalies or jetting of the fireball. This and other inhomogeneities in

19

the close-in region complicate interpretation and meaning of
data. Compressibility effects of the air also enter heavily
into analysis of the data from measurements at high overpressures.

Calibration accuracy is a major consideration in the high
overpressure regime. It is many times the case that great pains
are taken to calibrate the sensor as an isolated entity in the
laboratory while assuming no further calibration is required in
the field installation. Granted that often conditions of the
experiment coupled with fiscal constraints may restrict or even
preclude field calibration. Measurements are made for which a
portable calibration system is not feasible. These extenuating
circumstances do not alter the fact that sensors do not always
perform the same in a laboratory as in the field environment when
installed as part of a measuring system. An ultimate goal for
any measuring system is an end-to-end dynamic calibration of the
system after installation.

The influence of particulate matter in the flow cannot be
ignored. Most measurement systems are as sensitive to the
effects of dust and debris are they are to the desired physical
parameter. There is dust and there are particulate detonation
products, e.g. carbon, which influence the gage reading and
perhaps they should not be treated the same way. Dust is
largely a characteristic of the ground surface and therefore
subject to large variations depending upon the locale of a test.
Particulate detonation products are characteristic to the
particular HE used. With TNT, an oxygen deficient explosive,
large quantities of carbon can be expected. For close-in
measurements this will impose a force on the gages (or targets)
and should be part of the hydrodynamic calculation predictions.

Highly accurate measurements in Zone 1 therefore call for
transducers and/or application of technqiues that account for
and/or circumvent the effects of dust. An alternative is to

quantify the dirty environment at each measurement station and apply corrections to the data in an effort to cancel or compensate for the "error" signal. This approach seems impractical in view of the calibration problems faced and the requirement for a detailed and localized time history of the flow contamination associated with each measurement, not to mention the unknown effects of detonation products on the gas properties.

3.1.2 Physical Quantities of Interest

This report deals specifically with our capability to perform measurements of the fundamental physical quantities in an air blast. Included are direct and indirect methods for measuring pressure, density, velocity, and temperature. Because the shocked medium in Zone 1 is not a perfect gas, the relationships in Appendix A are only approximations. The degree to which these approximations are valid becomes more uncertain as the measurement is moved in closer to the blast source.

For this reason, it is imperative to independently measure as many parameters as possible because the inference of one by knowledge of another is not necessarily valid nor is it always known whether or not the relationships hold. Thus, the cross correlation afforded by independent measurements provides an insight into the flow conditions, as well as added confidence in the validity of the measurements.

Unfortunately, the desired measurements are not readily made (if at all) or they may not be cost effective and the experimenter often must live with shock front Mach number and peak overpressure as the only available measured data from the high overpressure region. Air tables have been extended to very high pressures and temperatures so that with shock Hugoniot

21

equations (A-16 to A-18) one can determine other properties at the shock (such as temperature, density, internal energy, etc.) although one may not be able to measure them. At other points in the blast field, it is a different story with additional measurement data required for definition of the flow conditions.

3.2 Pressure Measurement

Four important connotations of pressure are associated with an air blast: 1) Static overpressure, 2) Reflected over-pressure, 3) Total pressure and 4) Dynamic pressure. Each measurement requires different techniques and gage installation considerations. These will be defined and discussed in some detail in this section of the report.

It is noted by the author during the course of this study that there exists a general ambiguity and tendency toward careless usage of terms regarding pressure. No doubt the user has a clear understanding of the meaning and connotation of the term but its use (or misuse) can present a source of confusion to the reader or listener. For this reason, a glossary of terms commonly encountered in air blast work is included as Appendix C to clarify the meaning of the terms as used in this report.

One can urge the air blast technical community to agree upon the meanings of terms and adopt standard terminology for use, particularly in conversation but also in the literature.

Pressure is one of the most readily measured air blast parameters and has become a standard measurement on virtually every test. The types of pressures are presented in order of increasing measurement difficulty with dynamic pressure the most elusive of all since it is not measured directly. Only through indirect means is the dynamic pressure derived. In principle, one type of pressure transducer could be used to measure any of the first three pressures by installation in an appropriate probe that is mounted with proper orientation to the blast wave. In practice, it is often found advantageous to use different transducers that will de-emphasize the imperfections and take advantage of the desirable features of each according to the situation.

Three major problems are common to all pressure measurements in the extreme close-in region of the blast. First, the very survival of the gage and associated electrical cables as a functional unit is a significant accomplishment in engineering design. The transducer must also be insensitive to or isolated from thermal and mechanical shocks as well as a severe acceleration environment. Now, assuming these first two problems are solved, one is still faced with the problem of providing an inertially stable mount to assure that the measurement is made at a location with spatial coordinates that remain fixed during the measurement. It is certainly a tall order to expect to record much more than the peak pressure for any measurements attempted inside the radius of a crater from a surface or near-surface burst because of the extreme ground movement and ejecta flow.

3.2.1 Transducer Thermal Protection

Virtually every active pressure sensing element known will respond to a transient thermal stimulus to a significant degree. In the high overpressure region the thermal environment is always severe and becomes a major factor to address when blast pressure measurements are planned. The inherent design of

23

certain sensors provides a built-in time lag before the thermal effects are seen. Differential cancellation methods are often used in a wide variety of innovative schemes in the product design.

For the user who is not involved in a design program with a transducer manufacturer, the options available for minimizing thermal effects relate to shielding or delaying the thermal pulse from reaching the sensitive transducer sensing elements until the critical measurement period is over. Several methods are used with varying degrees of success. Test conditions and the transducers being used will often preclude use of one technique and indicate another. Examples of protection and time-delaying thermal barriers in current use are:

1. Vacuum grease
2. Black electrical tape
3. Asbestos-loaded silicone rubber
4. Metal screen or ported plate
5. Fluid-coupled plate
6. Powdered lead-loaded silicone rubber.

Combinations of more than one technique are sometimes used. Any of the above measures can be expected to degrade the transducer frequency response and should be carefully evaluated in light of specific test requirements. Isolated examples may be found where additional damping will actually enhance a transducer's response characteristics. Frequency response considerations and requirements for pressure measurements are discussed in some detail in Section 3.2.9.

A desired bonus from any of these schemes is the added protection afforded against physical damage to the transducer diaphragm by debris impact.

Blast transducer designs that utilize an exposed surface
of a crystal as the force summing area will exhibit pyroelectric
and photoelectric response to heat and light. Vacuum grease
will not provide adequate shielding for this situation. For
such cases, the thermal barrier must also be opaque to optical
radiation.

Thermal protection afforded by black electrical tape
Scotch brand type 88 is very commonly used and often adequate,
however many available materials are an improved thermal
insulation. For example, Scotch brand type 433 tape has been
found to be significantly more effective in tests using pulsed-
laser radiation to simulate the thermal blast source.

Silicone rubber compounds are available that are far
superior to tapes for delaying thermal effects. Two of these
in common use are General Electric #TBS-758 and Dow Corning #589.
Both of these materials offer better thermal and mechanical
properties; however, at the expense of increased difficulty for
use.

As the blast environment becomes increasingly more severe,
a new problem appears. It is obviously important for the thermal
barrier to remain in place during the measurement period. The
tape and silicone products are readily stripped away by the blast.
At pressures around 700 N/cm^2 (1000 psi) mechanical measures are
required to enhance or replace the function of adhesive to hold
the material in place. The pressure level at which these
additional precautions are indicated depends upon conditions of
the test, being heavily influenced by the amount of debris
entrained in the blast and the impulse.

A retaining ring is shown conceptually in Figure 2 that
is designed to hold the silicone compound captive to the
diaphragm. The debris screen offers additional protection for

25

SILICON SENSING
ELEMENT (~.5 mm)

PROPOSED DEBRIS SHIELD
(SCREEN)

TRANSDUCER CASE THREAD
3 8 - 24 UNF

THERMAL BARRIER
RETAINER

PORT

CAVITY

THERMAL
BARRIER
TBS 758
(~1.2 mm)
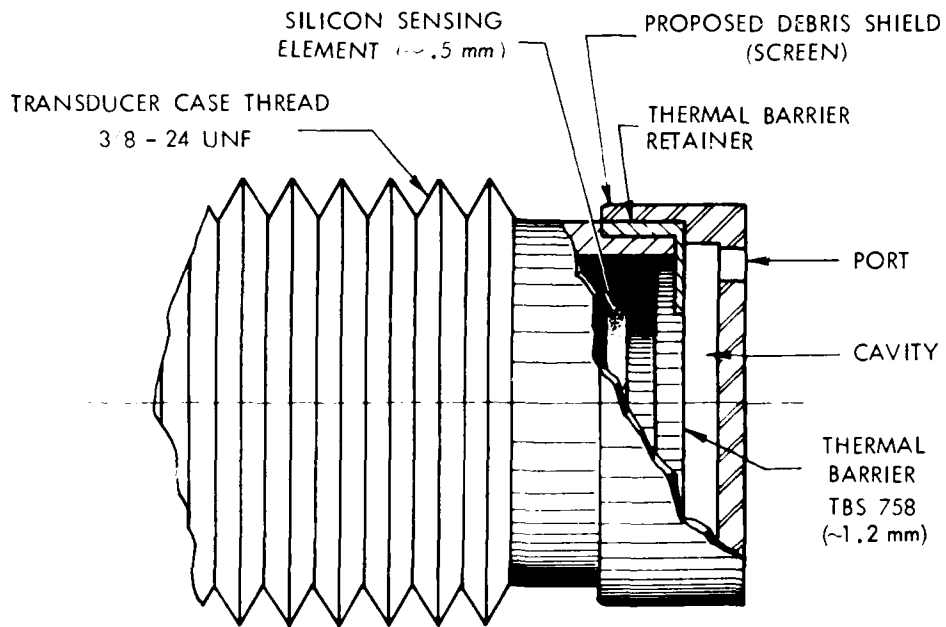
a) DEBRIS SCREEN AND THERMAL BARRIER RETAINER
(PER AFWL)

PROTECTIVE
HEAT & DEBRIS
SHIELD
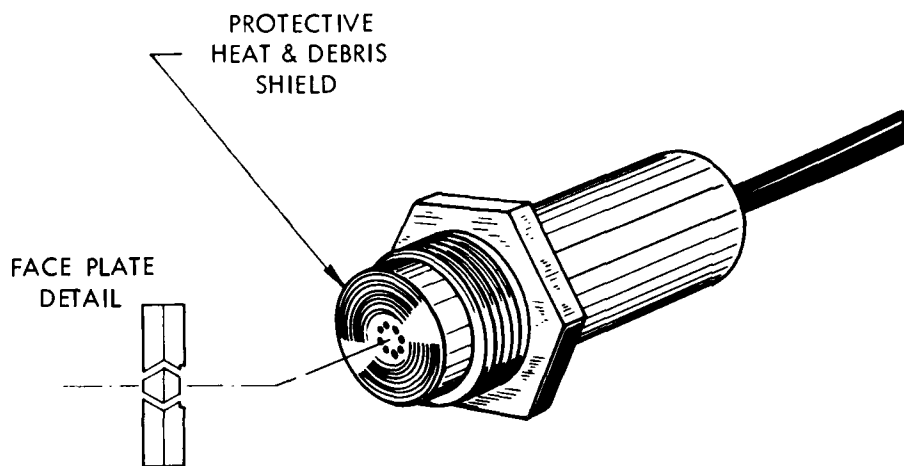
FACE PLATE
DETAIL

b) FACE PLATE WITH ANGLED PORTS
(PER BRL)

FIGURE 2   TRANSDUCER PROTECTION DESIGNS FOR HIGH
BLAST OVERPRESSURE

26

the transducer. The figure also shows a transducer with a face plate design that has been widely used for blast measurements. This somewhat higher degree of protection uses a pair of thick plates with a pattern of holes drilled at an angle and aligned so as to eliminate any direct line-of-sight path to the diaphragm. Obviously, this technique provides very effective protection in a rather extreme debris environment as well. Two disadvantages are the resulting degradation of frequency response and the tendency for holes to clog with debris. The screen or ported face plate can be expected to limit the frequency response to values from 5 to 20 kHz depending on the hole sizes and cavity volume.

Measurements in the most hostile environments are usually accomplished by indirectly coupling the pressure to the sensing element via an intermediate medium. Two examples of such extreme measures are shown in Figure 3. The fluid coupled plate is used to measure plasma pressure in the Horizontal-Line-Of-Sight (HLOS) pipe during an underground nuclear test. The pressure is coupled to the transducer by means of a fluid filled cavity. The piezoresistive bar gage utilizes strain gages on the sides of a long bar to measure strain in the bar that is induced by the pressure at the end surface.

The protective measures all have a tendency to degrade the frequency response and need to be evaluated carefully before application to assure that the system performance will be acceptable. The degree of change depends largely upon the method and transducer selected.

3.2.2 Transient Thermal Response Tests

A number of test methods have been devised and used in screening tests for selection of the best transducers and protective measures for use in the transient thermal environment

27
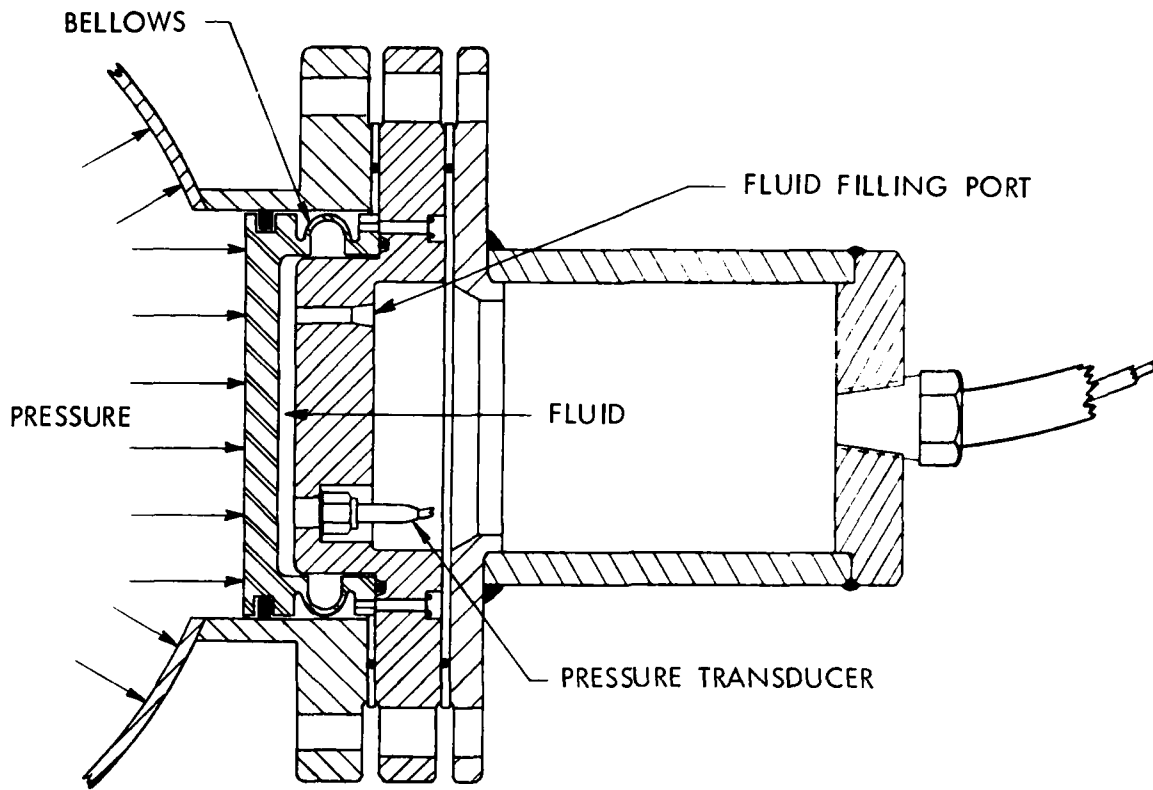
(a) FLUID COUPLED PLATE (FCP) (SANDIA)
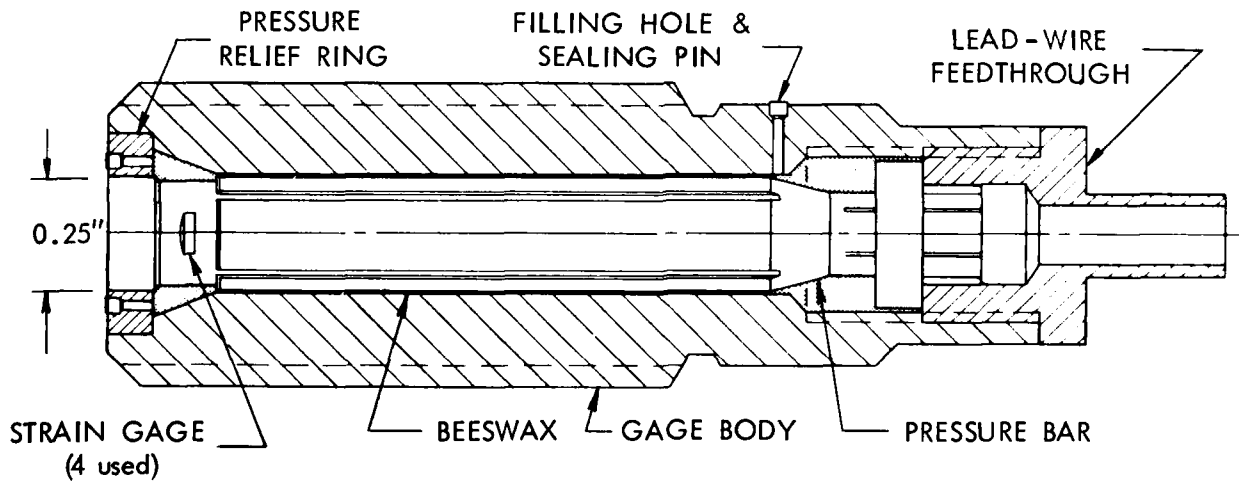
(b) PIEZORESISTIVE BAR GAGE (AFWL)

FIGURE 3   PRESSURE TRANSDUCERS FOR HIGH OVERPRESSURE
           APPLICATIONS

28

of an air blast. Standard procedures and judgment criteria have not been adopted for guidelines in transducer or thermal barrier selection by the experimenter. At the present time, each user tends to design and conduct his own selection criteria and test methods. One can argue that the simulated thermal pulse is not a true representation of the field environment. At the same time it is reasonable to expect better performance from a transducer with a thermally-induced zero shift of 1/2 percent of full scale than from one with 200 percent, for example. The test results should therefore not be considered as an absolute but rather a qualitative evaluation for guidance in transducer selection.

The National Bureau of Standards (NBS) has developed and reported on methods for testing response of pressure transducers to thermal transients[1,2]*. Reference 1 describes a method using laser energy as the thermal source while the more recently developed technique presented in Reference 2 uses photographic flash bulbs as the source. A current project at NBS involves testing and evaluation of various thermal barriers. These test results will be documented in a NBS Tech Note with expected publication in the near future.

Thermal transient tests are reported by TRW for the Susquehanna ST-4 at levels up to 4600 W/cm^2 and for the PCB 113A21 at 825 $W/cm^{2[3,4]}$.

A variation on the NBS technique was developed by BRL to test the candidate pressure transducers for the DNA shock-on-shock rocket sled tests at Holloman Air Force Base. These tests involved application of a pulsed thermal source up to 520 W/cm^2 with a simultaneous shock-tube-generated pressure step.

---

*Numbers in brackets refer to List of References.

Transducers tested were the PCB models 115 MO4 and 113A and a Kulite Model XTEL-1-190. A number of adhesive tapes were tested for shielding effectiveness also. Scotch brand type 433 was found far superior in resisting the laser radiation effects[5]. Under the given BRL test conditions the PCB-113A was proven least sensitive to thermal transients. This test may or may not be appropriate for aerodynamic heating since the source was radiant thermal heat. Yet, the screening test must be judged satisfactory in view of the successful sled test data return.

Sandia Laboratories (SLA) have also conducted thermal response experiments in a shock tube at pressures up to 350 N/cm^2 (500 psi) static overpressure. The test involved evaluation of the Kulite XTS-1-190 and HKS-7-375 model transducers with silicone grease packed into the cavity between the debris screen and the diaphragm. Not only is improved frequency response noted but the thermal protection is improved. The transducer sensitivity becomes a strong function of temperature with adverse effects on static and dynamic sensitivity at lower pressures. As with other methods, this technique is not a general purpose cure-all but has application for certain test conditions[6].

Reference to specific thermal sensitivities of transducers has not been made because non-uniformity in test procedures makes direct comparisons somewhat misleading. The reader is directed to the references cited for further details of test results.

3.2.3 Static Overpressure

Static overpressure is the transient differential pressure in the air blast relative to the ambient pressure just before

arrival of the shock wave. Mathematically it is expressed as

$$\Delta p_s = p_2 - p_1 \tag{1}$$

where the absolute pressures before and after shock arrival are denoted p_1 and p_2 respectively. It is measured with a pressure transducer whose diaphragm or force-summing area is oriented in a plane that is parallel to the flow velocity vector. Many other commonly used adjectives for static overpressure include incident, side-on, free-field or free-air overpressure.

From a sensor point of view, it is the easiest, therefore the most common pressure measurement. The exposure of the active sensing area to direct radiant energy of the fireball is much reduced as well as the hazard of debris impact. Interpretation of the data is not complicated by factors of kinetics and gas compressibility. The static pressure levels are lower than total or reflected pressures (to be defined later) at any given range. The transducer orientation to the blast for static overpressure measurement is favorable to minimize the mechanical shock and vibration effects, which are commonly very small for excitation in the plane of the diaphragm.

The measurement is however considerably more sensitive to probe geometry and alignment than the others. Misalignment of the transducer baffle with the flow introduces a source of measurement error that is not readily detectable by study of the data. Probe design considerations are presented in Section 3.2.8.

Measurements of static overpressures in the region from 7,000 to 14,000 N/cm^2 (10,000 - 20,000 psi) are reported with reasonable probability of success. Above this range, the probability diminishes, with added difficulty in recording the total

positive pressure phase duration, the period of positive pressure. Reports of data above 14,000 N/cm^2 (20,000 psi) static overpressure are quite spotty. Vortman (SLA) reports on very recent tests, a measurement of 27,000 N/cm^2 (39,000 psi) that is in line with the prediction[7]. A peak of 45,500 N/cm^2 (66,000 psi) was measured on Event TINY TOT and is one of the highest reported overpressure measurements noted in the course of this review.

Three basic installation configurations have evolved for the pressure transducer to measure static overpressure. They are:

1. The surface-flush ground baffle;

2. The disk probe; and,

3. The pencil probe.

Typical field installations for each type are seen in photographs in Figures 4, 5, and 6 respectively.

The pressure adapter seen in Figure 4 is used for field calibration and is removed prior to shot time to expose a flush surface to the air flow. Many variations on this basic installation are implemented to accomodate particular test requirements. Figure 7 is a drawing that illustrates several desirable features for the ground baffle. The teflon bushing provides electrical as well as mechanical isolation. The electrical isolation is required to avoid ground loops that are a source for electrical noise in the signal. Since all pressure transducers are sensitive in some degree to case strain, the teflon bushing serves further to isolate the pressure transducer from shock and vibration.

The usual field installation procedure for the ground baffle is to pour the concrete block in situ providing the maximum coupling to the surrounding earth media. Recent experience
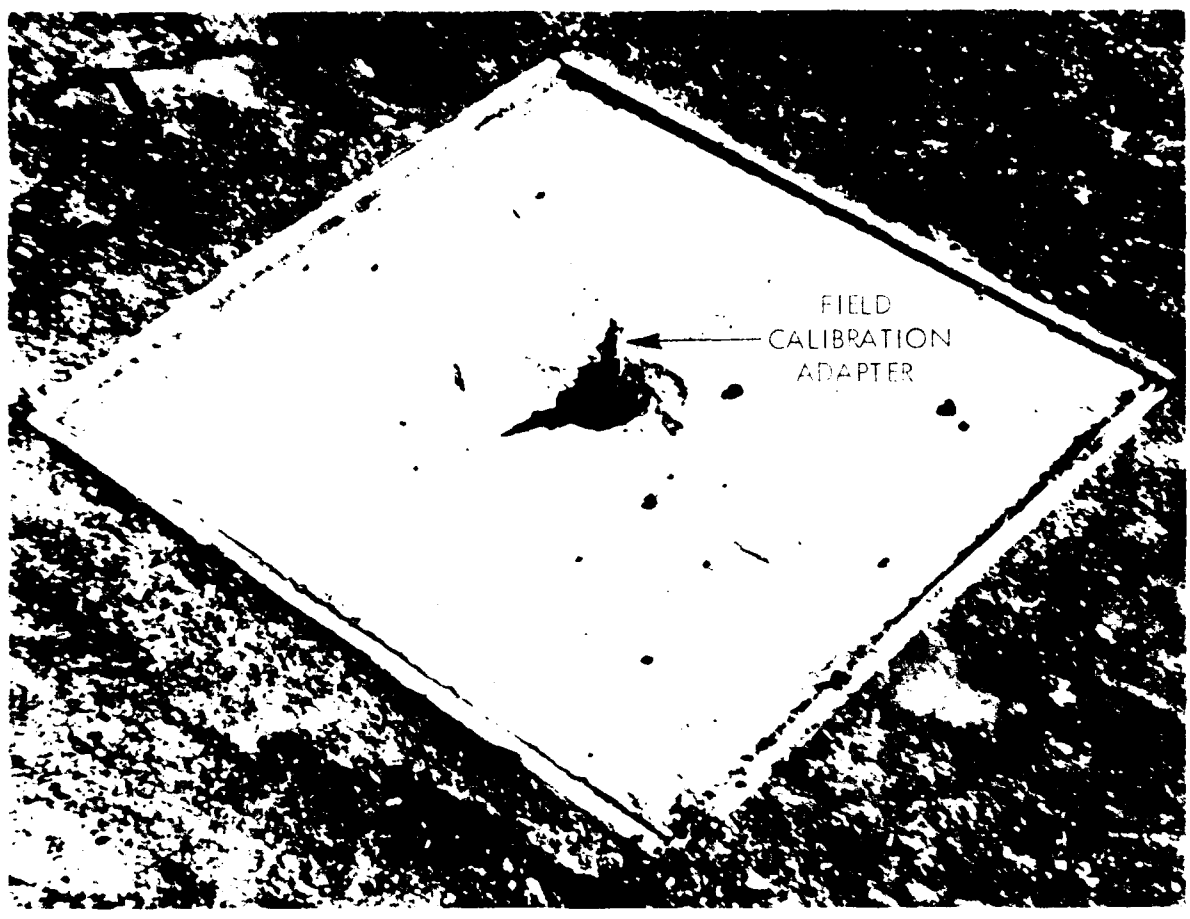
FIELD
CALIBRATION
ADAPTER

FIGURE 4   SURFACE FLUSH GROUND BAFFLE FOR
OVERPRESSURE MEASUREMENT

33

STATIC
OVERPRESSURE
DISC PROBE

PRESSURE
TRANSDUCER

EXPECTED
BLAST FLOW

TOTAL HEAD
PRESSURE PROBE
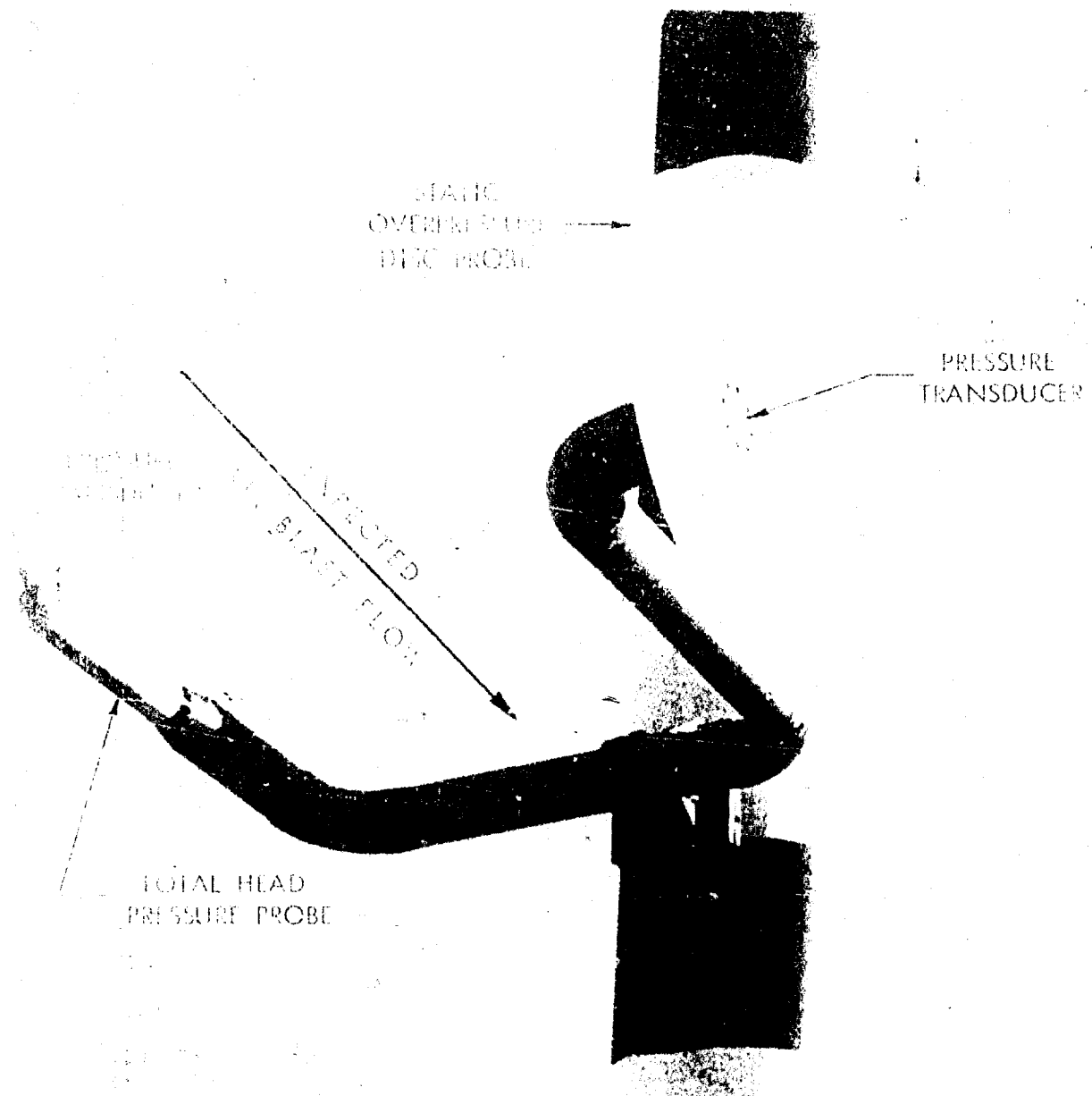
COURTESY OF BRL

FIGURE 5 FREE-FIELD BLAST PRESSURE PROBE INSTALLATION
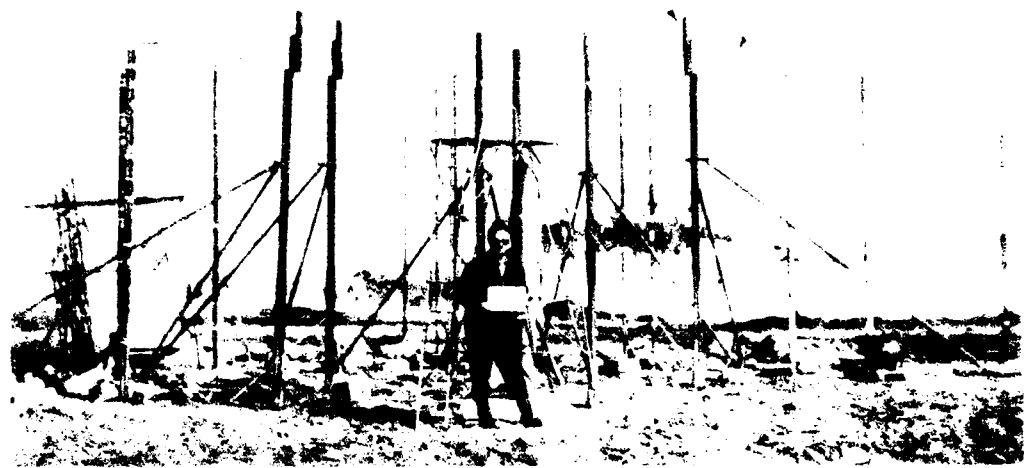
FIGURE 6   FIELD INSTALLATION USING PENCIL PROBES FOR
STATIC OVERPRESSURE MEASUREMENT

TRANSDUCER
TEFLON BUSHING
CAST LEAD
LIFTING PINS

COVER PLATES
TRANSDUCER MOUNT
INSTRUMENTATION TROUGH IN CONCRETE PAD
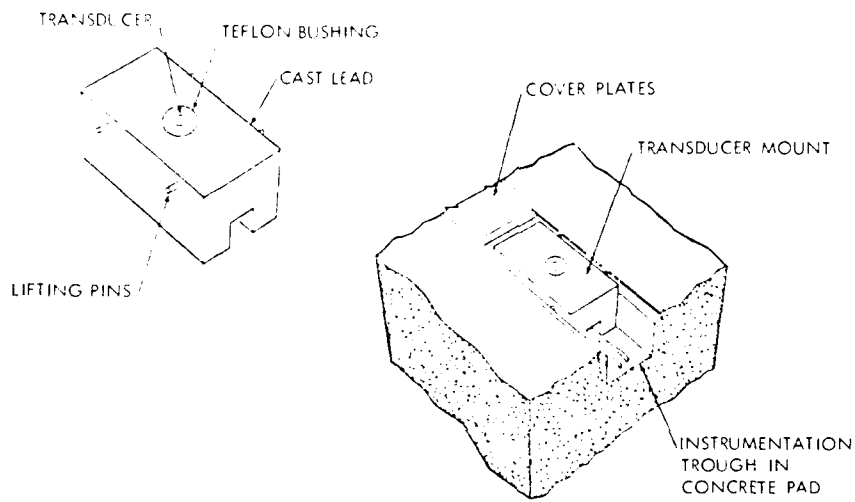
COURTESY OF NWC

FIGURE 7   TRANSDUCER MOUNT FOR STATIC TEST SITE

in the Pre-DICE THROW test resulted in a longer recording time
at close-in stations by use of precast mounting blocks.
While the holes were back filled after placement of the concrete
blocks, no special effort was taken to tamp the earth to restore
the soil to its undisturbed character. The backfill material
used was crusher fines or sand. This decoupling of the mounting
pad from ground motion probably contributed to the increased
record length, although this hypothesis has not been proven by
controlled experimentation.

Installation requirements such as size of the concrete
ballast and cable protection measures will vary widely depending
upon factors such as overpressure levels and predicted ground
motion.

The ground baffle offers excellent physical protection for
the transducer and this geometry has been used to successfully
measure some of the highest blast overpressures on record[8,9,10].

It is noted here that the overpressure measured at the
ground surface does not represent the free-field static over-
pressure at some height above the surface. The overpressure
measured at the surface is strongly influenced by surface
conditions, reflected air shocks and ground-induced air shock,
particularly in the close-in regions. Experience on high-
explosive charge tests indicates that in the high overpressure
regions, peak static overpressures measured at ground level
are depressed and the waveforms tend to be non-classical[11].
Pressures measured in the region of Mach reflection will
generally be about twice the amplitude of the incident free air
blast wave front. It is therefore of general interest to
measure static overpressures above the surface of the ground
at various radii, elevation and azimuth angles to more fully
characterize the pressure profile and symmetry of the air
blast environment.

Pressure measurements within the blast flow field require the introduction of a pressure transducer into the flow. One immediately faces the classical measurement problem of altering the physical quantity under study by the act of measurement. The objective is then to design a sensing probe that minimizes the perturbation of the flow field by its presence.

The disk probe design (see Figure 5) is seen to be omni-directional for flow within the plane of the disk. This probe geometry is particularly vulnerable to damage caused by mis-alignment in the flow because of the large surface area and relatively weak construction design inherent in the thin disk.

A variation of the disk baffle is available in a "lollipop" configuration. While this design is less susceptible to damage by misalignment, calibration is much more sensitive to flow Mach number and turbulence because of the complex aerodynamic shape. Figure 8 shows a commercially available lollipop probe for blast overpressure measurement.

The pencil probe design seen in Figure 6 is commercially available from Susquehanna Instruments (ST-7) and Celesco Industries (LC-13 or LC-33). Both types of probes utilize synthetic crystals that are quite responsive to temperature changes. The calibration stability is notably inferior to quartz sensors and should be considered before selection of these probes. The ST-7 probe may be ordered to accept a PCB model quartz transducer for improved temperature stability.

Figure 9 shows an installation detail that is recommer.:ed by Denver Research Institute for use with the pencil probe. The nylon adapter serves to provide electrical and mechanical isolation for the transducer sensing element as well as to provide a transition from the probe diameter to the supporting structure made of water pipe.
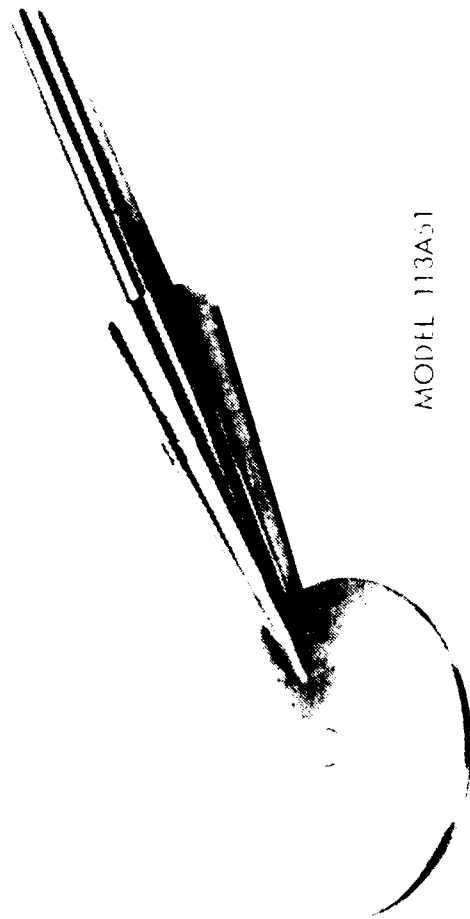
MODEL 113A51

FIGURE 8 PCB LOLLIPOP STATIC OVERPRESSURE PROBE

PENCIL BLAST
GAGE

NYLON
ADAPTER

1¼" WATER PIPE
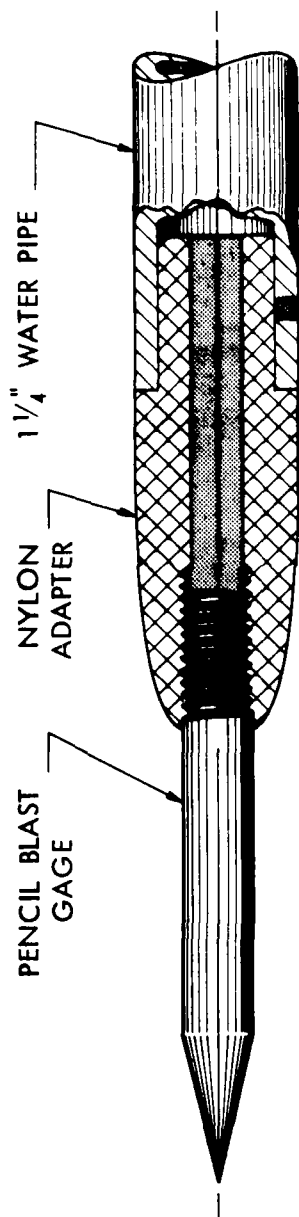
(per DRI)

NOT TO SCALE

FIGURE 9   STING ADAPTER FOR PENCIL PROBE

Refer to Section 3.2.8 for a discussion of design considerations of these and other probes for making pressure measurements in an air blast environment.

3.2.4 Reflected Overpressure

When a shock wave encounters a rigid surface in its path that is not parallel to its direction of motion, a reflected shock wave is formed. Figure 10 will be helpful to describe the reflection and for definition of terms.

The figure depicts a normally reflected wave in which the shock velocity (U_s) is perpendicular to the reflecting surface. The reflected overpressure (Δp_r) as measured at the wall by transducer "A" may range from 2 to 8 times the static overpressure for an ideal gas as seen by consideration of the equation that predicts the peak value of normally reflected overpressure for an ideal blast wave which is given by

$$\Delta p_r = 2p_2 \left(\frac{7p_1 + 4p_2}{7p_1 + p_2} \right) . \tag{2}$$

In this equation p_1 is the ambient pressure ahead of the shock and p_2 is the peak pressure behind the shock front as indicated in Figure 10[12]. In an actual field test with effects from ionization, dust, and products of combustion, the reflected overpressure ratio ($\Delta p_r/p_2$) could go as high as 20. Reflected pressure is often used in shock tube calibration of pressure transducers as a means of amplifying the pressure pulse to a higher level than obtainable with static overpressure alone.

An important point is that the above equation relates to normally reflected waves. Obliquely reflected waves are also often encountered in pressure measurements such as with flush transducers placed on the surface of the ground close-in to

41
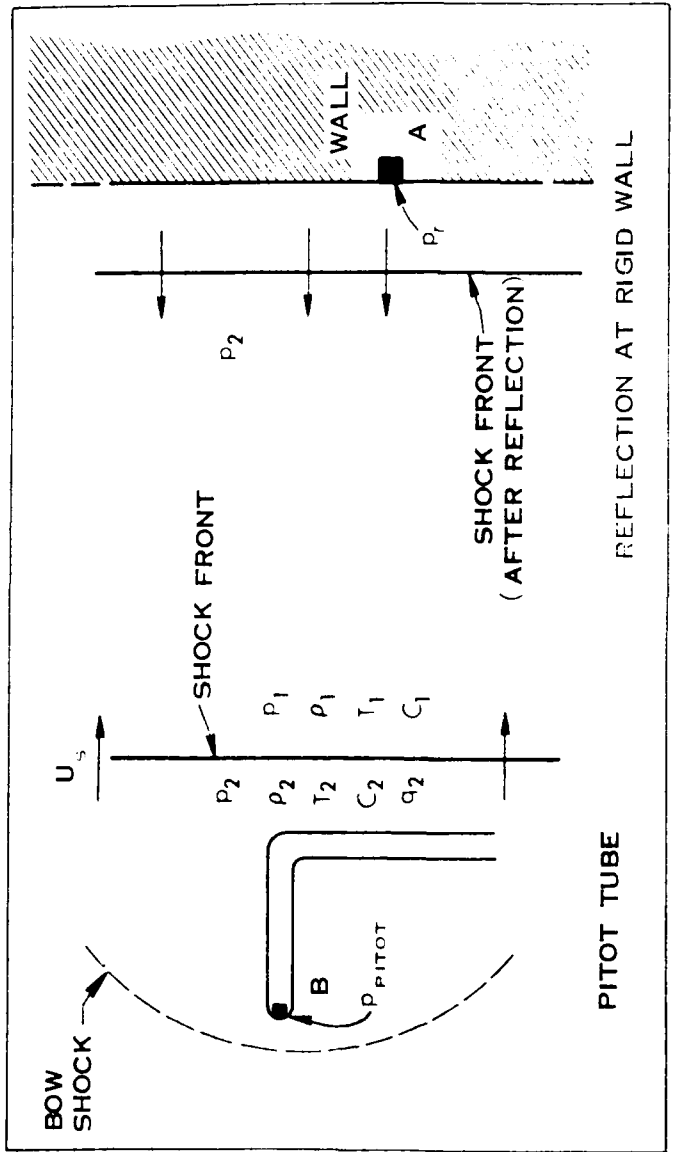
FIGURE 10 DESCRIPTION OF TERMS, PITOT TUBE AND REFLECTED PRESSURES

42

large charges (e.g. the 500-ton TNT tangent spheres). These measurements are often made before the formation of the Mach stem and sense an obliquely reflected blast pressure that is neither static pressure nor is it normally reflected pressure.

The reflected pressure can represent a significant increase in the impulse delivered to a target exposed to air blast. It may also appear on pressure-time histories as a confusing signal added to the pressure measurement from a pitot tube. Turning attention to the pitot tube shown in Figure 10, transducer "B" necessarily must present a reflecting surface area to the approaching shock wave. The resulting transient pressure peak is rapidly relieved around the probe as quasi-steady flow conditions are established around the probe. Figure 11 is shown as representative of such a measurement which distinctly shows a sharp spike on the leading edge of the record. The clearing time for establishment of flow around the probe is seen to be very short and the peak pitot pressure may be estimated by fairing and extrapolation from the overall pressure profile.

The amplitude of the reflected overpressure that is recorded depends upon the probe design and the bandwidth of the measuring and recording system. Many of the systems in use today have limited bandwidth that filters the signal to eliminate the peak reflected pressure spike[11].

Another manifestation of reflected pressure is seen in the data record of Figure 12. This instance shows shocks reflected from nearby surfaces. While the strength of these may be of interest in isolated cases, as a general rule, the data record is difficult to interpret or loses its meaning after the arrival of stray reflected shock waves.
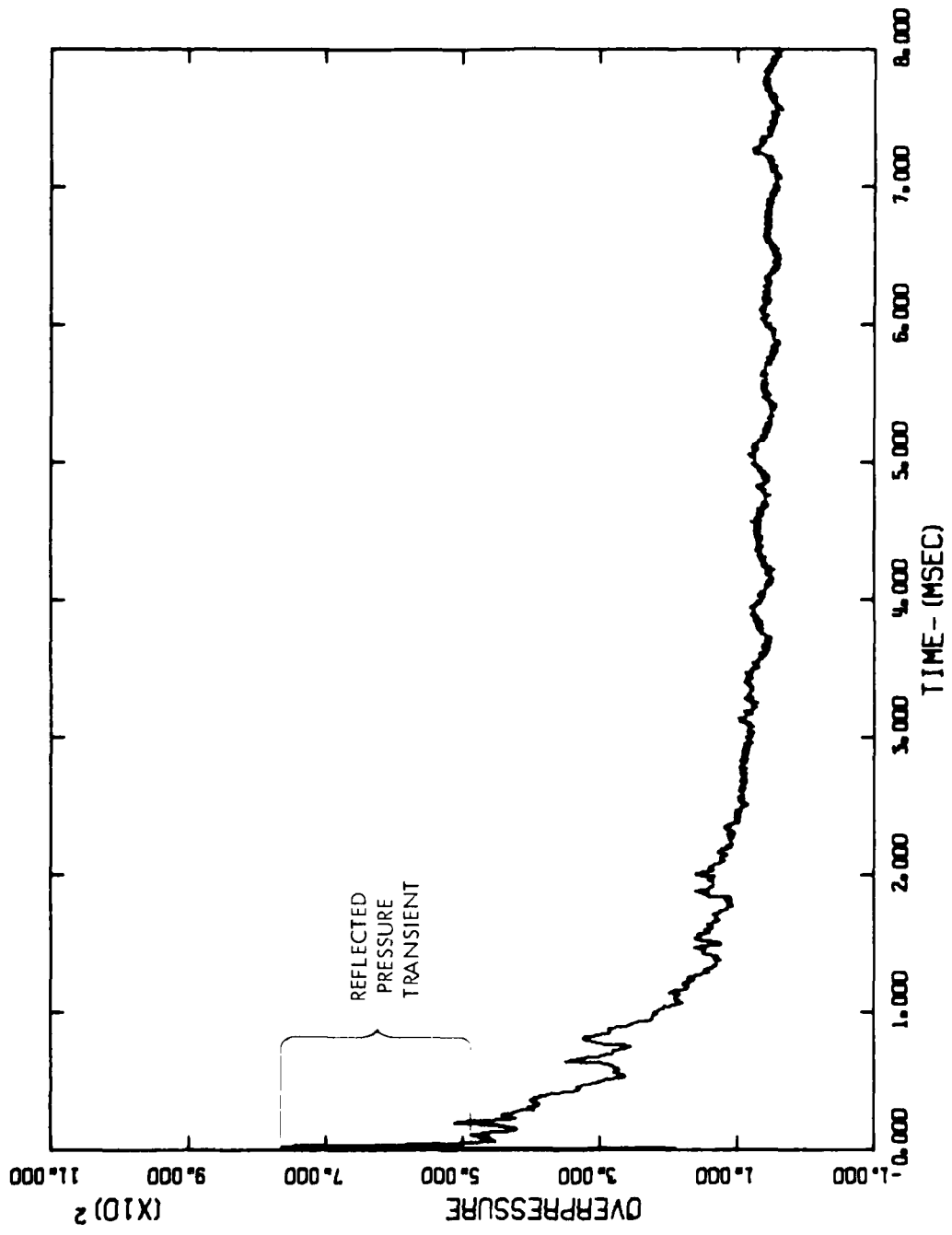
FIGURE 11 TOTAL HEAD PRESSURE WITH REFLECTED PRESSURE SPIKE
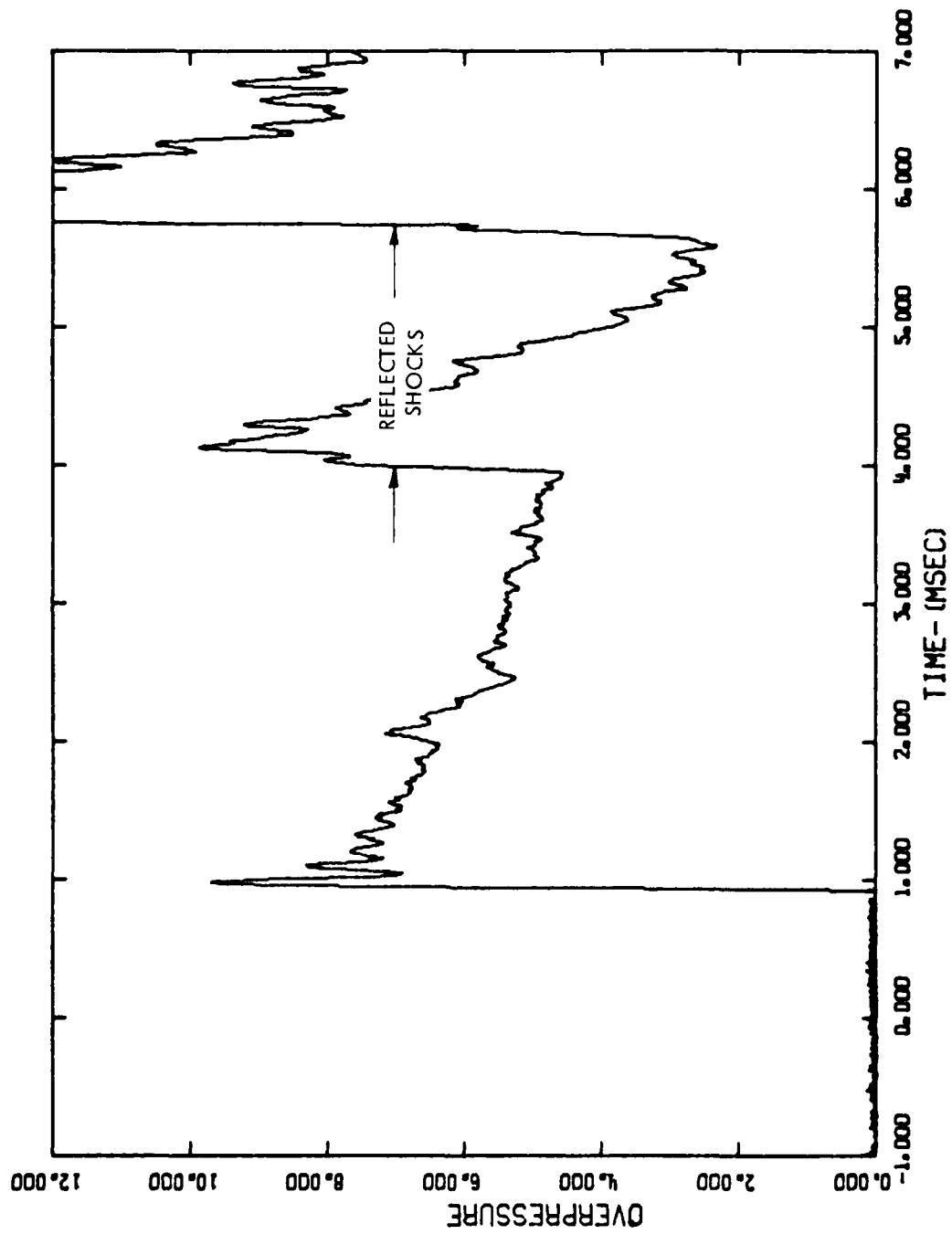
FIGURE 12 OVERPRESSURE RECORD WITH REFLECTED SHOCKS

45

Often measurements are made in a region of the air blast
known as the Mach stem which is formed by the coalescence of
the main air shock wave front with a reflected shock, commonly
the reflection from the ground plane. This is a somewhat
complex shock interaction and is mentioned to bring out the
point that it is essential to be aware of the region in which
the pressure measurement was made for proper interpretation of
its meaning.

Measurement of normally reflected pressure requires the
active force summing area of the transducer to be perpendicular
to the shock wave velocity vector. This specifies that the
transducer must face the blast source (with associated debris
and thermal environment) which is a much more severe requirement
than for measurement of static overpressure.

Reflected pressure measurements in the very high overpres-
sure region will generally require the type of transducer
protection shown in Figure 13 that provides a high degree of
isolation for the active sensing element. Not so much because
the overpressures are so high, but rather because it is neces-
sary to protect the element from debris and the extreme thermal
environment that accompanies the air blast.

The limitation for this measurement on a routine basis in
the air blast environment is on the order of 5000 N/cm^2 (7300
psi) using protective measures over the active force summing
area. An example of one method that has proven to be very
effective is seen in Figure 13. This ported face plate concept
can present a serious frequency response limitation for wide-
band measurements much above 5-20 kHz. The actual boundary for
reflected pressure measurement is very difficult to establish
because of the strong relationship it has to the air blast
source. In a shock tube with a cleaner environment, measurements

NYLON OR TEFLON INSERT

PRESSURE TRANSDUCER

HEAT & DEBRIS SHIELD

O-RINGS

SHOCK MOUNT CASE $1\frac{1}{8}$" – 12 THREAD

(Per BRL)

FACE VIEW OF
HEAT & DEBRIS SHIELD
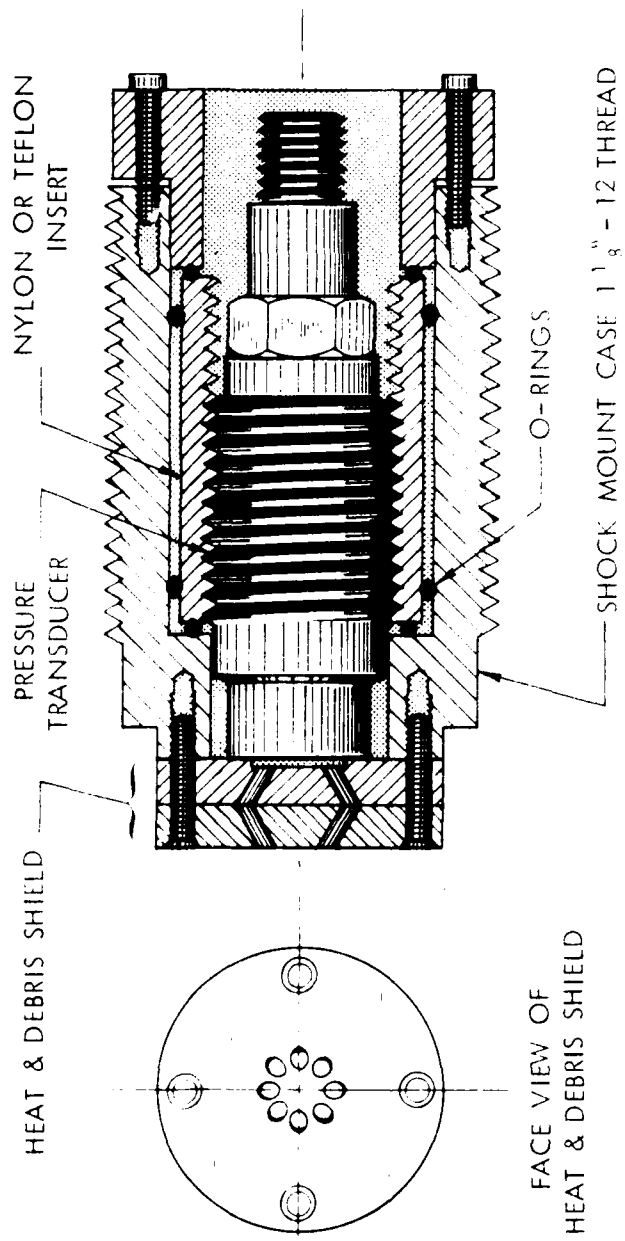
FIGURE 13 TRANSDUCER ISOLATION ADAPTER FOR EXTREME ENVIRONMENTS

47

as high as 20,000 N/cm^2 (29,000 psi) reflected pressures may
well be possible.

Reflected pressure measurements are usually associated
with target loading and response studies. The transducer is
installed flush to the surface of the model or structure at
the point of measurement. The installation techniques are
similar to the ground baffle for static overpressure. In fact,
the measurement of reflected pressure directly underneath a
charge above the surface would utilize a ground baffle.

As stated earlier, the reflected pressure measurement is
commonly associated with a target that is subjected to the air
blast loading. Pressure transducers are then installed flush
to the reflecting surface. Special precaution is taken to
avoid direct coupling of stress that is induced in the struc-
ture to the transducer case. Most pressure transducers will
respond to case stress (*some more than others*) and need
mechanical isolation from the high stresses that are induced
in the mounting surface of a representative target. Further
discussion of mounting considerations is found in Section 3.2.8.

3.2.5 Dynamic Pressure

The dynamic pressure is that component of stagnation
pressure that arises from the kinetic energy of the mass flow.
It is commonly denoted as q and is defined as

$$q = \frac{1}{2} \rho u^2 \tag{3}$$

where ρ is the gas density and u is the gas particle velocity
in the flow.

The dynamic pressure is not directly measured but is a computed value based upon measurements of other parameters. The Rankine-Hugoniot relationships presented in Appendix A are used with measurements of static overpressure, stagnation pressure and shock wave Mach number to calculate dynamic pressure at the shock wave[13].

For incompressible fluid flow, the dynamic pressure is the difference between static and stagnation pressure. At low overpressures the effects of compression are negligible, however at the levels of overpressure under consideration the dynamic pressure (q) is not simply related to static and stagnation pressure. It is usually obtained from the static pressure (p) and the Mach number (M) using the relation for perfect gas that

$$q = \frac{1}{2} \gamma \, pM^2 \qquad (4)$$

where gamma (γ) is the ratio of specific heats. It is readily observed that this calculation requires that several conditions are met; namely, the flow is adiabatic, the density and composition of the gas is consistent with the value of γ used, and it obeys the perfect gas laws.

Another approach to obtaining the dynamic pressure is to measure the drag forces on a calibrated target that is placed in the free-stream flow. The target may be a cylinder that has been tested in various environmental situations of dusty and clean air flow encountered in sled tests, shock tubes and wind tunnels. The drag coefficient is thus established and the forces of blast loading are measured during field test. The dynamic pressure is then calculated using the relationship that

$$q = \frac{F}{C_D A} \qquad (5)$$

where F = blast loading force

           C_D = average drag coefficient

               = $f(M, R_e, \theta, \phi_d)$

           A = presented area of the target

           θ = angle of incidence

           ϕ_d = dust momentum flux

and R_e = Reynolds number.

Unresolved problems or limitations to this method center around the inherent low frequency response because of the clearing time needed to establish steady flow around the target and the uncertainty of ϕ_d and its effect.

The establishment of dynamic pressure by differential pressure measurement techniques shows promise for low Mach number low pressure applications. This method has been used by BRL in the past with encouraging results and is under continued investigation for refinement of the technique[14]. An essential element for successful measurement using this technique is that both pressure sensing channels must be identical in sensitivity. This differential method is not so promising for application to the high pressure regime because of the non-linear corrections necessary for M > 1.

An obvious approach for determining q is to measure the density and gas particle velocity directly and then compute the dynamic pressure from the definition. While this can be done conceptually, very limited means are available for measurement of these two quantities in a field application. The topics of density and velocity measurements are discussed in Sections 3.3 and 3.4 respectively.

50

In summary, dynamic pressure is an important yet extremely difficult measurement to make in the high overpressure regime; it is not satisfactorily measured at the present time in the region of $\Delta p_s > 140$ N/cm^2 (200 psi). The major limitations are related to problems associated with measuring total pressure which are discussed next.

3.2.6 Total Pressure

The concept of total pressure is very important and is the source of considerable confusion on the subject of compressible fluid flow, particularly when the free-stream velocity is supersonic. Other related terms, some of which are synonomous, are: total head pressure, stagnation pressure, head pressure, impact pressure, and pitot pressure. A clear definition of these terms and a discussion of the total pressure measurement will help to eliminate some of the cloud surrounding the subject.

Total pressure in fluid flow is by definition the pressure that would exist if the flow were brought to rest isentropically. The flow is said to be stagnated when the flow velocity is zero. Thus, total pressure is commonly referred to as the stagnation pressure which is perfectly correct as long as the flow has been stagnated isentropically. This is the important point that is often overlooked. The clear understanding of the two thermodynamic processes is essential to this discussion; isentropic and adiabatic. Each will be defined before returning to the subject of total pressure. An adiabatic process is one in which no heat is transferred and an isentropic process is defined as one of constant entropy. Although one may imagine an irreversible constant-entropy process which is not adiabatic, from any practical viewpoint the term isentropic is generally understood to mean reversible adiabatic.

Returning to the discussion of total pressure, the measurement procedure is to install a pressure transducer in the nose of a probe that is oriented facing into the flow (toward the blast source). Figure 14 is a photograph of a total pressure probe developed by the Ballistic Research Laboratories (BRL) for measurements in high blast overpressure environments[15,16]. The face of the pressure transducer is protected with a debris and heatshield similar to that shown in Figure 13. Note that the transducer is recessed in the probe to provide a stagnation region with no flow over the face of the transducer. In a subsonic flow, the fluid will in fact be brought to rest over the face of the transducer isentropically and the measured pressure will be the true free-stream total or stagnation pressure.

However, such is not the case in supersonic flow. A detached bow shock wave forms ahead of the probe that involves an irreversible adiabatic process. The pressure transducer senses a stagnation pressure but it is not the desired free-stream stagnation pressure that is measured. The measured pressure behind the detached bow shock wave is known as the pitot pressure. On the stagnation streamline (at the face of the transducer) the shock is normal and the ratio of true total pressure (p_{01}) to measured pitot pressure (p_{02}) is given by

$$\frac{p_{01}}{p_{02}} = \left(\frac{2\gamma}{\gamma + 1} M_1^2 - \frac{\gamma - 1}{\gamma + 1} \right)^{1/(\gamma-1)} \left(\frac{1 + \frac{\gamma - 1}{2} M_1^2}{\frac{\gamma + 1}{2} M_1^2} \right)^{\gamma/(\gamma-1)} \tag{6}$$

where M_1 is the Mach number ahead of the bow shock wave and γ is the ratio of specific heats for the gas. Subscripts 1 and 2 denote conditions ahead of and behind the shock respectively (see Figure 10).

52
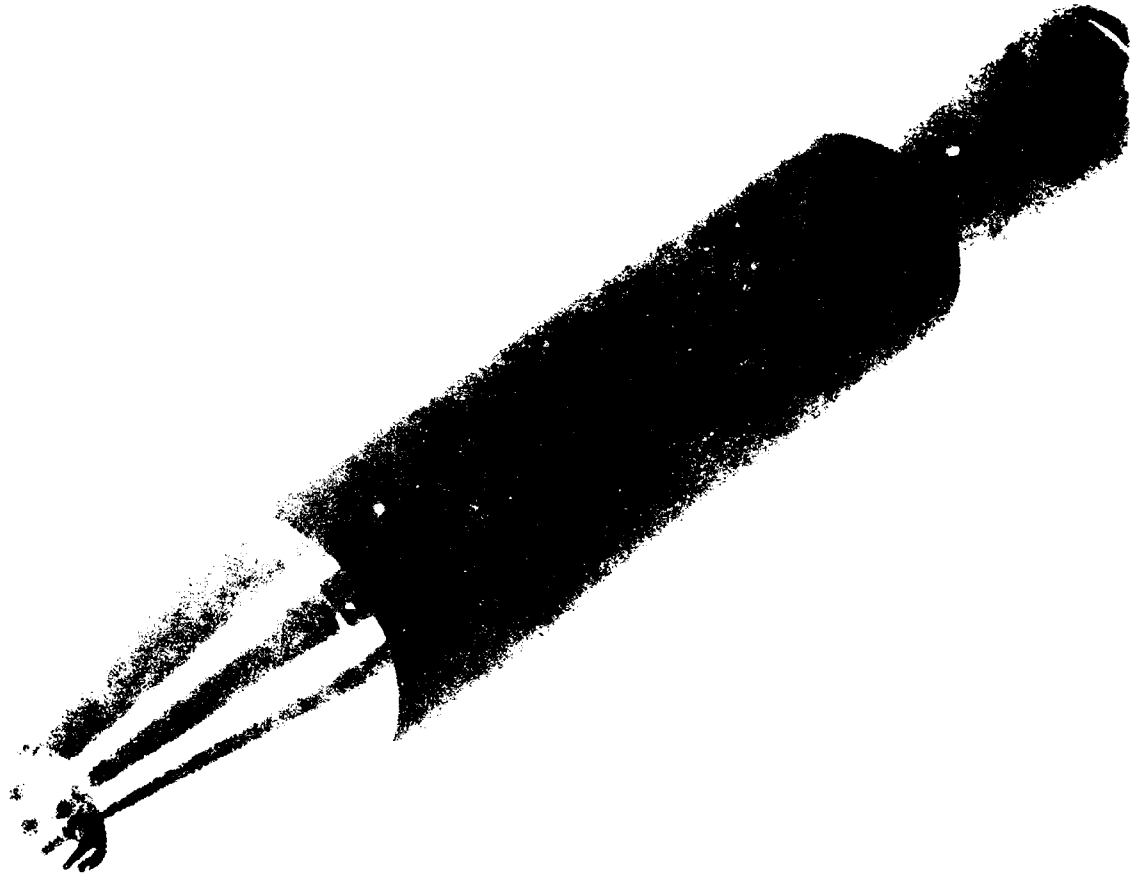
FIGURE 14 TOTAL PRESSURE PROBE

If the flow is subsonic, the pitot pressure measured is the true total pressure and the pressure ratio is given by the isentropic relation

$$\frac{p_0}{p} = \left(1 + \frac{\gamma - 1}{2} M^2\right)^{\gamma/(\gamma-1)} \tag{7}$$

where p is the static pressure.

Note the subscripts have been dropped since there is no bow shock wave formed in subsonic flow. For supersonic flow the Mach number may be obtained by combining the above equations to eliminate the total pressure ($p_0 \equiv p_{01}$) by division of Equation (6) by Equation (7). This gives the Raleigh supersonic pitot formula which is

$$\frac{p}{p_{02}} = \frac{\left(\frac{2\gamma}{\gamma + 1} M_1^2 - \frac{\gamma - 1}{\gamma + 1}\right)^{1/(\gamma-1)}}{\left(\frac{\gamma + 1}{2} M_1^2\right)^{\gamma/(\gamma-1)}} \tag{8}$$

The reduction of data from stagnation pressure measurements in supersonic flow is seen to be anything but straightforward and involves a number of assumed values and conditions along with iterations between Equations (8) and (6) along with predetermined gage calibration factors. For reasons such as these, confidence in total pressure measurements diminishes rapidly at overpressures much above 140 N/cm^2 (200 psi).

The Air Force Weapons Laboratory (AFWL) is involved with an experimental program to significantly advance the current capability for measurement of total pressure (and thus dynamic pressure). This program entails both transducer and probe development and considerations of data reduction and analysis

54

techniques. Figure 15 shows the AFWL wing-shaped probe used for multiple gage installations in their Dynamic Air Blast Simulator (DABS) program. DABS is a large explosive driven expendable shock tube for providing high overpressure and dynamic pressure environments over large test volumes. Stagnation pressures ranging from 2100 N/cm^2 (3000 psi) upward to 3400 N/cm^2 (5000 psi) have been repeatedly measured using the bar gage (seen earlier in Figure 3b) as the pressure transducer.

A major problem with measurement of stagnation pressure at high overpressures is the influence of dust and particulate matter that is an inseparable part of the field test environment. In review of past history, a number of attempts have been made to account for the effects of particulate matter in the flow. The Sandia Greg and Snob gages along with the SRI-MAD (for measurement of air and dust) are notable examples of probes that have been designed especially for the purpose of determining the separate contributions of air and dust components[13,17].

The Greg and Snob gages were designed and used during the days of atmospheric nuclear testing and are described in Reference 13 which is dated 1959. Aside from the development of the MAD gage by Stanford Research Institute (c.a. 1963) for measurement of dusty air blast effects no other significant recent effort has been uncovered relating to development of instruments that deal specifically with the contribution from dust effects to the total measurement.

The measurement of parameters in the high overpressure regime necessitates measurements in environments that are heavily laden with dust, debris and combustion products. It seems apparent that proper interpretation of such measurements

55
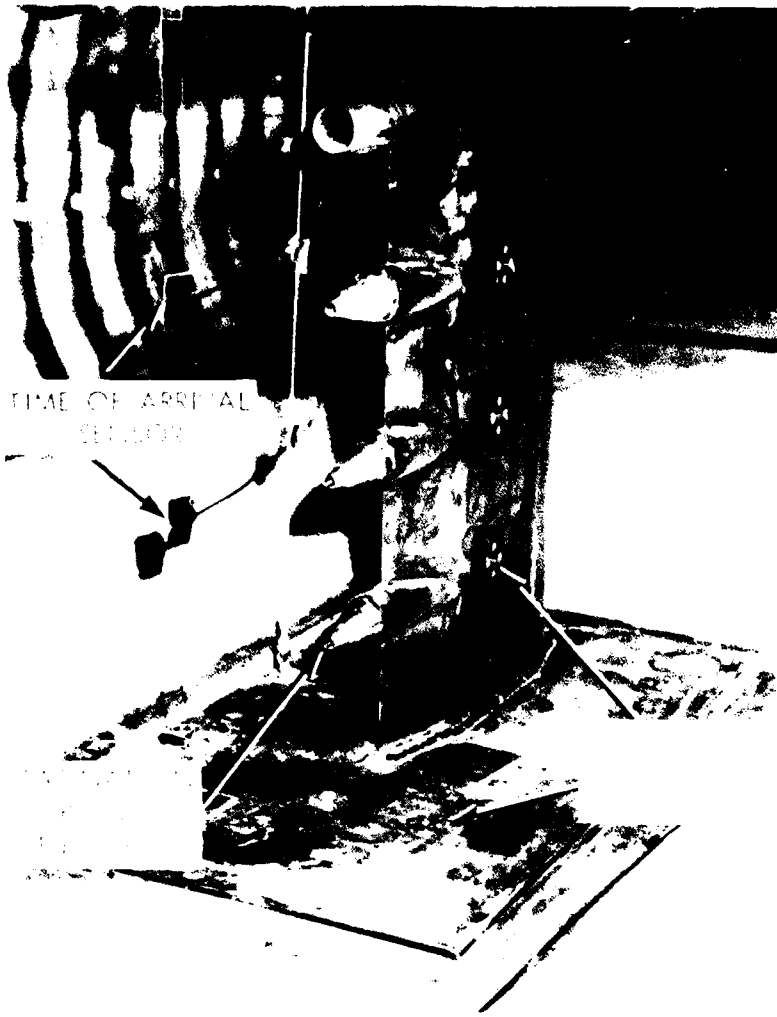
TIME OF ARRIVAL
SENSOR

FIGURE 15   MULTIPLE GAGE INSTALLATION FOR DABS SHOCK TUBE

calls for a basic understanding of the effects and influence of these factors on the measurement as part of the larger problem of air blast phenomenology.

3.2.7 Impulse

The impulse (I) from a blast wave is given by the area under the pressure-time (p-t) curve. Mathematically it is expressed as

$$I = \int p \ dt.$$

The impulse is usually calculated from numerical integration of one of the pressure measurements previously described. From many viewpoints, the impulse is a more interesting parameter than pressure: Structures respond to impulse. The nature of the measurement involves a smoothing or averaging process. Consequently, correlation of impulse measurements with predictions generally leads to less scatter in the data.

Positive impulse is defined to be the area under the overpressure-time curve during the interval that this pressure is positive. Similarly, the negative impulse is the integral of the negative portion of the overpressure curve.

A "flying plug" has been proven useful for measurement of reflected impulse at high overpressure levels[18,19]. The technique involves exposing a lightly constrained plug in a large fixed plate normal to the blast wave. The flight of the plug is recorded using high speed photography and application of impulse-momentum considerations to the trajectory data. The accuracy of data thus measured is reported to be in the neighborhood of ±2 percent[18].

An advantage to measurement of impulse using the flying plug or similar approach is that it may provide a reliable data point in a region where most measurements are not presently made.

3.2.8 Probe Design Considerations

The presence of a pressure transducer in an air flow will necessarily perturb the flow field and alter the parameter being sensed. For this reason, it is essential that the sensor be installed in a probe that has been designed with due appreciation and understanding of the aerodynamic aspects of the measurement. Not only must the probe be designed for minimal perturbation of the flow, but consideration must be given to the optimum location of the sensing element in the probe. This is especially critical for air blast measurements in a high overpressure region because pressure distribution and flow conditions around the probe will change drastically during transition from supersonic to subsonic flow.

The successful measurement of blast pressure depends on a priori knowledge of the blast direction since none of the available transducers are omni-directional. It will be seen that certain probes and mounting designs are less sensitive than others to blast orientation.

Books have been written dealing with the aerodynamics of flow around probes and the influence of probe geometry distortion of the free-stream flow. Two points are made here: 1. The subject is a study in itself and will not be treated in depth in this report; and 2. Much attention and theoretical work is focused on wind tunnel testing and only limited work has been done on probe design considerations for blast study

58

programs in the field. This is not to discount the fine work
that has been and continues to be done by laboratories such
as BRL, SLA, SRI, AFWL and others.

A very few U. S. manufacturers of blast-type pressure
transducers offer, as standard catalog products, sensors
installed in aerodynamically shaped probes for measurement of
static overpressure. While these probes are widely used for
measurements in a supersonic blast flow environment, aerodynamic
calibration or performance specifications are sparse or totally
unavailable from the manufacturer. Responsibility rests with
the user to determine calibration factors and the suitability
of the probe for the intended application. This is understand-
able from the viewpoints that the transducer manufacturer is;
(1) unlikely to have an aerodynamicist on his design staff,
(2) the shock tubes and wind tunnels represent major test
facilities that would not be a financially cost effective
investment and (3) the volume of business for air blast
instrumentation represents a relatively small portion of the
pressure transducer market.

Three commercially-available probes that are used for air
blast measurements are the ST-7 probe by Susquehanna Instruments
and the LC-13 and LC-33 probes by Celesco Industries (formerly
Atlantic Research). The name "pencil" probe is commonly given
to this design.

Photographs of the ST-7 and LC-33 probes in Figure 16 show
the probes to be streamlined and slender. The LC-13 that is not
shown is smaller than the LC-33 but similar in shape.

Design considerations for this streamlined probe are
deceptively complex. In supersonic flow, a detached bow shock
wave will form off the tip of the probe. This disturbance will

59
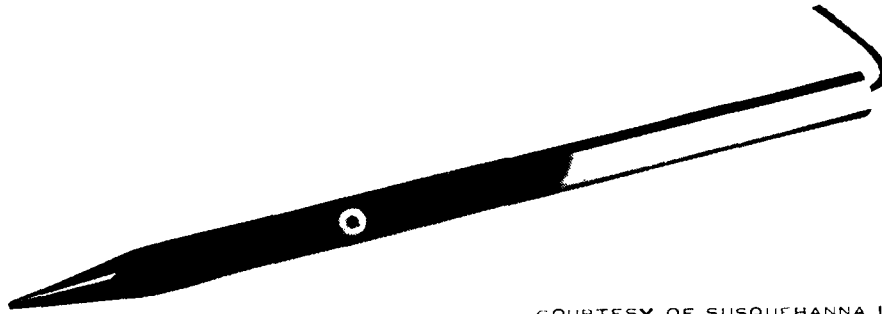
(a)   ST-7 PROBE
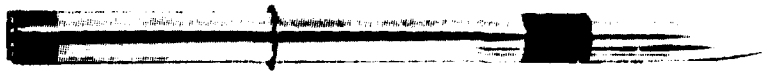
(b)   LC-33

FIGURE 16   PENCIL PROBE BLAST PRESSURE TRANSDUCERS

cause a surface pressure gradient along the length of the probe making sensor location a critical concern.

Representative pressure distributions for two probe geometries are seen in Figure 17. The first probe (Figure 17a) is similar to the ST-7 while the second is more like the LC-13 and LC-33 design. The abrupt shoulder at the cone-cylinder junction causes the air to be expanded and the pressure drops to below the free-stream static value. The pressure on the surface of the probe asymtotically approaches the true static pressure to within 1% at 10 to 15 diameters downstream from the shoulder.

The blunt-nosed Celesco probe geometry makes use of the fact that a smooth transition from the cone to cylinder will eliminate the expansion wave and change the pressure distribution to look like 17b. Location of the pressure transducer sensitive area at B allows a much shorter probe than the design in 17a. However, the location of point B is more sensitive to flow Mach number than is point A. From a study of published design information[20,21] the overall calibration for variable Mach number for the probe with the transducer at least 10 diameters back is expected to be more accurate.

Figure 17 is given to illustrate that the geometry is a critical consideration in design of a probe for static overpressure measurement. The surface pressure distributions indicate that the optimum location of the active sensing element is not an arbitrary choice. The pressure distributions are dependent upon Mach number (M) and the most accurate measurements require use of a correction factor that is a function of M. The pressure (ρ) measured by the cone-cylinder model, with sensor location at least ten diameters downstream from the shoulder,
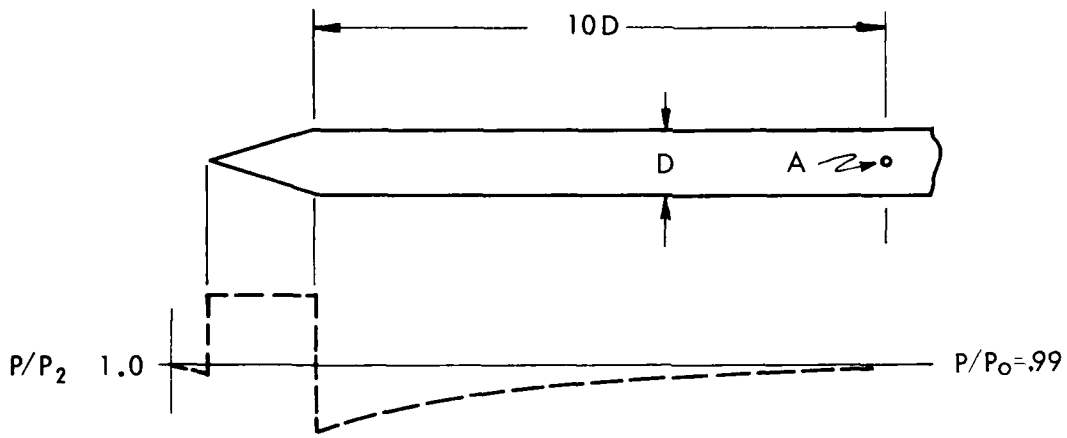
a) CONE-CYLINDER PROBE
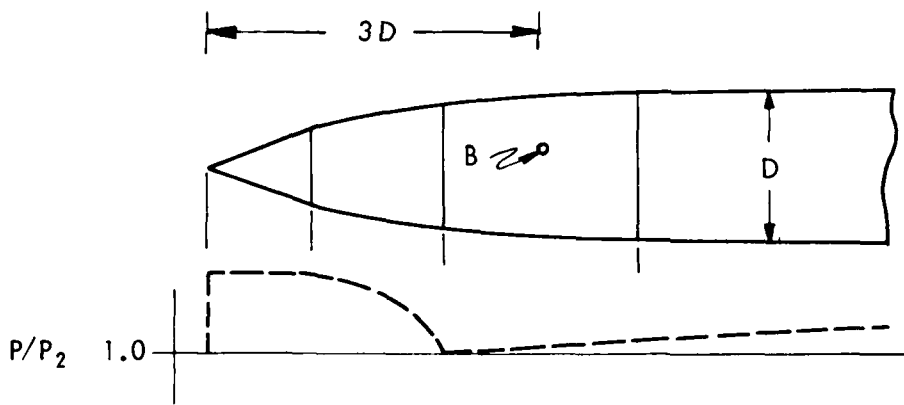
b) BLUNT-NOSED PROBE

FIGURE 17   PRESSURE DISTRIBUTIONS ALONG SLENDER PROBES
            (REFERENCE 21)

62

is expected to be within one percent of the desired free stream pressure (P_o) for widely variable M[20]. Calibration for the blunt-nosed geometry will be more dependent upon M; the particular probe shape and sensor location having been optimized to provide a short probe for special purpose application over a limited range of M[21].

A number of variations on the disc probe are also used to measure static overpressure. The BRL 18-inch diameter disc baffle seen in Figure 5 uses a flat surface with a flush-mounted transducer in the center. This probe design has been widely used for a number of years with proven results. It is susceptible to damage from flow misalignment at higher overpressures because of the large exposed surface area. This probe calibration may be quite sensitive to alignment error also. For example, consider the pressure distribution over the surface of the disc to behave as a thin airfoil. At '6 degree angle of attack one would predict a corresponding '30% error at the mid-chord position.

The probe design of Ruetenik and Lewis described in Reference 22 is considerably less sensitive to alignment while at the same time more rugged from a blast damage viewpoint. Figure 18 shows the outline dimensions for this probe which incorporates two sensors instead of one. When the probe is misaligned with the flow, one transducer will sense a pressure that is higher than the free-stream static overpressure while the other one is too low. To a large extent the errors are compensating so that the average output approaches the desired value. The difference between the two output signals gives a measure of the flow vector. As with all differential measurements, accuracy of this type of probe is strongly dependent upon a dual channel measuring system that is presumed to be identical. This requires a carefully matched system from the sensor to recorder.

63
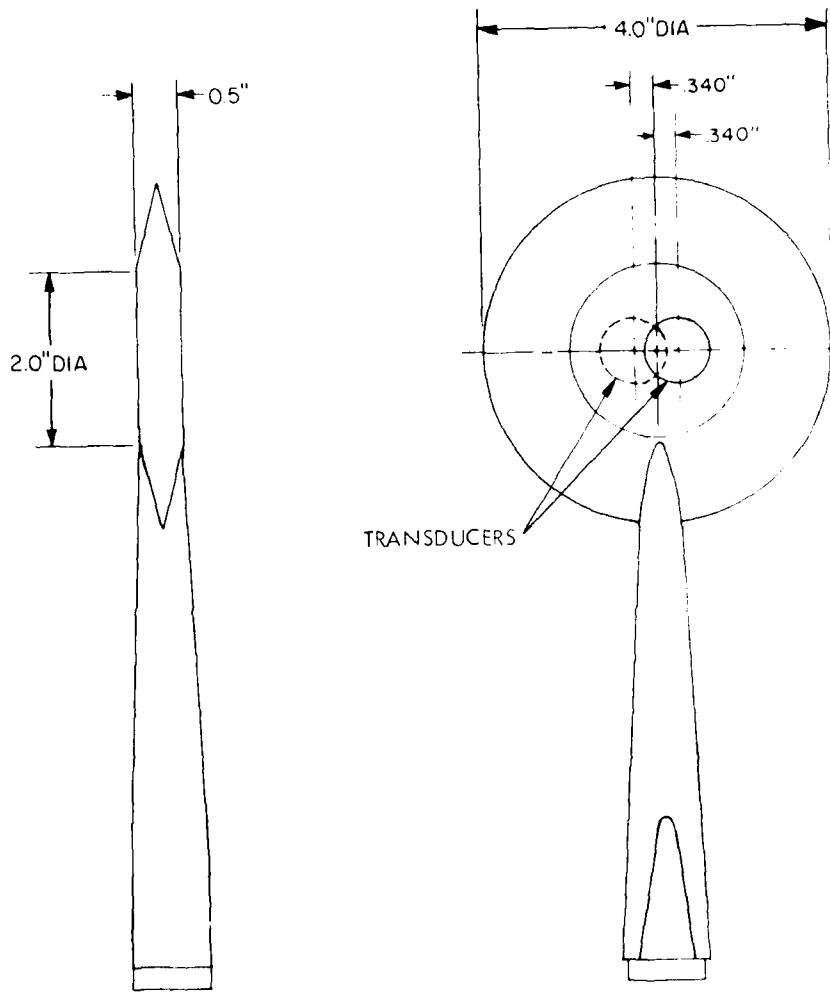
FIGURE 18   SKETCH OF DUAL-TRANSDUCER PRESSURE PROBE

Figure 19 is a sketch of a commercially available lollipop probe (PCB Piezotronics) that is interesting to consider in light of the foregoing discussion. The success of this probe as with the others is dependent upon calibration and application to the proper situation. Note that there is virtually no flat surface parallel to the plane of the free-stream flow. The pressure distribution across the diameter would be generally above the ambient along the slope ahead of the sensor and below ambient behind the sensor (toward the sting mounting). The sensing element is located in the transition region where the calibration at different Mach numbers and angles of attack might be a difficult problem.

One should not ignore the error that is introduced in a static overpressure measurement by misalignment of the flow with the baffle (disk). This problem is especially serious for large overpressures where the dynamic pressure is not small compared with the shock overpressure. The error introduced by the "angle-of-attack" effect is essentially independent of the probe size. Equally important for transient blast measurements are considerations of aerodynamic response time of the probe. The pressure transducer itself may have a response time of a few microseconds (depending on the particular one chosen) but the time for the flow surrounding the probe to come to equilibrium following diffraction of the shock wave by the probe will be considerably longer. Any ports or cavities in the transducer installation or adaption to the probe will increase the basic transducer response time by effectively including an organ pipe and/or a Helmholtz resonator in the system. The acoustic resonances of these devices may seriously limit the response of the probe and must be considered[23].

.375

3.0 dia.

.218 dia.
SENSING
SURFACE

10.6

1.13 dia.

4.06

.50 dia.

.50

BNC CONNECTOR

COURTESY OF P. B. PIEZOTRONICS
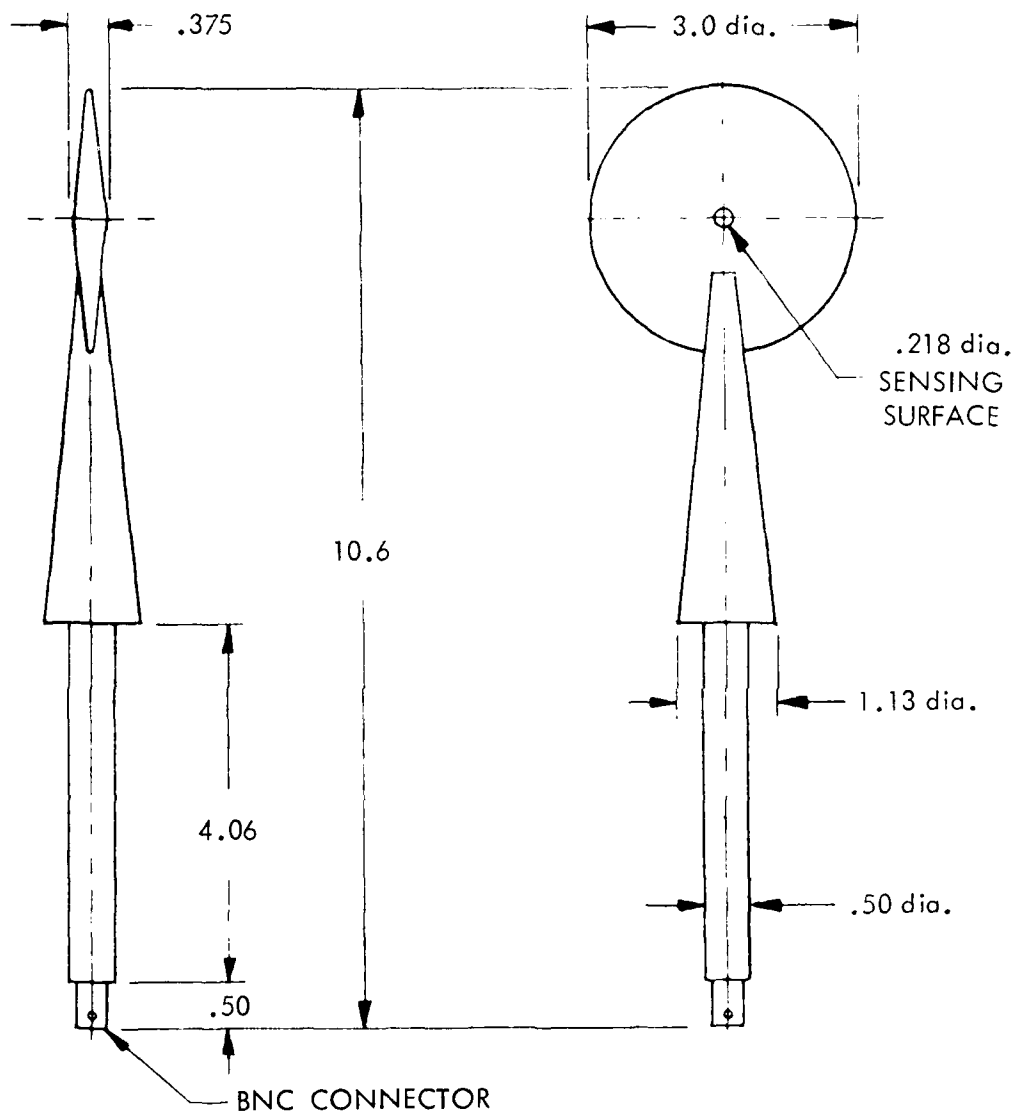
FIGURE 19   FREE-FIELD BLAST PRESSURE TRANSDUCER
(MODEL 113A51)

The point being made regarding probe design is that the probe will disturb the flow field being measured and the optimum location of the sensing element is critical. The correction factors and pressure distributions measured in wind tunnel and shock tube tests will also be sensitive to flow turbulence levels for most probe geometries.

Careful study and consideration thus needs to be given to selection of the probe and gage mount for measurement in an air blast environment.

3.2.9 Frequency Response

Considerations of frequency response and interrelated parameters of the measuring system are contained in this section. The discussion is given in the context of pressure measurements only because this is the physical parameter most commonly measured in the overpressure regime above 140 N/cm^2 (200 psi). The definitions and comments may be generalized to apply equally well to transducers and measurement systems for other parameters.

Several definitions are quoted from the Instrument Society of America (ISA) "Standards for Electrical Transducer Nomenclature and Terminology" (1969). These terms will be discussed as they apply to requirements for successful transient measurements.

"Frequency Response - The change with frequency of the output/measurand amplitude ratio (and of the phase difference between output and measurand), for a sinusoidally varying measurand applied to a transducer within a stated range of measurand frequencies.

Response Time - The length of time required for the output of a transducer to rise to a specified percentage of its final value as a result of a step change of measurand.

Resonant Frequency - The measurand frequency at which a transducer responds with maximum output amplitude.

Rise Time - The length of time for the output of a transducer to rise from a small specified percentage of its final value to a large specified percentage of its final value as a result of a step change of measurand. (Unless otherwise specified, these percentages are assumed to be 10 and 90 percent of the final value.)

Time Constant - The length of time required for the output of a transducer to rise to 63 percent of its final value as a result of a step change of measurand."

These terms have been defined by the ISA as properties of transducers. The definitions certainly have a broader meaning and can be applied to a probe or measurement system as well as a transducer.

Before considering the frequency response requirements for measurements in a blast environment it will be helpful to review relationships between rise time, time constant and frequency response. These relationships are well known and their bases are given in many texts on frequency analysis (e.g. Reference 24).

The rise time (10-90 percent) t_r, for a single degree of freedom system, is given by the equation

$$t_r = 2.2\tau \tag{9}$$

where τ is the time constant of the system.

The upper 3-dB frequency f_2 is related to τ by

$$\tau = \frac{1}{2\pi f_2} \; . \tag{10}$$

By combining Equations (9) and (10) we obtain the very useful relation that

$$t_r = \frac{0.35}{f_2} \; . \tag{11}$$

It can be further shown that for n systems in cascade the overall rise time is given by

$$t_r = 1.1(t_{r1}^2 + t_{r2}^2 + \ldots + t_{rn}^2)^{1/2} \; . \tag{12}$$

These equations are strictly true for a single degree of freedom system yet they are useful close approximations for the more complex systems.

It is important to note that the measurement system frequency characteristics are determined by the combination of the transducer, the probe (or installation details), signal conditioning circuits and the recording system. The entire system must therefore be evaluated to establish the adequacy for making a desired measurement or validity of a given data record. Distinctions of the difference between sensor and system characteristics need to be fully understood by the experimenter.

69

A transducer that is exposed to a step pressure change
will be excited at its resonant frequency if the rate of
pressure rise is sufficiently fast. The rise time for a
shock wave will vary, depending upon the blast source and
intensity, distance from the source and gas dynamic properties
of the shocked medium. Nonetheless, rise times can be
expected to be less than a microsecond particularly for the
static overpressures of concern to this study which are
above 140 N/cm^2 (200 psi). Damped oscillations will show up
on the output of virtually any air blast pressure measurement
that is not overdamped since very few (if any) sensing
elements have natural frequencies that would not be excited
by high frequency energy in the shock wave.

Referring back to Figure 12 as an example, this ringing
response is clearly evident in the initial response of the
transducer. Sources of this oscillatory response may be
mechanical resonance of the transducer sensing element, acoustical
resonance of ports and cavities or aerodynamic oscillations
in the flow set up by diffraction of the initial and succeeding
shocks and rarefaction waves over the probe. Another potential
source might be the signal conditioning and recording system,
although existing technology in these areas is sufficiently
advanced so that this source can be eliminated by careful
selection of these system elements.

The resonant frequency of a measurement system will impose
a limitation on the useful frequency response (bandwidth) of
that system. A rule of thumb for system design is to limit
the system frequency response to not more than 20 percent of
the lowest resonance in the system. As the system response is
crowded toward the resonance, frequency selective distortion
will be introduced in the output signal.

Compensation methods have been developed for unfolding the distorted data signal in situations with inadequate bandwidth. These methods can be especially productive when the deficiency is discovered after the measurement has been made or where a better measuring system is not available. Most compensation methods are based on use of the Fourier transform operating on the data in the frequency domain and an inverse transform to the corrected data. An alternative approach is to perform the compensation by time domain deconvolution (TDD)[25]. Either method requires additional test information that defines the transfer function. This is commonly given by an analytic expression, modulus and phase versus frequency tabulations, or appropriate input and output time response pairs.

Frequency or time domain corrections can be applied to each stage of the measurement system or as an overall end-to-end correction. Each method has its own merits and most suitable application. It is worthy of note that the TDD approach may offer certain advantages to measurement systems that tend to be oscillatory. The frequency domain transfer function for such a system changes radically in the region of the resonant frequency and mathematical operations with the function may introduce large errors in this region.

The response time required for pressure measurements is dependent upon the size of the detonation and the pressure level being measured. Consider for example, a 2.2 kg (1 lb) versus a 2200 kg (1000 lb) spherical charge of TNT in free air. At the 350 N/cm^2 (500 psi) level of peak blast pressure, the positive phase duration lasts 114 and 1140 microseconds respectively. From another viewpoint, the positive phase duration is 1140 microseconds for the 2.2 kg charge at a peak pressure of approximately

71

48 N/cm^2 (70 psi)[26]. If the interest in the measurement is primarily to measure impulse, a much lower frequency response measuring system will suffice than if the peak pressure and initial character of the blast are to be defined.

A 20 kHz bandwidth measuring system is perfectly adequate for most measurements in the large-charge field tests with charge sizes of many hundred tons. As the charge weight decreases and/or the peak overpressure increases,the frequency response requirements increase and the selection of a suitable transducer is more difficult. Equations (9) through (12) are helpful in determining the frequency response required by the measurement system elements after the expected pressure level and waveform have been established.

3.3 Density Measurement

The temporal measurement of gas density does not lend itself readily to the field test environment. The moderately successful blast wave density-time gage for this application is a beta-ray densitometer used on Events PRAIRIE FLAT (1968) and DIAL PACK (1970). The maximum overpressure in which these densitometers were tested was 17 N/cm^2 (25 psi).

The results of these measurements are presented in References 27 and 28 along with a description of the system used and some theory of application. The densitometer has been designed for subsonic flow measurements and would need some re-design for use in supersonic flow. Another perhaps more serious limitation of the beta-ray densitometer is its high sensitivity to even low concentrations of dust entrained in the air.

Photographic means for density measurements are being developed that utilize high-speed photography of smoke tracer particle trajectories. This method is further described in Section 4.2.2.

The schlieren system is a photo-optical method that depends upon the density gradient from which one can (in principle) obtain quantitative measurements that may be integrated to give the density field. Practical application of this method to high overpressure blast environment in the field has not been demonstrated. The same statement can be made for the Mach-Zehnder interferometer which is so widely used in wind tunnel tests for density gradient representations.

Thus, density remains as a very desirable blast parameter for which adequate field worthy measurement techniques have not been developed for overpressure in the region above 35 N/cm^2 (50 psi) or in other than clean-air conditions.

3.4 Velocity Measurement

Two distinct velocities associated with air blast are identified as important to this study: One, the velocity of the shock wave front (U_s); and two, the gas particle velocity (u) in the flow behind the wave front. In dust-laden flow the velocity distribution of the particulates is noted as being a separate quantity that is not currently measured satisfactorily in the field.

3.4.1 Shock Wave Front Velocity

The shock wave front velocity can be counted among the more readily measured air blast parameters. Two basic methods are available to the experimenter with either continuous or discrete resolution. The degree of sophistication ranges from

73

the simplicity of an open-circuited coaxial cable for sensing
an ionized shock wave front to the complexity of a radar
system. The tradeoff is a single data point at a small cost
versus a continuous measurement with resolution of a few
centimeters at a relatively high cost.

The most usual method is to use air blast time-of-arrival
detectors (ABTOAD) at discrete locations to measure shock wave
front arrival at particular locations to complement pressure
measurements. Average velocities are then readily calculated
as the spacing per differential arrival time. The ABTOAD
consists of a piezoelectric crystal, foil strain gage, carbon
gage or any other pressure or shock sensitive detector -
effectively an inexpensive, uncalibrated pressure transducer
that is designed to provide a positive indication of blast
arrival at the sensor. Several different home-made sensors
are used; examples are an aluminum foil between two electrical
contacts that is blown apart by the blast arrival, a diaphragm
that "makes" a contact under blast loading, etc. The resolution
for such ABTOADs is closely related to the spacing between the
gages although, of course, response time of the recording
system is an important parameter of the measuring system.

A considerably more sophisticated alternative to ABTOADs
is a doppler radar system that is aimed at the air blast
source. A unique feature of such a system is that the radar
will trace the propagation of the shock right from the booster
charge with near-continuous resolution. Again, the radar
system is relatively costly but it can provide a lot of data.
The value of such a continuous measurement system must be
weighed against the extra cost.

3.4.2 Air Particle Velocity

Passage of the shock wave front through the air sets the gas in motion giving it a velocity (u) which is known as the gas particle velocity. A peak overpressure of 38 N/cm^2 (55 psi) will result in a gas particle Mach number of 1 for a perfect gas initially at atmospheric pressure according to the Rankine-Hugoniot relationships. The Mach number approaches a theoretical limit of 1.89 for air as the peak overpressure is increased without bound, but the actual limit is much higher because the air is not a perfect gas.

The direct measurement of particle velocity is seldom attempted in the air blast environment because of technical difficulties. The photographic measurement of trajectories of low inertia smoke particles is described in Section 4.2.2. Other methods using velocity sensitive elements that are calibrated in a flow are used in the field to a fairly limited extent.

Hot-wire and thin-foil anemometry is not particularly adaptable for use in the high overpressure environment because of the relatively fragile sensing elements. The hot-film anemometer is estimated to have an upper limit in air blast work at about 50 N/cm^2 (72 psi) peak overpressure.

The Kaman vortex shedding anemometer (VSA) is shown in Figure 20 with the top plate removed to expose to view the vortex generating obstruction and frequency sensing ports. This device has been proven field-worthy in air blast environments for measurement of air particle velocity when M < 1[29,30]. Frequency response of the VSA is a function of the velocity with an estimated 700 μsec response time at 300 m/sec increasing proportionately to 1000 μsec at 150 m/sec.

FIGURE 20   ANEMOMETER WITH TOP COVER REMOVED SHOWING
            FLOW OBSTRUCTION AND TRANSDUCER PROBES

76

Among the latest innovations for gas particle velocity measurement at high overpressures is the radar doppler measurement using an aluminum foil target and a radar "gun" of the type used by highway patrols for measuring speed of automobiles[31]. This system has successfully measured gas particle velocities on the order of 1400 m/sec. It is noted that this method does not provide a local measurement, as the target is swept along with the flow of the gas. A limitation of radar doppler system is encountered when the shock wave front is ionized as the radar would then see the shock front as the reflecting surface.

3.5 Temperature Measurement

The measurement of temperature in an air blast environment is indeed a difficult problem even at relatively low overpressures. Assuming an adequate frequency response, a temperature sensor placed in the gas flow environment will come to an equilibrium temperature that is different from the desired gas temperature. The temperature sensed by the probe will be the net sum of direct radiation from the air blast source, heat transfer rates, conduction effects, and local gas velocity and pressure which contribute to frictional heating caused by flow around the probe.

These factors are all difficult to deal with and collectively contribute to the fact that direct measurement of gas temperature is not usually attempted in an air blast environment, particularly in the high overpressure region. The temperature measurements reported by TRW on Event MIDDLE GUST IV are an exemplification of the problems encountered and complex analysis required to interpret the recorded measurement data. These measurements were made at approximately 20 and 40 N/cm^2 (30 and 60 psi) peak overpressure test stations

using hot-film anemometer probes in a study to characterize the boundary layer development behind a blast wave. The highest peak temperature of slightly above 600°C was measured at 50 N/cm^2 (72 psi)[4].

Perhaps the greatest promise for successful temperature measurement is held forth by techniques that utilize remote sensing such as radiometry and optics technology.

4. PHOTOGRAPHIC MEASUREMENTS

It is the purpose of this chapter to present capabilities
and features of available cameras and photographic equipment
that are of interest and have application to measurement of
the air blast environment. Current applications and techniques
for measurement of specific parameters are included.

This chapter is primarily concerned with photographic
methods used as instrumentation for large-scale HE tests;
however, many of these techniques are used for small explosive
tests, also. In addition, this chapter is not an attempt to
list or detail every camera or optical technique available,
but rather to present today's technology. In general, emphasis
has been placed on commercially-available products rather than
camera systems or techniques which have been invented or are
in use at only one laboratory. William Hyzer has authored
two excellent texts for those needing specific reference to a
particular camera system. These texts are listed in the
bibliography[32,33].

4.1 Photographic Equipment

The camera has been successfully used with experimental
field tests for documentary records that are of a generally
qualitative nature. It is also proven as a very productive
and versatile instrument for making numerous highly sophisticated
quantitative measurements. One particularly attractive aspect
of photographic measurements is that the remote observation
does not perturb the environment being studied as is character-
istic of transducers that require insertion into the flow field.

Photographic measurements are in contrast to those from a
transducer that senses a single parameter of the environment
at a fixed location. One frame of a photograph is a spatial

record of all the camera "sees" at a single instant in time. An electronic data channel (or even a self-recording transducer) is usually designed for measurement of a single parameter at one point in space, to the exclusion of all others. Continuous observation within a recording interval or time window is possible and characteristic of most transducers and electronic recording systems.

The high-speed motion picture camera provides data that are both temporal and spatial in nature and also has a frequency response that is comparable to the frequency response of electronic systems used for measuring blast parameters. In addition, the two types of measurements are highly complimentary of one another, each lending insight into the interpretation and analysis of the other.

This section will identify a variety of photographic equipment available along with its capabilities and applications to air blast parameters. Important camera parameters are optical resolution, framing rate, and total recording time. Optical resolution is given by line pairs per millimeter. This designation refers to the number of lines that are clearly resolved within one millimeter. The lines must be individually distinguishable, without blur, on the film. A specification of 80 line pairs per millimeter is excellent. However, it should be pointed out that this quality of resolution is seldom achieved under field conditions. A resolution of 80 line pairs per millimeter is usually achieved statically on a single frame using high contrast film and printing paper. Field conditions typically limit the optical resolution to approximately 50% of the manufacturers specifications. Manufacturers' resolution numbers are given, however, since field conditions vary so greatly between different events or users as to be the predominating factors in determining the quality of the optical system results.

The framing rate of a camera is simply the number of
pictures photographed per second, while total recording time
is the real time interval during which an event may be photo-
graphed. Classification by framing rate is given in the
paragraphs that follow.

Photographic instrumentation typically falls within five
speed categories: 1) Still camera, 2) low speed, 3) high speed,
4) very high speed, and 5) ultra high speed. Industrial
sources of these instrumentation cameras have designed techniques
which allow an overlap of speed ranges, thereby increasing the
versatility of any single camera type. Many optical techniques
are used to obtain the versatility of speed ranges among the
available cameras. Among these techniques are intermittent film
movement, rotating prisms, rotating drums, rotating mirrors, the
image-converter, and Kerr cell cameras.

4.1.1 Still Cameras (Single Frame)

This type of equipment is generally characterized by the
capability for single frame exposures. Polaroid, single lens
reflex, and view cameras are examples of still cameras. Some
still cameras are equipped with electromechanically actuated
shutters for remote control of the film exposures. Other
cameras have automatic motor-driven film advance techniques
for time-lapse sequential exposures up to one photograph per
second.

Numerous high quality still cameras are commercially
available, and none will be identified by name here for this
reason. Auxiliary shutter techniques which can be used with
still cameras will be discussed in Section 4.1.7 of this
report.

4.1.2 Low-Speed Framing Cameras (5-400 fr/sec)

Framing cameras provide a sequence of exposures with a
known time interval between frames. Low-speed framing cameras
use intermittent film drive where the film is advanced during
a closed shutter, held stationary during exposure of the film.
A subsequent repeat of the film transport sequence yields
many frames. The low-speed framing rate is 5-400 frames per
second. The limiting factor is the rate at which the film can
be accelerated from position to position without tearing.
Optical resolution available with this style camera is 80 line
pairs per millimeter. Total recording time available depends
on the length of the film spool, but typically ranges from
10 seconds to 2 minutes. Numerous commercial sources are
available for this type of camera. Several that have been
successfully used in the field are the D. B. Milliken, Hulcher,
Locam, and Photosonics.

An advantage for this type of camera is that the film is
pin registered and held stationary during exposure, thereby
increasing the resolution obtainable as compared to higher
speed cameras which must shutter the image onto film which is
in continuous motion.

The Hulcher camera is a low-speed camera with a framing
rate from 5 to 20 frames per second. Shuttering is accomplished
with two discs which form an aperture which is continuously
adjustable from 1° to 180°. This disc system gives very short
exposure times to give excellent ability to freeze motion.
Combined with a stationary film, the well controlled exposure
time and fine optical system allows excellent resolution.

4.1.3 High-Speed/Very High-Speed Cameras
(400-300,000 fr/sec)

Industrial sources of instrumentation cameras have developed an overlapping frame rate capability in these categories. High-speed cameras generally have a frame rate of 400-10,000 frames per second, while very high-speed cameras have a frame rate of 10,000-300,000 frames per second. The speed limitation of the low-speed camera is overcome by elimination of the requirement to start and stop the film transport between each frame. These higher speed cameras use rotating prisms to effectively shutter the image on the film and thereby prevent a blurred image, although at the expense of a slight decrease in resolution.

Red Lake Laboratories produces the Hycam camera with an optical resolution of 60 line pairs per millimeter with a 16 millimeter frame, and a framing rate of 11,000 frames per second. By reducing the frame size and imaging four frames rather than one, the framing rate can be quadrupled to 44,000 frames per second. A disadvantage is that the frame size is reduced by this process to 2 millimeters. The recording time at the maximum rate is limited to approximately one second, allowing time for the camera to come up to speed.

The Cordin Company produces the Dynafax camera which has a framing rate of 35,000 frames per second with a frame size of 16 millimeters. The optical resolution of the Dynafax is approximately 50 line pairs per millimeter. Advantages of this camera are that it is continuously accessible at full framing rate with a large film format of 16 millimeters. An auxiliary shutter system may be required to prevent multiple exposure (rewrite) if the event being photographed is luminous or illuminated for more than one cycle of the film. Several high-speed shutters are described in Section 4.1.7.

83

4.1.4 Ultra High-Speed Cameras (>300,000 fr/sec)

Entirely different techniques are used for ultra high
framing rates of $300,000-10^6$ frames per second. One type of
ultra high-speed camera operates by holding the film stationary
and accelerating a small mirror to extremely high rotational
velocities. The rotating mirror is used to sweep the event
across the film plane, the final image being formed by secondary
lenses. At these extremely high framing rates, total recording
time is necessarily limited. Since the writing rates of these
cameras are so high, the exposure times are very short and,
consequently, enormous illumination is required for proper
illumination of the subject. Self-luminous events such as the
fireball are easily photographed; however, non-luminous events
require sophisticated generation of large amounts of light.

The only known commercial source for these cameras is the
Cordin Company. Optical resolution for the Cordin cameras is
approximately 20 line pairs per millimeter. Beckman-Whitley,
now owned by Cordin, was a source for ultra high-speed cameras
(10^6 frames/second), and many of these are still available for
use. Also, several special cameras have been built at labora-
tories such as Naval Surface Weapons Center (NSWC) which may
be made available for government-sponsored projects.

A variation of the rotating mirror framing camera is the
streak camera. Briefly, it uses the rotating mirror principle
to obtain a continuous record of motion versus time at a
single point of observation , rather than many pictures at
sequential time intervals. Writing rates of 20 millimeters
per microsecond are available with an optical resolution of
80 line pairs per millimeter. A disadvantage of the camera
is that only one discrete point of information may be obtained
without clever external optical techniques. The Cordin Company
manufactures several streak cameras.

4.1.5 Image-Converter Cameras

Image-converter cameras offer exposure times as short as 5 nanoseconds. To obtain these extremely fast exposures, an adaptation of cathode ray tube techniques are used. As a brief explanation, the object photographed is transformed into photoelectrons by the image converter tube photo cathode. These photoelectrons are amplified and accelerated to the fluorescent screen of the cathode ray tube, and the light subsequently emitted from the fluorescent screen is photographed by one of the photo-optical technqiues described previously.

Both Quad-Tran and Cordin Company supply the necessary equipment in one assembled package for an image-converter camera system. The Quad-Tran image-converter has a streak or framing camera option. The Cordin image-converter can use beam splitter techniques and two electronic packages to form two sequential frames recorded on 70 millimeter film. The optical resolution is about 20 line pairs per millimeter with the Cordin Company camera. An advantage of image-converter camera is the extremely short exposure times.

Recently, an image converter camera has been reported which has a nanosecond exposure time. This camera has been reported in the Journal of Technical Physics, 16, 2, 185-195, 1975. The title of the article was "A Camera With Nanosecond Exposure for Research Into Rapid Dynamic Processes," and was authored by Z. Ziolkowski and H. Derentowicz.

4.1.6 Kerr-Cell Cameras

Another camera technique which can be used at ultra high-speed framing rates is the Kerr-cell camera. This camera technqiue uses the Kerr-cell effect to act as an extremely fast shutter. The Kerr effect notes that certain materials, such

as benzene, become birefringent when stressed by an electric field. The construction of a Kerr-cell requires that two polarizing optical elements are oriented 90° with respect to one another. A birefringent material, such as benzene, is placed in the optical path between two orthogonal planes of polarization. No light will pass through the system until the benzene is stressed by an electric field. Then bi-refringence occurs and light is able to pass through the second polarizer to the camera optics.

Cordin Company makes a special order Kerr-cell camera. This camera system consists of six beam splitters that project the image through six Kerr cells onto six (4x5) film planes. The application of the electric stress to each Kerr cell can be sequentially timed to obtain six frames of information. Advantages to the Kerr cell camera are the extremely rapid photographs which may be obtained. A disadvantage is that approximately 50% of the light may be lost through the Kerr cell, thereby limiting the camera to highly luminous events.

4.1.7 High-Speed Shutters

Very high-speed and ultra high-speed cameras often require auxiliary shutters to prevent double exposure of the film. This rewrite problem is inherent to all rotating mirror or rotating drum cameras. These cameras may be used to record fast time events which are either artificially illuminated or self-luminous for long periods of time. If the late-time extraneous light is not stopped from reaching the film during the second revolution of the mirror or drum, a double exposure and possible destruction of the optical record occurs. The double exposure can be stopped by the use of high-speed shutters which close directly after the desired event is recorded. Mechanical shutters supplied by the manufacturers typically actuate in 1/50 of a second. For high speed events,

86

this shutter speed is obviously not intended to prevent rewrite. The camera requires an auxiliary high-speed shutter such as one of the high-speed shutters that are described here.

Blast shutters are typically constructed by placing a thin sheet of glass between two lucite plates on the optical axis. Two blasting caps (used to detonate explosives) are placed on different edges of the glass. After the desired event has been recorded, an electrical signal detonates the blasting caps, sending shock waves propagating into the glass. The shock wave fractures the glass and causes an opaque screen to develop between the two sheets of lucite.

A variation of the blast shutter technique is to use mirrors in the optical transmission of the light such that the camera views the event through the reflection from the mirror surface. When the event to be recorded is completed, the mirror is destroyed by blasting caps and, as a result, the light from the event cannot enter the camera optics.

Blast shutters are commercially available from the Cordin Company.

Kerr cells utilize several basic principles of physics to close off extraneous light to the camera system. These principles have been described earlier in the operation of the Kerr cell camera in Section 4.1.6.

Kerr cells are available from Cordin and Kappa Scientific.

Faraday magneto-optic shutters work on similar principles to the Kerr cell. Most importantly, however, a magnetic field is used to activate solid crystal materials to become doubly refracting. Similarly, the pockels cell shutter works by

application of an electric field to a piezoelectric crystal. The removal of the field causes the shutter to close off light from entering the camera optics. No known source of these shutters is available as a standard commercial product.

Lead-vapor shutters are also used successfully where fast shutters are required. They are not commercially available but are readily fabricated by the experimenter. The principle of operation is based upon condensation of vaporized lead on the surface of a plastic window placed in the optical path of the camera.

In practice, a pancake spiral of lead wire is wound with approximately 6 mm spacing between the turns. This spiral is then assembled as a sandwich between two plates of lucite, taking care to avoid shorting any of the turns by the center wire as the leads are brought out of the assembly. The lead blockage will reduce the light to the camera a negligible amount but will not appear as an image on the film because it is not placed within the focus of the camera. The lead wires are connected to a high energy capacitor bank through a switch that permits rapid discharge of the capacitor bank through the lead spiral. When the capacitor bank is triggered, the wire is vaporized by I^2R heating and the vapor is deposited on the lucite surfaces causing it to become opaque.

Depending upon the intensity of the light to be blocked, sometimes three plastic windows with two lead coils are used.

4.2 Measurement Applications

Applications of the camera and photographic techniques to air blast and related measurements that are presented in this chapter have been classified in six categories:

88

1. Shock Wave Front Velocity and Profile

2. Air Particle Velocity and Density

3. Charge Detonation Symmetry

4. Fireball Development

5. Crater Ejecta Trajectories

6. Cloud Development.

Strictly speaking, only air particle velocity, density, and shock wave front velocity are air blast parameters. However, in many cases the equipment and techniques needed to measure the last four categories are very similar, and, indeed, can often be obtained from the same photographic records. For this reason, all six applications are discussed briefly in the paragraphs that follow.

4.2.1 Shock Wave Front Velocity and Profile

Visual observation of the main shock wave profile in the vicinity of instrumented transducer measurements is particularly useful to establish whether the measurement was made in a regular or an anomalous portion of the air blast. It is not uncommon to record two entirely different measurements of pressure, for example, along two radials that are the same range but with different azimuth angles. Aerial photography that shows a jet extending toward one of the transducer stations quickly resolves the reason for the differences.

The same types of cameras and framing speeds used for fireball studies are used for shock wave front recording although often field of view and orientation is more tangent to the shock wave front in the region under observation. Often different filters, film types and exposures are also indicated to optimize the particular measurement being made.

Quantitative measurements of the shock wave front velocity
are usually made with the aid of a back drop having a geometric
pattern. Distortion of the pattern enhances visualization of
the shock wave front. This is particularly required for weak
shocks. Fiducial targets in the camera field of view allow
correction of the apparent distances on the film. Average
velocities of the shock wave front may be calculated by
measuring its position from frame to frame. Accurate timing
marks along the edge of the film provide a measure of inter-
frame time as well as an absolute time from detonation zero.

Figure 21 is a photograph from the recent DIPOLE WEST
series that shows a representative geometric backdrop pattern
to enhance the shock wave front. Often diagonal lines are
used instead of a polka dot pattern. The dimensions of the
geometrical design are dependent on properties of the shock,
such as velocity and orientation. Resolution will also depend
on the design dimensions and camera framing rate. Smoke trails
are useful for observing shock profiles (similar to the striped
backdrop) and, in addition, are useful to observe shocks at
further distances than are practical with backdrops.

Shock wave front velocity measurements from photographic
records are used to calculate the peak values of other
parameters at the shock front. The Rankine-Hugoniot relation-
ships uniquely define peak values for the pressure, temperature,
density, and particle velocity assuming the shock Mach number
and ratio of specific heats (γ) are known. Static overpressure
measurements are sometimes used with real gas tables and shock
Mach number to establish γ to use in other computations. While
this is a very satisfactory method of measuring the peak
values, it does not yield accurate data regarding the time
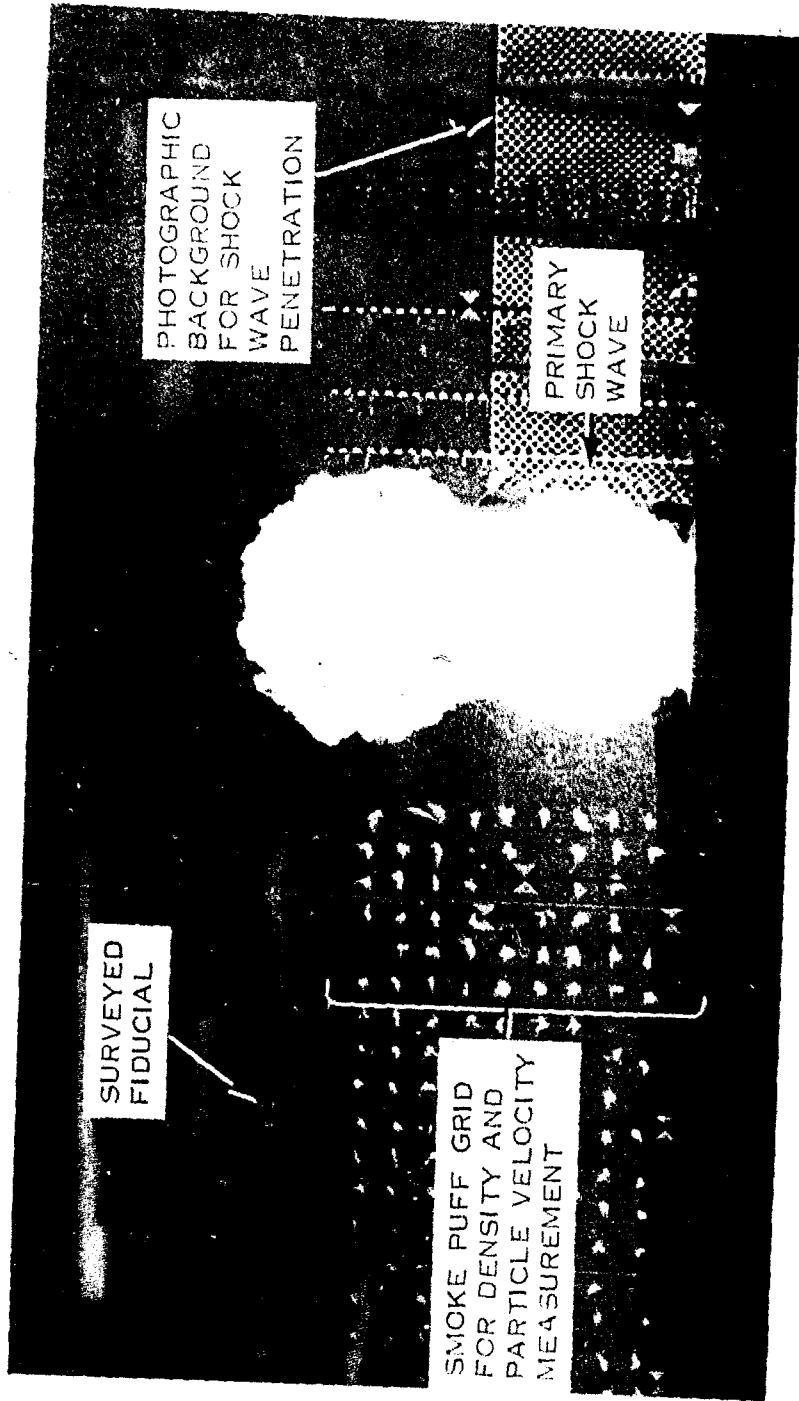history of the parameters.

FIGURE 21   PHOTOGRAPH FROM DIPOLE WEST PROJECT SHOWING GEOMETRICAL
BACKDROP AND SMOKE PUFF GRID

91

Thus, it is clear that the photographic measurement techniques are very complementary to fixed point measurements with transducers but they do not replace them.

4.2.2 Air Particle Velocity and Density

Techniques are currently under development to improve the measurement of air particle velocity and density using photographic data. The method involves the use of smoke particles as tracers that may be considered to have negligible inertia. Gross measurements of this type were made on early atmospheric nuclear tests using an array of smoke-generated rocket trails. Measurements in shock tubes have used crossed smoke streams to form a grid[34]. By high-speed photography, temporal measurements of the grid distortion are used to calculate particle velocity and density.

Recent effort to refine the application to field test measurements was included in the DĪPOLE WEST project[35]. In these experiments a grid of smoke puffs were initiated at time zero to establish a geometric pattern of particles whose trajectories could be traced from the film records. The initial coordinates (x_o, y_o) and the coordinates (x,y) at time t are measured and fitted to the parametric equations

$$x = X(x_o, y_o, t) \tag{13}$$

$$y = Y(x_o, y_o, t) \tag{14}$$

Rectilinear components of the velocity are calculated by the equations

$$u = \frac{\partial X}{\partial t} \tag{15}$$

$$v = \frac{\partial Y}{\partial t} \tag{16}$$

The density may also be calculated as

$$\frac{\rho_o}{\rho} = \frac{x}{x_o} \begin{vmatrix} \dfrac{\partial X}{\partial x_o} & \dfrac{\partial Y}{\partial x_o} \\[2ex] \dfrac{\partial X}{\partial y_o} & \dfrac{\partial Y}{\partial y_o} \end{vmatrix} \qquad (17)$$

These techniques have been successfully used in laboratory measurements and are now being applied to the field test measurements from DIPOLE WEST. A paper presenting the theoretical background for this technique was presented at the 4th International Symposium on Military Applications of Blast Simulations at Foulness, England in 1974[36].

It is noted that the data reduction procedures for these measurements are complex and quite time consuming owing to the manual tracing of trajectories requiring frame by frame analysis of the film. However, particle velocity and density measurements are extremely elusive and at present, no better methods are in usage.

4.2.3 Charge Detonation Symmetry

Early-time observation of the charge detonation phenomena is recorded with ultra high-speed cameras operating in the speed range 2.5×10^5 to 5×10^6 frames per second. These very short interframe times on the order of a microsecond per picture are used to measure detonation velocity, detonation symmetry and relative temperature over the surface of the charge.

The average detonation velocity is calculated as the charge radius divided by the transit time of the detonation shock wave to the charge surface. This is conventionally

measured with an ionization probe (or probes) placed in and/or
at the charge surface to detect the detonation front arrival,
or through the use of photoelectric devices. Ultra high-speed
cameras are also useful for this purpose, and are sometimes
a valuable aid in evaluation of the data. In recent experiments
in which photoelectric measurements were made (i.e. to determine
detonation velocity), the photoelectric signal gave an anomalous
value for the average detonation velocity when one used the
nominal charge radius in the calculation. Photographic measure-
ments, however, indicated an asymmetry in the light breakout.
This fact led to the discovery that there was a non-uniform
construction of the charge in that the cap radius was 0.63
feet less than the nominal base radius. The average detonation
velocity was re-calculated and yielded an answer comparable to
that measured using ionization probe data. Therefore, ultra
high-speed cameras can give excellent results for detonation
velocity measurements[37].

The ultra high-speed camera is extremely helpful for
indicating the detonation symmetry by recording relative light
intensities that are proportional to temperature. Failure of
a detonator and other irregularities in the detonation are
readily detected which aid in interpretation and understanding
of an unexpected behavior or measurement. These records are
also very useful for future charge designs, as was the case
in the Pre Dice Throw series.

It has been mentioned that the relative temperature can
be inferred from the light intensity in various areas of the
charge (or fireball) surface. Relative temperature from one
test to another may be inferred in the same manner if the
records are made under controlled conditions (i.e. same exposure
time, f-stops distances, etc.). State-of-the-art techniques
permit absolute temperature measurements using blackbody
radiation assumptions.

94

A non-uniform breakout of the fireball from the charge surface is readily observed in the photographic records. As measurements are attempted moving closer to the source, effects of anomalous behavior are more pronounced. The insight provided by early-time photographic data is increasingly more valuable for meaningful interpretation of the data from the transducer signals recorded on close-in electronic channels.

4.2.4 Fireball Development

Photography of the fireball as it expands from the charge surface is of primary interest as it enables visual observation and study of the growth of anomalies as they develop into jets and irregularities that distort the symmetry of the blast wave.

The camera required for this application uses a wider field-of-view and a more moderate framing rate commensurate with the need for longer recording time. Framing rates and field of view are variable depending upon the charge size but are generally slower than required for early-time detonation studies. The rates may range from 250,000 frames per second requiring an ultra high-speed camera to 400 or less frames per second. Commonly, this coverage will utilize several cameras with various speeds.

The average radius of the fireball is readily measured from the film and may be converted to plots of radius and velocity versus time.

4.2.5 Crater Ejecta Trajectories

Crater ejecta studies are outside the scope of this study project but the application is mentioned here briefly because of the close relationship between different measurements using photographic techniques.

Typically 70 mm cameras are used to record the ejecta particles at framing rates on the order of 5 to 24 frames per second for about 30 seconds. In addition, short exposure times are used to stop the motion of the particles. The coordinates of ejecta are tracked and digitized as input to computer-aided data reduction that provides mathematical solutions of the position-time data yielding information on the origin, size, trajectory drag constant and drag coefficient.

4.2.6 Cloud Development

Photography of the cloud development and dispersion is generally covered with a combination of low-speed motion picture for early time formation followed with time-lapse photographs taken seconds and minutes apart. As with crater ejecta studies, the cloud development is not considered in the scope of this project as an air blast parameter and is included only to mention the various applications and measurements of the camera.

4.3 Summary

The equipment descriptions and applications as discussed in this supplement have been summarized in tabular form for convenient reference. The data in Table 1 are organized according to camera classification and lists important features of each type. Table 2 is oriented toward the air blast measurement and identifies the equipment often used for the various applications. It is understood that the information contained in Table 2 is quite general and subject to the variation of individual test conditions.

TABLE 1   CAMERA CLASSIFICATIONS AND CAPABILITIES

CAMERA CLASSIFICATION	MAXIMUM FRAMING RATE (fr/sec)	TOTAL FRAMES AT MAX FRAME RATE	CAMERA DESIGN	RESPRESENTATIVE CAMERA TYPES
Still, Time Lapse, Motor Driven	NA	NA	Mechanical Shutter	SLR, View Camera
Low Speed	5-400	NA	Intermittent Film Drive, Rotating Disc Shutter	Milliken, Locam, Hulcher
High Speed/Very High Speed	400-10,000 10,000-300,000	10,000 for Hycam 224 frames for Dynafax	Rotating Prism	Hycam, Dynafax, Fastax, Nova
Ultra High Speed	300,000-10^6	25 Frames	Rotating Prism	Cordin
	>10^6	3 Frames	Image Converter	Quad-Tran
		1 or 2 Frames	Image Converter	Cordin
		6 Frames	Kerr Cell Camera	Cordin

97

TABLE 2   PHOTOGRAPHIC APPLICATIONS

MEASUREMENT	CAMERA CLASSIFICATION	SPEED RANGE (FRAMES/SECOND)
Charge Detonation	Ultra High Speed	10^6
Fireball Development	Very High Speed High Speed	250,000 400
Shock Front Velocity and Profile	Very High Speed High Speed	250,000 400
Gas Particle Velocity & Density	High Speed Low Speed	400 5-24
Ejecta Studies	70-mm Low Speed	5-24
Cloud Development	Time Lapse Still 16-mm Low Speed	5-24
Documentary	4x5 Press Camera 35-mm Still 16-mm Low Speed 35-mm Low Speed	5-24

5.   EXTENSION OF CURRENT TECHNOLOGY

Consideration is given in this chapter to measures and development programs that show promise of extending the existing capabilities for measurement of air blast parameters with a moderate investment of resources. The suggestions are largely based on variations or modifications of currently available methods and instrumentation and are felt to be cost effective in relation to payoff on investment. Many of the ideas presented apply in a general sense to any measurement being made while others are specifically applicable to a particular measurement or sensor.

Primary recommendations in this chapter call for emphasis on the following items:

1. Workshops or symposia to encourage a spirit of cooperation and technological interchange between laboratories, government contractors, and agencies that are actively engaged in experimental air blast programs.

2. Dynamic field calibration of measurement system.

3. Dynamic laboratory calibration of pressure transducers at overpressure levels above 2000 psi.

4. Probe and mounting fixture design.

5. Mechanical and thermal protection of the transducers from the environment.

6. Development of pressure transducers and application technology for ranges 70,000 N/cm^2 (100,000 psi) and above.

7. Development of gas particle velocity anemometer with improved frequency response.

It is evident that Items 1 through 5 listed are applicable to the measurement of many of the air blast parameters discussed in this report; Items 6 and 7, however, are associated with the extension of development of two specific sensors.

Discussions of these recommendations and considerations leading to them are given in the remainder of Chapter 5.

5.1 Air Blast Instrumentation Workshops

Many persons who are involved with air blast measurements have been contacted during the course of this study project. From the ensuing conversations, it is evident that there is room for improvement in the intercommunication between these technical communities. One senses some degree of jealousy between laboratories that stems naturally from the competition for business, both in the private and government sectors.

Workshops and conferences can provide effective catalysts as well as a forum for exchange of experiences and techniques that are helpful to all. The spirit of cooperation is strengthened by the friendships that develop and are renewed during associations that accompany the group activities.

The DNA-sponsored D+60 instrumentation meetings following underground nuclear test events have demonstrated the viability of such a program. Contractors and various government agencies with many different private interests, many times in direct competition, joined together and freely discussed common problems and their solutions. One reason for the success of

these meetings: The attendees are largely those who actively participated in the experiment rather than administrators who often have a tendency to direct such meetings to political confrontations.

This recommendation is based upon the premise that much duplication of effort can be avoided by information exchange and new ideas will be triggered by group discussion of common problems.

5.2   Dynamic Calibration

While this report is not directed specifically at the problems of calibration, it has been observed that transducer and system calibration are a major factor.

An immediate enhancement of measurement capability is effected by improving upon the calibration accuracy. Both field and laboratory calibration methods are deficient in many areas of measurement. This is particularly true when considering the dynamic response of the transducer or measuring system because of the high levels of excitation required to simulate the blast environment to be measured.

5.2.1   Laboratory Calibration

With particular respect to pressure transducers, dynamic calibration is a problem. The principal methods in current usage employ shock tubes up to a maximum of approximately 1400 N/cm^2 (2000 psi) peak reflected pressure. Above this range, calibrated pentolite spheres are useful up to 8300 N/cm^2 (12,000 psi). Sandia Laboratories have developed a procedure for direct application of tamped sheet explosives (Deta sheet) to a transducer using a layer of felt between the diaphragm or

force-summing area and the explosive. Peak pressures of
17,000 N/cm^2 (25,000 psi) are generated by this method.
Both of the explosive procedures rely heavily upon repeatability
from charge to charge which is sometimes difficult to control.

The disagreement among the community regarding validity of
high overpressure dynamic calibration methods is an indication
of the confidence each has in the accuracy of another's
measurement.

While this presents a politically sensitive problem, a
step toward resolution and mutual agreement would be a program
of comparative evaluation by round-robin calibration of the
same transducers at the various facilities. This program could
also simultaneously compare the performance of transducers from
several commercial sources as well as special developmental
models such as the bar gage (AFWL), the fluid-coupled plate under
development at Sandia and others.

5.2.2 Field Calibration

It is well known that the end-to-end calibration of
measuring system installed in a field is not synonomous with
that of the sensor installed in the isolated laboratory environ-
ment in which it is usually calibrated. However, complications
of in-situ field calibration and the press of schedules in
preparation for the test execution often lead (or force) the
experimenter to neglect a dynamic calibration of the entire
measuring system.

Methods of data compensation have been shown to be effective
for certain situations where total system calibration is not
known but frequency response characteristics for component
elements have been determined[25]. These methods have not been
generally adopted and are not used to the extent they could be if

people had more confidence in the results and understood the limitations and capabilities of the procedure. When these and other data compensation methods are applied, it is strongly recommended that the unretouched data records be reported along with the final results. A complete description of the manipulations of the data helps the reader in his own evaluation of the measurement and validity of the compensation.

The recommendation is that more emphasis be placed on total system calibration and system response measurements in the field. This can be implemented by development of a capability to simulate the expected input stimulus with equipment. An example is a portable shock tube for pressure transducer calibration[38]. This approach is not always feasible; as an alternative (albeit less desirable), the dynamic sensor calibration is performed in the laboratory with the response of the rest of the measuring system carefully determined and data compensation methods applied when required.

5.3 Probe and Fixture Design

Pressure transducers with adequate range and dynamic response characteristics are available from commercial vendors up to 70,000 N/cm^2 (100,000 psi). The key to a valid pressure measurement lies in the correct selection of a probe and mounting fixture design to provide for placement of the sensing element in the flow with the desired orientation without disturbing the parameter to be measured. Poor correlation between similar measurements is sometimes traceable to differences in probe geometry that were initially believed to be unimportant. In other cases, this has not been shown but can only be speculated to be the cause.

Numerous instances were noted by the author wherein pressure measurements have been made using probes in supersonic flow conditions that have not been dynamically tested under conditions of use. A paucity of information exists from the transducer manufacturers who offer probes with factory installed sensing elements as a single package. Several probes are offered on the market and in common usage for which the aerodynamic response time is not known nor is the pressure distribution over the surface of the geometrical shape known.

It is probably not reasonable to expect a commercial vendor to have on his staff an aerodynamicist for probe design or have test facilities to verify the aerodynamic response of probe/ sensor packages. The responsibility is then imposed on the user to insure that the sensor is in fact properly applied in the field to measure the desired parameter. It has been observed that this responsibility has sometimes been avoided or side-stepped by assuming a design that might have worked well in subsonic flow would also be adequate in the supersonic regime.

It is suggested that wind tunnel and shock tube tests be conducted to characterize existing probe designs that are in current use. Such tests have been done for some probes such as the BRL total pressure probe shown in Figure 14 (also Reference 15) and the static overpressure probe described by Ruetenik and Lewis in Reference 22.

Of particular note is the Ruetenik and Lewis probe which is of the lollipop design but using two sensors, one on each side of the disc for an averaged measurement. Thus, when the probe is at an angle of attack the sensor on one side measures too high while the opposite side is too low giving a degree of self compensation.

In light of advances in pressure transducer technology
during the last ten years it seems probable that the Ruetenik
and Lewis probe design could be miniaturized to improve the
aerodynamic response time. An additional possibility would be
to relate angle of attack to the pressure ratio and difference
between the two sensors.

5.4   Mechanical and Thermal Protection

One of the major problems encountered upon placement of a
probe in an air blast environment is the protection from both
thermal effects and physical damage caused by the high energy
debris impacting the probe and/or active sensing area.

Protective measures in current usage are reported and
discussed in Chapter 3. Most of these are stop-gap measures
with varying degrees of influence on the frequency response of
the transducer. Along with the requirements to measure
parameters at higher overpressures and in more severe environ-
ments comes the need for more effective protection of the
measuring device.

The National Bureau of Standards has been pursuing projects
relating to transient thermal response and protection methods
for transducers. Much good information has been compiled and
methods developed as a result of this effort. Continued
support of this and similar projects is needed to extend the
capability for measurements in hostile environments.

While most of the emphasis is on pressure transducers, it
is pointed out that this recommendation applies generally to
protective measures for other types of instruments equally as
well.

5.5 Pressure Transducer Development

The upper range of commercially available pressure transducers is in the neighborhood of 70,000 N/cm^2 (100,000 psi). Current experimental programs indicate the desirability of measuring pressures up to 350,000 N/cm^2 (500,000 psi). This represents a giant step from present capabilities, both in sensor availability and measurement technique. It is probably possible to extend the range of the quartz pressure transducer to 140,000 N/cm^2 (200,000 psi) by adapting high strength materials in existing basic designs.

5.6 Advanced Gas Particle Velocity Anemometer

The vortex shedding anemometer (VSA) was developed for measurement of air particle velocity in an air blast environment (Reference Figure 20). Used in one event of the DISTANT PLAIN series the instrument performed very well and was subsequently used to obtain air particle velocity profiles in the conical shock tube facility (DASACON) at U. S. Naval Weapons Laboratory, Dahlgren, VA. The reduced data obtained on the DISTANT PLAIN event is shown in Figure 22[30].

Two notable limitations of the anemometer are found in the response time and the Mach number range.

The diameter of the vortex generator described in Reference 29 is 0.665 inch which determines the shedding frequency (f_s). The response time is not only dependent on the diameter (d) but also is seen to be a function of the free stream velocity (u) from the equation

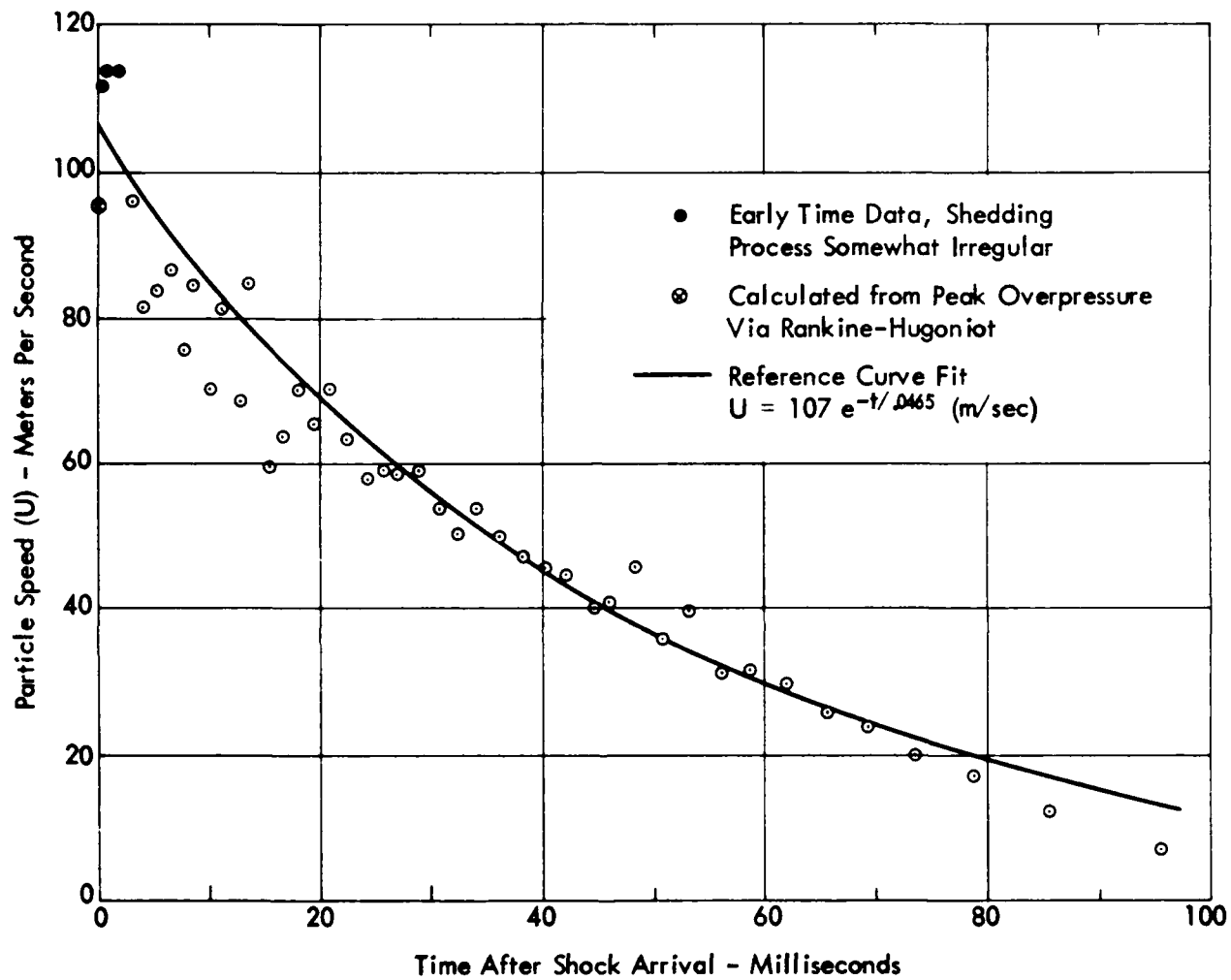$$f_s = S \cdot u/d \qquad (18)$$

106

FIGURE 22   PARTICLE VELOCITY COMPUTED FROM VSA
TRANSDUCER OUTPUT
(20 TON TNT CHARGE, RANGE = 149 m)

where the dimensionless number S is called the Strouhal number.
Clearly, the frequency is increased for a given velocity if
the diameter is reduced. While the velocity information is
recognized to be contained in the frequency, the amplitude of
the signal is speed dependent. Thus, as the diameter is
decreased, the sensitivity of the pressure transducer must be
increased. Transducer technology has advanced considerably in
the direction of smaller diameter and higher sensitivity since
the VSA was developed in 1966. It is technically feasible to
adapt presently available miniature pressure transducers to an
advanced model of the VSA. The immediate result would be to
improve rise time from an estimated 1 millisecond to perhaps
200 microseconds by use of a transducer similar to the Kulite
CQ-080 series which has 0.080 inch diameter. This would also
effectively lower the Reynolds number away from the critical
region to improve stability of the vortex shedding process
which should be helpful in extending the range of the instru-
ment.

In tests performed with the present instrument, there were
encouraging indications of velocity dependent wake fluctuations
at speeds in excess of Mach 1.0. These were masked by the
presence of a velocity independent signal in excess of 10 db
stronger than the one being observed. Spectral analysis was
required to establish the presence of the signal being used to
indicate velocity. By use of such devices as a tracking filter,
it is possible that continuously varying velocity dependent
signals could be selected in the presence of high background
interference. Techniques for data processing of this nature
would likely be most effectively utilized during playback of
recorded data from magnetic tapes.

Figure 23 contains spectral density plots of the VSA
output signal showing the progressive development of an inter-
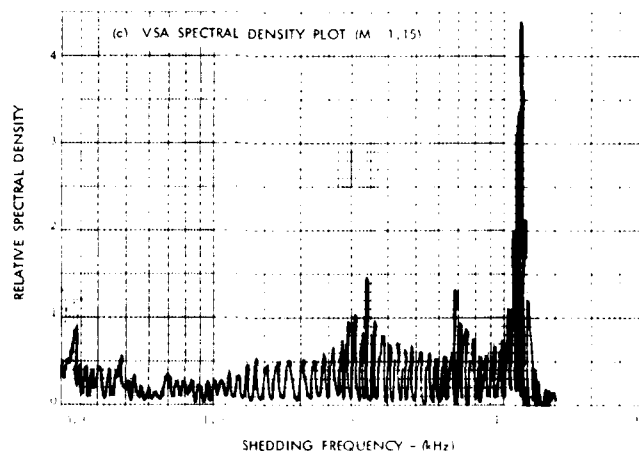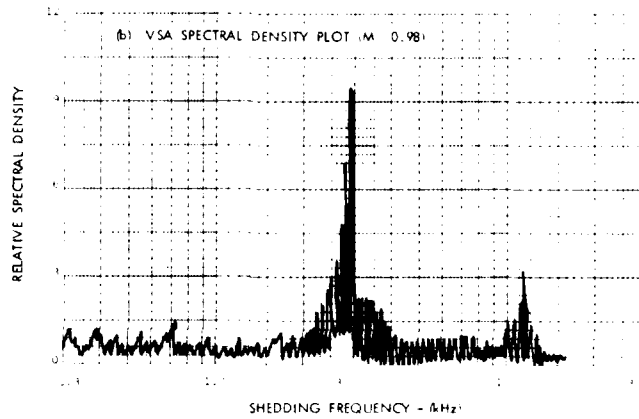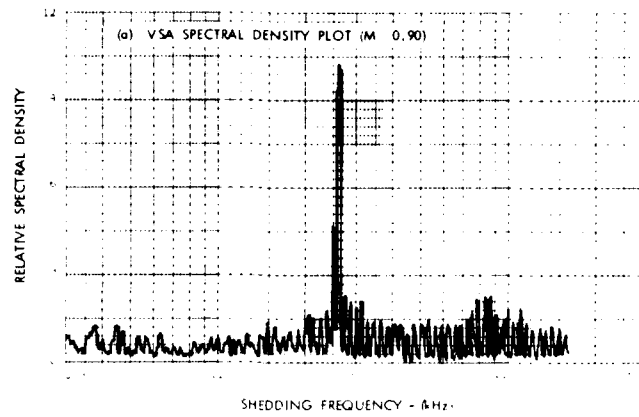ference signal as the Mach number is increased. Note the

108

FIGURE 23   VSA SIGNAL SPECTRUM FOR VARIOUS
MACH NUMBERS

109

total absence of any interference signal for M = 0.90, the
appearance of a weak signal for M = 0.98 and finally the
predominance of interference at M = 1.15. Although the
signal of interest is swamped out with the alien frequency,
it is possible, with spectral analysis, to observe the
3350 kHz element that is velocity dependent.

Improved frequency response is accepted as a realistic
design goal. Extension of the range to $M \geq 1.0$ is recognized
as an objective for which there is considerable question. At
the present time, not enough is understood regarding influence
of the bow shock on the vortex shedding frequency. The
mechanics of supersonic flow may very well restrict application
of the VSA to Mach numbers less than 1. It is recommended
that a significant effort be directed toward a better definition
of the vortex shedding process in the transonic region. Since
work of this nature tends to be highly empirical, these studies
should be complemented with experimental testing in the wind
tunnel.

In view of the satisfactory results obtained from
development of the existing anemometer, it is felt worthwhile
to investigate its properties and behavior more thoroughly.
In particular, its response to environmental conditions
(temperature, density, etc.) should be explored.

5.7 Summary

Chapter 5 contains a number of recommended activities
and programs that could lead to a moderate extension of
present capabilities in needed areas with a modest investment.
Certainly, the list could be extended, almost without bound,
and there is no question that many of the items would share

110

equal promise and priority with those found in Chapter 6.
One can presume that selected specifications for almost any
existing transducer could be extended by concentrated effort.
Some benefits will be more easily obtained than others.

The items suggested in this chapter meet three qualifica-
tions in common: The payoff will be cost effective, they
address a timely need, and the results can be anticipated in
a relatively short time frame.

Workshops and symposia are recommended as a means of
dispersing knowledge that is already known by some among
those interested and working in air blast.

Improved calibration methods are urged because most air
blast instrumentation, as it stands, has the stability and
performance capability to yield far more accurate measurements
if the overall dynamic calibration of the measuring system was
better characterized.

Probe and mounting hardware design is reccgnized as a
major factor in the application of a transducer to measurement
in the transient flow environment from an air blast. Two
serious problems in design of a measurement system are the
effect of the probe on the measurement being made and
protection of the sensor from physical damage by the environment.
It is observed that both of these aspects of the measurement
science could be improved within existing state-of-the-art to
effect an immediate advancement in air blast measurement
capabilities.

As the pressure measurements are attempted at even higher
and higher levels, the selection of available transducers
becomes more restrictive. There is an increasing requirement
to measure pressure at overpressure levels for which existing

sensors and probes are inadequate. In this area, as with others, the calibration and data interpretation are an integral part of the program to extend the measurement technology.

The direct measurement of gas particle velocity and density are important as they combine to provide an independent measurement of dynamic pressure. The beta-ray densitometer[27] and the vortex-shedding anemometer (VSA)[29] are suitable for subsonic measurements in clean air. A limitation of the VSA lies in its frequency response. Laboratory tests show promise that the frequency response could easily be improved and with a slim hope for measurements above $M = 1$.

6. NEW CONCEPTS

This chapter is devoted to consideration of concepts that might be applied to measuring air blast parameters by use of emerging new technologies or innovative application of existing technologies that show promise for improved or extended measurement capabilities. It is emphasized that these are only ideas that show promise with a preliminary investigation. A feasibility study is the next logical step to more fully investigate the application of any of the suggested concepts to the measurement being considered. The results of such studies will no doubt show some of the concepts worthy of development while indicating that others should be dropped.

Concepts presented in Chapter 6 are:

1. Laser-Radar Velocity Measurement

2. Self-contained Instrumented Drag Sphere

3. Microwave Densitometer

4. Ultrasonic Gas Particle and Sonic Velocity Measurement

5. Laser Gas Density Instrument

6. Shock Wave Front Temperature Measurement.

6.1 Laser Doppler Anemometer

Light that is scattered from a moving target will experience a frequency change, relative to the source, as observed by a stationary detector. This frequency change (Doppler shift) is linearly proportional to the velocity of the target. In the Laser Doppler Anemometer (LDA) the Doppler frequency is sensitive to the velocity of light

scattering particles in the air. By measuring the velocity
of the particles, the air velocity may be inferred. An
attractive feature of the LDA is that only a light beam
need enter the flow, except for the presence of the target
particles (which may already be present). No external probe
is inserted to perturb the flow field.

Calibration of the LDA is dependent on the laser light
frequency, optical geometry and the index of refraction of
the air. Relating target particle velocity to gas particle
velocity (u) further depends upon knowledge of the drag
coefficient (C_D) for the target.

The LDA has been widely used for measurement of velocities
in steady flow, such as a wind tunnel. While it is not
difficult to find questions that are unanswered and problems
as yet unsolved, the LDA does hold promise for velocity
measurements in the transient flow of an air blast. This
section presents with brief discussion two conceptual
configurations of the LDA. One concept is based on the use of
a laser to record velocities of wavelength size reflectors
which are accelerated by the shock wave. Figure 24 shows how
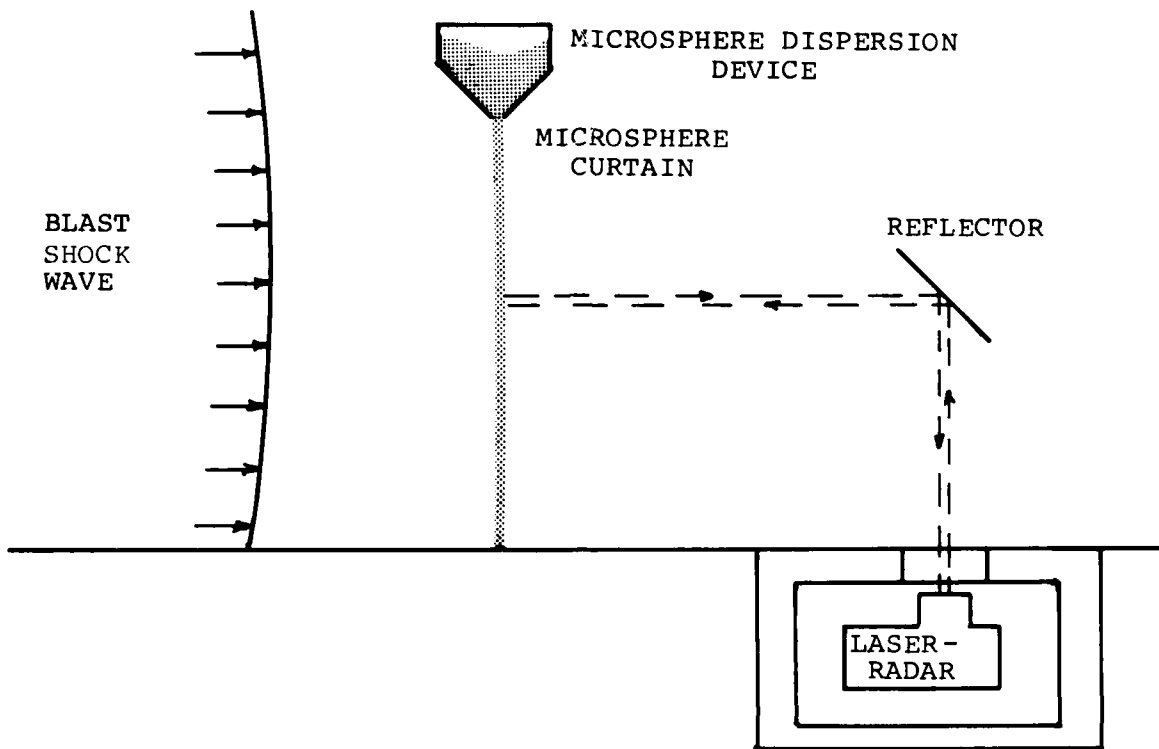such an experiment might be configured.

FIGURE 24   LASER-DOPPLER ANEMOMETER FOR AIR BLAST
            MEASUREMENTS

The laser targets are miniscule glass microspheres which
have been coated to provide high reflectivity at the laser
wavelength and are released from a container which is designed
to create a "curtain". These curtains can be placed at several
locations if desired. Microspheres are commercially available
in different sizes, density, and material. A critical factor
in selection is the ability to survive the passage of the
shock without fracturing. A typical glass microsphere has a
radius of 50 microns, density of 300 kg/m^3 and wall thickness
of 2 microns. A commercial source for microspheres is
Emerson & Cuming, Inc., Canton, Massachusetts.

Laser selection depends on microsphere radius but probably will be an infrared CO_2 continuous-wave type with a 10.6 micron wavelength. An interferometer type measurement will provide a Doppler signal whose amplitude is proportional to target velocity. Depending on overall geometry, two lasers and several detector stations might be used to get the microsphere velocity vector. Lasers and detectors will be placed in protective shelters. Data should be obtained until debris obscures the target view.

The relationship of the target microspheres to the air blast parameters may be estimated as follows. The drag force (F) on a particle which is immersed in a flow field which has a velocity relative to that particle is given by

$$F = C_D A q_p \tag{19}$$

where C_D - drag coefficient of target particle

A - presented area of particle

q_p - dynamic pressure relative to particle.

From Newton's Second Law of Motion we know that

$$F = m a \tag{20}$$

where m - mass of particle

a - acceleration of particle.

By combining Equations (19) and (20) and noting that the particle acceleration may be determined from the time derivative of the particle velocity we obtain

$$m \frac{d u_p}{dt} = C_D A q \tag{21}$$

116

where u_p - target particle velocity.

Now, the dynamic pressure experienced by the target particle is given by

$$q_p = \frac{1}{2}\, \rho\, (u-u_p)^2 \tag{22}$$

where
ρ - gas density at the particle location
u - gas particle velocity.

By substitution of the expression for q from Equation (22) in Equation (21), we obtain the desired relationship between gas particle velocity and the measured microsphere velocity.

$$m\, \dot{u}_p = \frac{1}{2}\, C_D\, A\, \rho\, (u-u_p)^2. \tag{23}$$

The drag coefficient and gas particle velocity are known to be time dependent as well as the microsphere velocity so that Equation (23) must be used with caution.

Equation (23) can be simplified during early time when the target particle velocity is small compared with the gas particle velocity. The equation is then approximated by

$$m\, \dot{u}_p \approx \frac{1}{2}\, C_D\, A\, \rho u^2 \qquad (u_p << u) \tag{24}$$

A more convenient form of this equation may be written in terms of the static overpressure (Δp_s) and flow Mach number (M)

$$m\, \dot{u}_p \approx \frac{1}{2}\, C_D\, A\gamma \Delta p_s\, M_2^2 \qquad (u_p << u) \tag{25}$$

where γ - ratio of specific heats c_p/c_v.

As an example, suppose the microspheres described earlier are used as the target and the air blast parameters are given as

$$\Delta p_s = 1000 \ (e^{-1000t}) \ psi$$

$$M_2 = 1.7$$

and $\gamma = 1.4.$

Using Equation (25) the target particle velocity versus time has been calculated and is plotted in Figure 25 up to the time when the target velocity has reached 10% of the gas particle velocity.
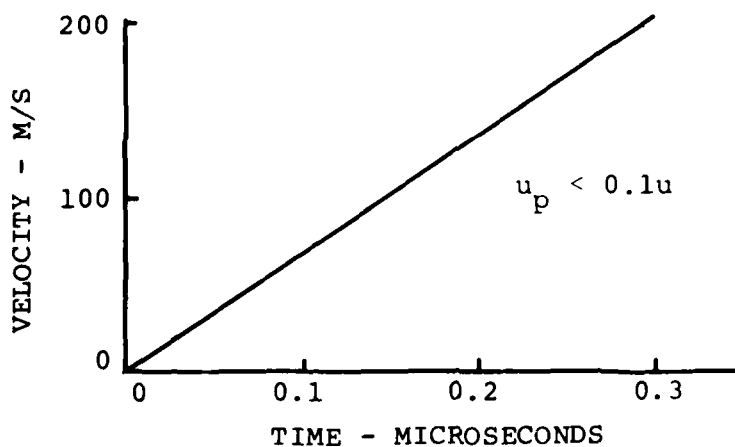

FIGURE 25   MICROSPHERE PARTICLE VELOCITY

The major conclusion of the data of Figure 25 is that the glass particles will be swept along immediately behind the shock having been accelerated to the gas velocity within a very few microseconds. Thus, the use of hollow glass microspheres permits a measurement of shock velocity.

118

From Figure 25, it can be seen that the laser detector bandwidth must approach 10 MHz to resolve this rapid acceleration with reasonable accuracy.

The major design considerations to be addressed with the LDA concept include the physical properties of the target particle (size, density, geometry, etc.) and development of an economical method of applying a suitable reflective coating. Other problems of significance are selection of actual laser hardware and optics, target scattering characteristics, and bistatic detector sensitivity requirements. The LDA system will be relatively costly and design of a blast hardened system for field application will insure not only the successful measurement but also the post-test survivability of the equipment for repeated use.

The laser-radar method described thus far will measure microsphere targets associated with the shock. There is need to measure particle velocity behind the shock at a stationary point in space as the blast wave moves by. A proposed method for accomplishing the latter is illustrated in Figure 26.
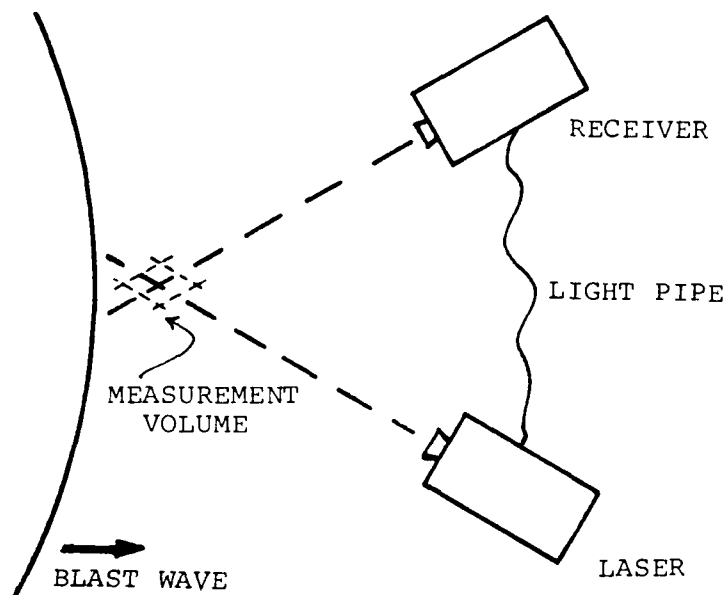
FIGURE 26 LASER REFLEFTION TECHNIQUE

In this scheme, the receiver will detect light scattered
by particles in the volume common to both the laser beam and
the well-collimated detector field of view. Receiver and laser
will be connected via a fiberglass light pipe to permit coherent
detection and Doppler velocities of particles to be measured.
The success of this technique depends both on the presence of
scattering material and good light transmission in the optical
paths which should present no problem in view of recently
developed measurement techniques for detecting turbulence and
atmospheric wind velocity by using backscattered light from
aerosols that are naturally present in the air[39,40].

This technique appears to be largely an adaptation of
recently developed technology to the transient air blast
measurement. The problems for primary consideration are light

120

absorption, refraction and scattering properties in and behind
the shock wave front which have direct bearing on its successful
operation. Development and packaging of a field-worthy design
is also a significant problem for optical systems of this sort
because of the mechanical stability required.

A variation on this laser anemometer would be the use of
a microwave system in place of the laser. Such a system could
be designed using frequencies that would provide useful data
after the optical path was obscured.

6.2 Instrumented Drag Sphere

The sphere has been used as a drag target in flow studies
for many years. High-speed photography of target trajectories
has also been used quite successfully. Neither of these two
techniques can be considered as new. Recent developments in
microcircuits have opened up the interesting possibility of
a self-instrumented drag sphere containing both measuring
transducers and a multichannel digital recorder.

Two techniques are suggested in this section: 1) A sphere
with an internal set of accelerometers and self-contained data
recorder or a UHF transmitter to telemeter data to a recording
ground station, and 2) An optical tracker or television-type
device viewing the sphere from the side to record the trajectory.
Both concepts center around measurement of the unrestrained
response of a drag sphere in the blast environment.

It is well known that the drag coefficient of spheres is
a variable with Mach number especially in the vicinity of
Mach 1[41]. Hoerner has provided data which are shown here in
Figure 27[42].

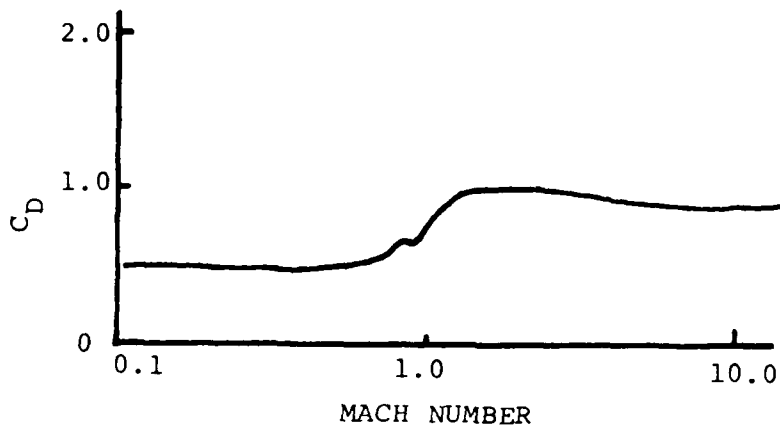121

FIGURE 27 SPHERE DRAG COEFFICIENT

These data, for high Reynolds numbers, indicate that with flows at $M_\infty < 0.6$ and $M_\infty > 1.7$, the assumption of constant drag coefficient is approximately true. Between those values, care must be used in experiment design and interpretation of the data.

A sphere with a set of accelerometers contained internally will continue to record data after the arrival of dust and debris has obscured the visual observation. It has been estimated that a sphere of 4 inches diameter has sufficient volume for accelerometers, batteries and a solid state recorder with enough memory capacity to store up to several seconds of data. This dimension could be even further reduced by a special purpose chip design effort. Such a course would be extremely expensive and should only be considered if a smaller sphere is seen desirable after initially testing and proving the value of the basic concept.

122

The last few years have seen vast changes in transient digital recorder technology. The development of advanced models of miniaturized recorders has been possible because of recent strides in microcircuit design. Consequently, it is feasible to consider packaging of a multichannel digital transient recorder in a drag sphere and to instrument that sphere with a set of accelerometers.

Similar self-contained instrumentation packages have been successfully applied to measurement of the acceleration experienced by 155 mm howitzer projectiles from launch to impact. This type of system has measured (and survived) peak accelerations of 1.65×10^6 m/s^2 (1.68×10^4 g)[43].

By adjustment or selection of appropriate density and area, a wide range of blast environments could be measured. It is estimated that by use of existing microcircuits, the total weight for a triaxial system would be 2 kg with 4096 samples (8-bit) per channel with a 4 kHz bandwidth. In consideration of the rapidly developing technology, it is probably not sensible to consider investment in a more advanced model at this time, because the current cost would be very high.

The recorder could be set to trigger normally upon command or to pre-trigger on the signal level. This mode of operation saves a predetermined number of samples that were taken prior to the time when the signal exceeds a set threshold value. After the test the sphere is recovered and the data are transferred to permanent storage for analysis.

The relatively light weight spheres from the example in Section 6.1 will be swept along by the shock wave thus providing a measure of the gas particle velocity directly behind the shock wave front. By using heavier particles (perhaps lead shot), velocity profile behind the shock could

123

be measured. The acceleration of such heavy particles by a
blast wave will provide data on dynamic pressure behind the
shock, but the measurement is complicated by uncertainties
associated with the establishment of gas flow around the
particle. Consider for example, the extreme case of a solid
tungsten sphere with a 2.54 cm radius. The velocity of the
sphere (u_t) in a blast wave with parameters used in the
example in Section 6.1 will be given by

$$u_t = 21.8(1-e^{-1000t})m/s$$

for the times during which the sphere velocity is low. Thus, a
heavy sphere will provide a good measurement of dynamic pressure
for many milliseconds into the wave, provided the aerodynamic
drag coefficient remains constant as assumed in the example.

Optical trackers are available commercially and function
via electronic servos to track angle positions of the target.
Accuracy is excellent and data would be good during the time the
optical path is clear. A television camera would provide
similar location data against a reference background grid; the
camera output would be recorded directly onto magnetic tape
for data analysis. Such tracking methods can be very effective
but are limited by the need for clear visibility of the target
and are subject to error from aberrations caused by viewing
through the shock wave front.

An alternative to the self-contained data recording method
might be to equip the sphere with a miniature UHF radio
transmitter and multiplexing system that would telemeter the
data to a ground station recorder. The self-contained
recorder, of course, obviates the problem of radio transmis-
sion through an inhospitable media.

Perhaps the most important factor for any of the drag sphere approaches lies in the analysis and interpretation of the measured data. The engineering problems associated with the design and fabrication of the system to measure and record the trajectory and response of the sphere involve relatively straightforward applications of existing electronic (and/or photo-optical) technology.

Problems to be considered are: High density packaging the electronics in a spherical configuration while maintaining the center of gravity at the geometrical center of the sphere, design of an omidirectional antenna for the transmitting sphere, signal processing circuits, etc.

6.3 Microwave Densitometer

A major problem associated with measurement of air blast parameters is the presence of dust and debris which is carried along a short distance behind the shock front. A significant proportion of the blast energy is contained in the accelerated debris; thus, to obtain a measure of the effective free stream dynamic pressure in that region requires a measurement of the density and velocity of both the debris and the gas.

Microwaves can be used to measure density, and possibly velocity, of a blast in which a significant percentage of dust is entrained provided the correct configuration is utilized. A proposed experiment layout is shown in Figure 28.
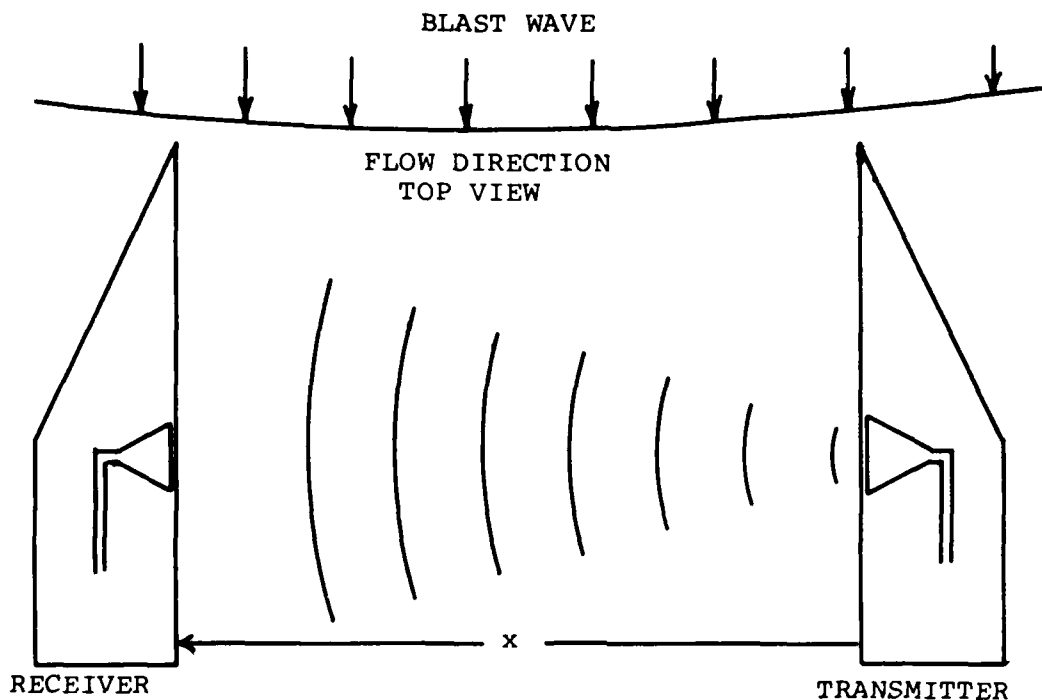
FIGURE 28 MICROWAVE TRANSMISSION MEASUREMENT

Several configurations are possible; the one shown may be advantageous because of the simpler electronics involved. Another configuration using a passive reflector and having one antenna for both transmission and receiving may be feasible also.

A measurement of both signal attenuation and path phase shift can be made with the setup shown according to the following expression

$$E_R = E_T \, G \, e^{-(\gamma x + j\omega t)} \tag{26}$$

E_R – received amplitude
E_T – transmitted amplitude

126

G - antenna design constants

γ - propagation constant = $\alpha + j\beta$

x - distance from transmitter

ω - angular frequency = $2\pi f$

t - time.

The flow variables are the attenuation per unit length, α, and the phase shift per unit length, β.

The attenuation will depend on several factors including dust particle density and particle size. Within physical size restraints, the particle size effect can be changed by changing wavelength of the transmitted energy. Provided sufficient energy is transmitted, attenuation should have little effect on β which is the variable parameter of interest.

Phase shift along a non-homogeneous transmission path depends on the particle material characteristics at the frequency used and on the particle size with respect to the wavelength. For small particles, with a fairly small loss tangent, the effect on the medium is that of increasing the average dielectric constant and hence slowing the microwave velocity. This is the expected effect of dust from soils which are sandy and dry. Using silicon dioxide as a representative material, Figure 29 illustrates relative phase shift due to debris levels up to 10% by volume (averaged over the path length) at a frequency of 1 GHz (λ_o = .3 meters).
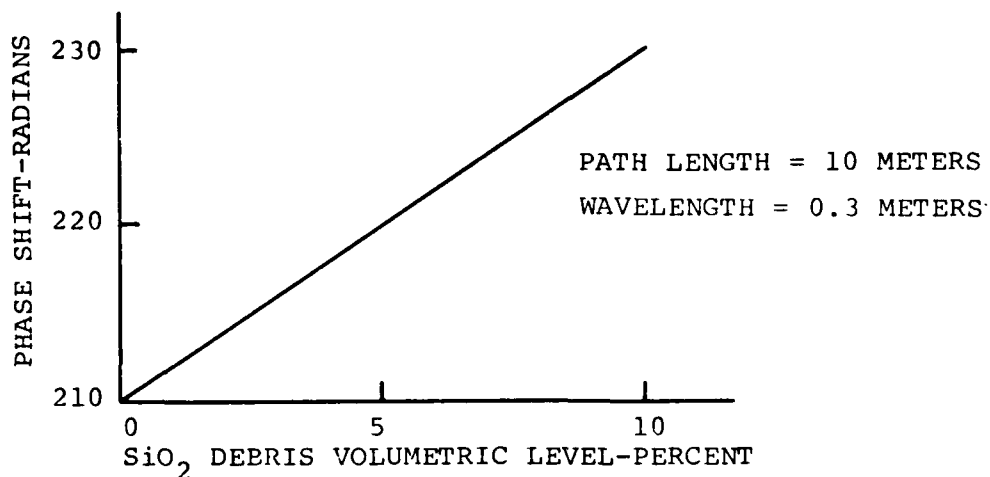
FIGURE 29   PHASE SHIFT VERSUS DEBRIS LEVEL

The sizable phase shifts shown in the figure indicate an
excellent resolution capability for this particular path length.
Shortening the path length to 1 meter will reduce the phase
shift scale by a factor of 10.

Since the microwave densitometer is also sensitive to gas
density, the measurement yields a net density that is determined
by the effective dielectric constant of the media in the
transmission path volume.

Another measurement using microwaves is that of using
debris particle backscatter to measure velocity by doppler
shift of the backscattered energy. The data obtained is
supplementary to the phase shift and would permit a separate
estimate of the kinetic energy of the dust and debris.

A simple laboratory setup could verify the feasibility of
the experiment just described. The design and implementation
of such an experiment utilizing poured fan-blown dust of differ-
ent particle sizes and compositions would help to assess the
merit of this concept.

The significant problems associated with the microwave
densitometer are related to calibration of the system because
the phase shift is a function of the media dielectric properties
which may be uncertain for a given field measurement. Parametric
calibration curves may be the answer by using particulate
sampling devices for post-test determination of calibration
factors. The design of hardware for the system is a fairly
straightforward problem using available technology and components.
Consideration is necessarily required for design of the aero-
dynamic shape for the antennae housings to insure that the flow
is not perturbed unnecessarily or in any unexpected fashion.
To reiterate, the success of this technique is heavily dependent
upon interpretation of the measurement.

6.4 Ultrasonic Measurement of Gas Particle and Sonic Velocities

The suggested measurement setup is shown in Figure 30.
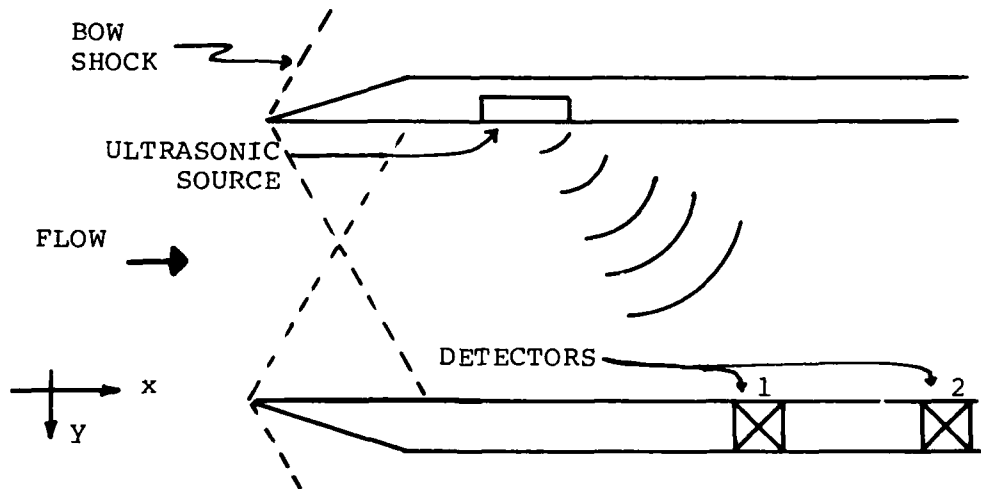
FIGURE 30   TEST GEOMETRY FOR GAS PARTICLE AND SONIC
VELOCITY MEASUREMENT

An ultrasonic source is mounted on a column and transmits atmospherically propagating waves which are detected by two detectors at selected locations. By a comparison of the relative phase of each detected signal both sonic velocity and gas particle velocity may be calculated. Sonic velocity permits an estimate of gas temperature and particle velocity is related to dynamic pressure.

A sinusoidal pressure wave (P) generated at the source propagates spherically according to the following equation:

$$P = P_o e^{-j(kr+\omega t)} \tag{27}$$

where

P_o - peak pressure

k - propagation constant of medium

r - total trajectory path length

ω - angular frequency

t - time.

For a low loss gas, $k = \frac{2\pi}{\lambda}$ and in a moving gas r would represent the total path length of a given pressure perturbation from a point on the source to a detector.

The wavelength (λ) depends on the frequency and on the sonic velocity in the gas over a wide range of gas conditions. The phase shift introduced by path length r depends on the sonic velocity and the magnitude of r. In the case for a moving medium, the distance may be evaluated from the vector equation.

$$r = \int_0^{t_n} (\vec{v}_q + \vec{v}_c) dt \tag{28}$$

where $\vec{v}_q$ - the gas particle velocity

$\vec{v}_c$ - the sonic velocity - the rate at which a pressure impulse moves from the source in still air

t_n - the time at which the impulse arrives at the nth detector placed at coordinates (x_n, y_n) with respect to the source $(0,0)$.

Considering only the two dimensional problem shown in Figure 30 at this time, we have

$$r = \int_0^{t_n} [i(v_{qx} + v_{cx}) + jv_{cy}]dt \tag{29}$$

and for non-varying velocities during the transit time

$$r_n = ix_n + jy_n = [iv_q + iv_{cx_n} + jv_{cy_n}]t_n \tag{30}$$

for the detector number 1

$$ix_1 + jy_1 = (iv_q + iv_{cx_1} + jv_{cy_1})t_1 \tag{31}$$

and the detector number 2

$$ix_2 + jy_2 = (iv_q + iv_{cx_2} + jv_{cy_2})t_2 \tag{32}$$

The positions (x_1, y_1) and (x_2, y_2) are known; t_1 and t_2 are measured from the phase of the detected signals. The result is an algebraic solution for the velocity components using the relaionship:

$$(v_{cx_1}^2 + v_{cy_1}^2)^{1/2} = (v_{cx_2}^2 + v_{cy_2}^2)^{1/2} = v_c. \tag{33}$$

131

In order to reduce the effects of variable velocity along the path, the distance from source to detector should be kept small. This also improves signal-to-noise ratio of the measurement. The frequency of the wave should be chosen to increase accuracy in the phase shift measurement.

Application of this technique in actual blast experiments will also be dependent on the effects of entrained dust and other debris which change radically the velocities calculated. Also, a high noise level background at the ultrasonic frequency of the source will reduce confidence in the results. However, even with background noise and dust, valid results should be obtained.

Further investigations are necessary into the impact of the ambient environmental conditions for the proposed application. Wideband measurements of background noise levels in proposed test environments are needed to determine not only the amplitude but also the spectral content of the transient noise.

Since dust appears to be a problem if sufficiently dense, a lab experiment similar to that proposed for the microwave technique should be considered, using dust showers or fans to generate this type of environment and to show feasibility.

While this concept has been presented with varied approaches before, it is introduced in this chapter because of the potential seen and the expectation that a fair research and development program is needed to perfect the system.

A similar system described in Reference 43 was used to measure flow Mach numbers of 3.26 and 2.70 at respective temperatures of $954^{\circ}C$ ($1750^{\circ}F$) and $1350^{\circ}C$ ($2460^{\circ}F$). The application described in the reference is for measurement of quasi-steady-state flow velocity from a rocket motor in an

experimental drag facility in which the composition of the exhaust products were well known.

Specific problems to be addressed for the ultrasonic measurement include the design of a sonic source, the detectors, system geometry and signal processing circuitry. While the design of electronic circuits requires no new technology and is a relatively direct problem in application engineering, the source and detectors required may well be quite specialized and as such are viewed as a major design problem. The sonic generator may be either pulsed or a continuous-wave discrete frequency device with detectors that are broadband or tuned to be frequency selective.

As with the other suggested measurement techniques, calibration, analysis and the data reduction/interpretation will be a significant portion of the development effort.

The use of multiple detectors may help to evaluate gradients within the test volume but the basic principle assumes uniform flow and a homogeneous media. For transient measurements, these assumptions certainly place restrictions on the application and limit the capability of such a system. These need to be investigated, carefully evaluated, and understood to assess the merits of this method of measurement.

6.5 Laser Gas Density Instrument

The basic idea on which the gas density instrument has been founded is that the index of refraction of air (n) is dependent on the density of the air (ρ)

$$n = n(\rho) \qquad (34)$$

Since this dependence is quite weak, it is appropriate to expand Equation (34) in a Taylor series in powers of the density. Doing so, one obtains

$$n = n(0) + k\rho + k_2\rho^2 + k_3\rho^3 + \ldots \tag{35}$$

The first term, $n(0)$, in this expansion is the index of refraction of a vacuum which is equal to 1. The terms involving the density to powers greater than the first are small except for exceedingly large densities. Thus, for a range of densities we have the following expression for index of refraction of air as a function of density.

$$n = 1 + k\rho \tag{36}$$

For air the constant k, which is known as the Gladstone-Dale constant, has the value $0.234 \, cm^2/gm$.

To study this dependence, consider an interferometer shown in Figure 31 with one arm exposed to the gas which is to have its density measured.
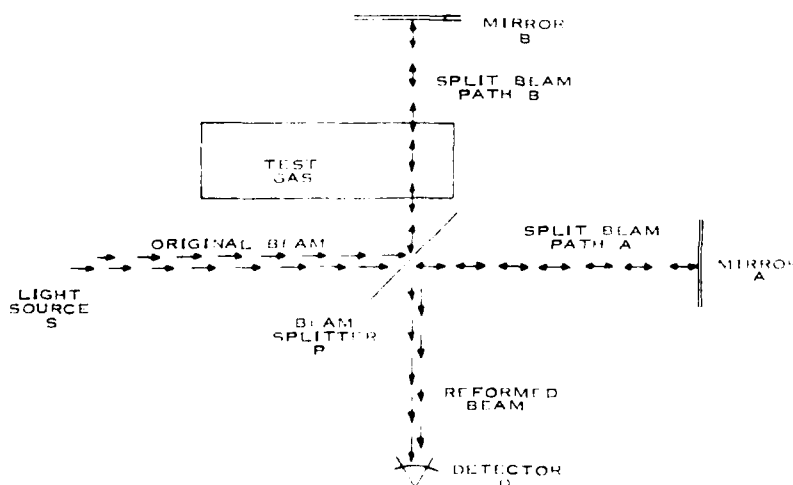
FIGURE 31 ALIGNED LASER INTERFEROMETER

134

As the density varies in the test arm, fringe shifts are observed by the detector. The number of fringe shifts (ΔN) observed for a change in the density ($\Delta \rho$) is given by

$$\Delta N = \frac{2kL\Delta\rho}{\lambda} \qquad (37)$$

where   k is the Gladstone-Dale constant

             L is the Length of the test arm

and λ is the wavelength of light produced by the source. One can obtain a feeling for the resolution possible with this sort of instrument by setting $\Delta N = 1$, choosing reasonable numbers for L and λ, and solving for $\Delta\rho$. In particular, using $\lambda = 6.328 \times 10^{-5}$ cm, the wavelength of the actual source used, and L = 12.45 cm, the length of the test chamber, one obtains a full fringe shift for a density change of 1.09×10^{-5} gm/cm^3, or more than 100 fringe shifts for a density change equal to one sea level atmospheric density.

As the density varies in one arm of a perfectly aligned interferometer, a single detector looking at the re-combined beam will see a single spot which blinks bright and then dark. Since this sequence is the same for both increasing and decreasing densities, such an instrument will provide ambiguous information as to the sign of the density change. To eliminate this ambiguity one might carefully misalign the interferometer (as in Figure 32). Having done this, the output of the optical system is, instead of a single spot, a fringe pattern of Figure 33. As the density varies, this pattern moves one way for a density increase and the other for a decrease. The sign uncertainty vanishes as one observes the direction of motion.
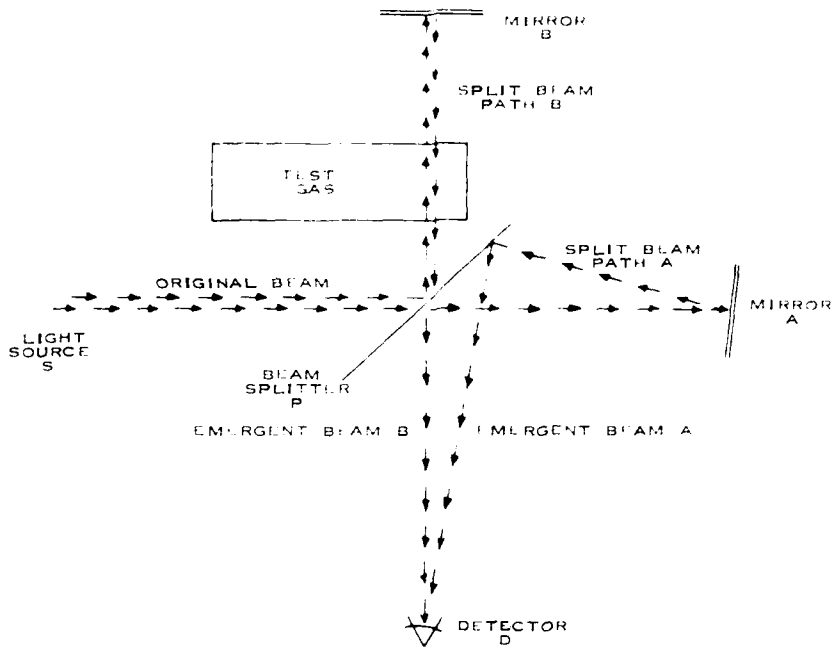
FIGURE 32   MISALIGNED LASER INTERFEROMETER

FRINGES MOVE LEFT
FOR DENSITY DECREASE

FRINGES MOVE RIGHT
FOR DENSITY INCREASE

FIGURE 33   FRINGE PATTERN FROM MISALIGNED INTERFEROMETER

136

The problem of automatically keeping track of the sign may
be handled as follows. A single photo detector observing the
interferometer output while the density varies will yield a
signal such as in Figure 34a. Suitably amplified and clipped,
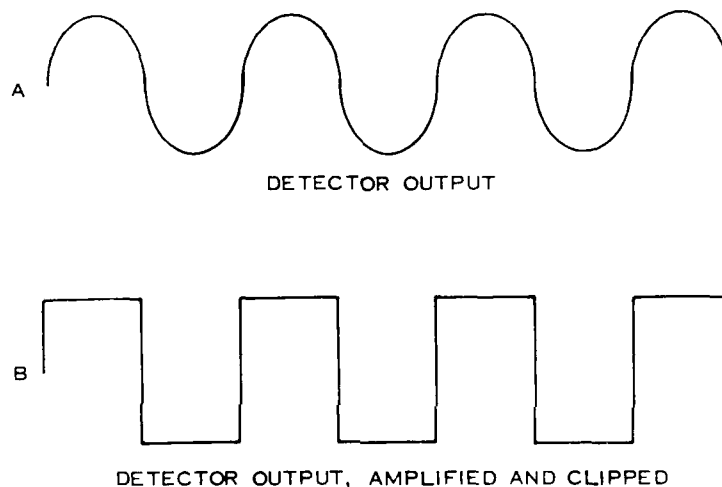this signal takes on the appearance shown in Figure 34b.

A

DETECTOR OUTPUT

B

DETECTOR OUTPUT, AMPLIFIED AND CLIPPED

FIGURE 34   FRINGE DETECTOR SIGNALS

If two detectors are placed less than a fringe width apart,
their outputs will have the appearance of Figure 35a when the
density increases, Figure 35b when it decreases.

137
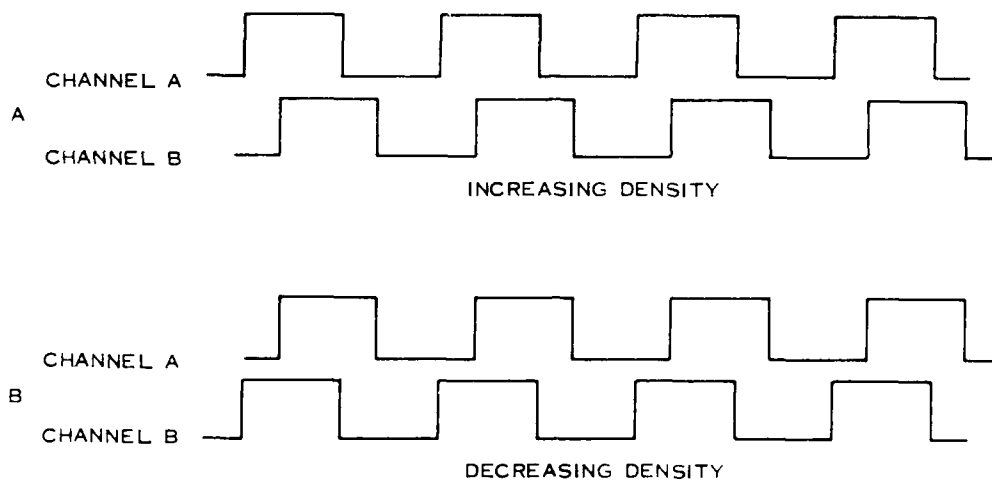
FIGURE 35   RELATIVE PHASE OF DETECTOR SIGNALS

One of these two signals (say Channel A) is now used to gate
two amplifiers. One of them is gated on when Channel A is in
its positive phase, the other on when A is in its negative
phase. The other signal is differentiated and clipped, leaving
only its leading edge, and then is fed to both amplifiers. One
amplifier now puts out a pulse when the density increases by
an amount corresponding to a single fringe shift. The other
puts out a pulse for a similar decrease. The output of one
amplifier is inverted, the two amplifier outputs are then
added and the coded density information is then presented as a
single signal.

The laser densitometer concept shown in Figure 36 has been
tested in controlled laboratory experiments[29]. The system
has not been developed to a field-worthy instrument and several
design problems remain unsolved.

At the outset of development of the densitometer, the goal
was to be able to follow a density change from 1 atmosphere to
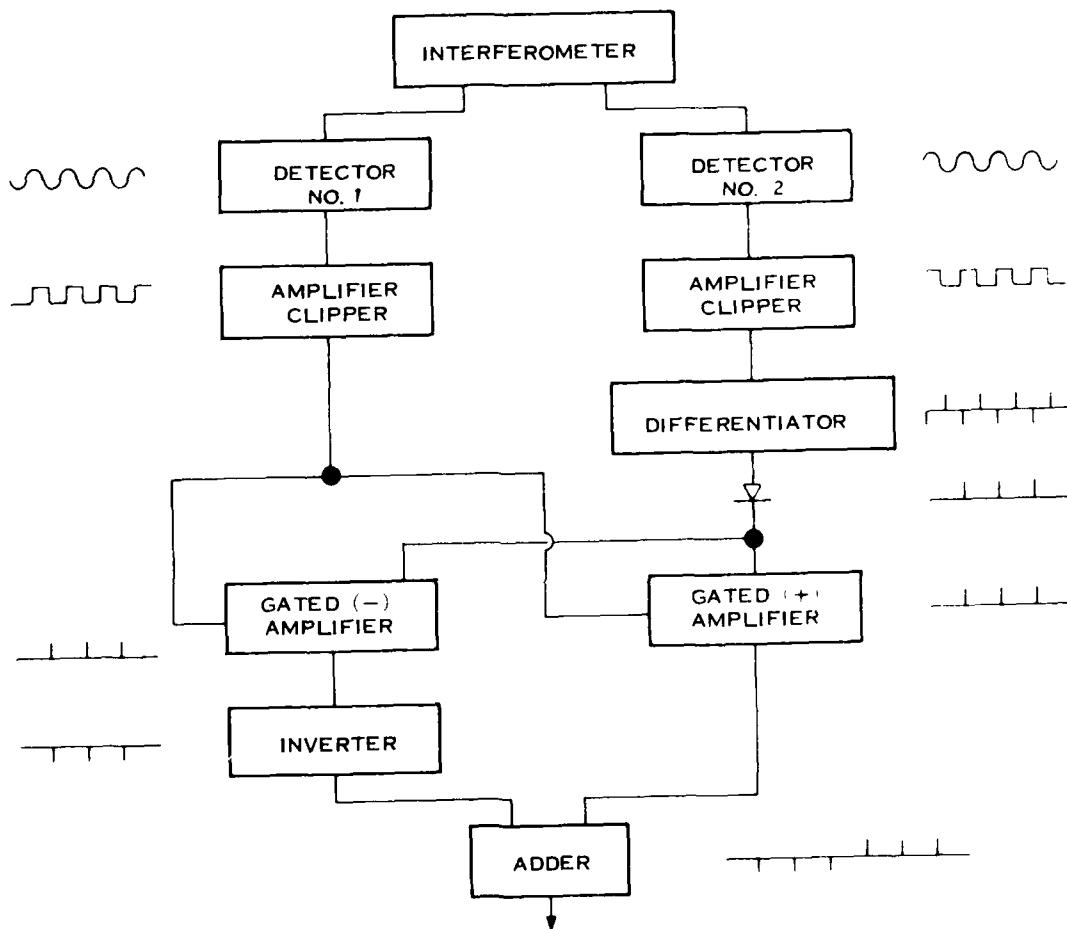4 atmospheres at sea level in 1 millisecond. Coupled with a

138

FIGURE 36 LASER DENSITOMETER BLOCK DIAGRAM

139

resolution goal of one hundredth of an atmosphere, this requires that fringes be accurately processed at a rate of 300,000 per second. This processing rate was not achieved except by stopgap methods which seriously degraded low frequency response. The problem appears to be a fairly straightforward electronics design problem.

The second major design question remaining unresolved is the packaging of the densitometer for field use. Because of the sensitivity of such a device to relative motion of its optical components, it is necessary that the package be extremely rugged. One version of the laboratory model was constructed so as to be able to withstand appreciable shocks without producing an output which looked like response to a density variation. This lends the encouraging feeling that sufficient ruggedness is attainable without undue mechanical design complications.

One solution to a potential mechanical design problem has been explored. In order to obtain sufficient resolution, the optical length of the sensitive arm is constrained to be of a certain minimum length. The difficulty in retaining internal rigidity increases at a rate greater than linear in the internal dimensions. With this in mind some effort was expended in folding up the optical path of the sensitive arm. This effort met with modest success, but needs further exploration.

The status of the densitometer is, in short, that a workable laboratory model has been constructed and that two well defined engineering problems lie between the present state of development and the production of a useful field instrument. Another problem that should be addressed is the influence of particulate matter in the flow whose dimensions are comparable to the laser wavelength. The calibration of the densitometer seems certain to be disturbed by these diffracting particles.

6.6 Gas Temperature Measurement

In nuclear weapons simulations utilizing underground tests or surface HE explosions, spectral emissivity data having good time resolution is desirable. These data, together with others, are used to characterize the temperature and geometry of the fireballs and shock wave in these events. The development and application of some simple, practical instrumentation to obtain these data are discussed in the following paragraphs.

6.6.1 The Value of Emissivity Measurements

Optical emissivity measurements have been used for a considerable period of time in diagnostics for nuclear weapon detonations. The blue-sensitive "bhangmeters" were one of the first sensors used, providing data which correlated well with yield and employed as one of the primary methods of measuring yield of events for a considerable period of time. Various filtered radiometers have been used to obtain spectral outputs of atmospheric nuclear events. The temperature of shock fronts has been determined using the spectral emissivity of the gases in the shock, together with pressure measurements. Both of these kinds of measurements are used primarily in experiments whose goal is to verify theories predicting the interaction of nuclear weapon energy with its environment. Capabilities for obtaining good optical data have been limited in the past by equipment limitations. The equipment is either large, bulky, and fragile with good spectral coverage or, relatively small, simple, and rugged with poor spectral coverage. For the small versions, in many wavelength regions, the response time was relatively slow.

Advances in optical component technology in recent years, in particular, have now made it possible to develop a series of very rugged, very fast response, narrow band radiometers. Very narrow fields of view are possible, permitting good spatial resolution and rejection of extraneous background energy. The shock front will probably not be very Planckian, but will instead obey the laws for high temperature gas emission. The theories which describe the emissivity of high temperature gases are quite complex because of the large number of transitions that contribute to photon emission. A number of simplified expressions have been developed, however, that are quite tractable. One of these is[45]

$$E_{eff} \simeq \frac{4.76 \times 10^7 \ hc \ E_O^4 \ (\exp \frac{E_O}{KT}) \ (2\delta\Psi\Phi q)}{26.4 (KT)^5 \ p}$$

where E_{eff} is the effective emissivity from a given transition

h is Planck's constant

c is the velocity of light

K is Boltzmann's constant

T is temperature

E_O is the dissociation energy of the molecule

δ is the thickness of the observed layer

Ψ is the concentration in molecules per air atom (temperature dependent)

Φ is the total oscillator strength

q is the ambient dynamic pressure, and

p is ambient undisturbed pressure.

This equation indicates that the effective emissivity is a function of temperature, pressure, the thickness of the emitting gas layer, the concentration of emitting molecules, the

oscillator strength of the molecules, and the energy associated with the particular transition which gives rise to the photon emission. For a given molecular transition, many of these parameters are fixed and the remaining ones which are variables are temperature, pressure, thickness of the emitting gas layer and concentration of the emitting molecules. If pressure is independently measured using fast response transducers, and if the composition of the air is determined using a gas chromatograph, and if thickness is established by the geometry of the experiment, then temperature will be obtainable from emissivity measurements. The geometry to be used is shown in Figure 37. It can be seen that if the radiometer is looking along a tangent to the spherical shock front, and that if the radial thickness of the front is greater than the diameter of the radiometer aperture, the maximum temperature of heated gas in the radiometer field of view may be determined with good accuracy. It is obvious, of course, that only the maxima of radiometer signals would be meaningful and that rapid response of the radiometers will be essential. The use of spectroscopy for gas temperature measurement is an old idea which has been described in the literature for the last several decades[46].

6.6.2 Signal Strengths

Some order of magnitude estimates of the signal-to-noise ratios which should be available were computed by using the expressions in Reference 45 to estimate the radiance of the heated gas and using the data on emission of the normal atmosphere from Reference 47. The results indicate that NO emission will provide signal-to-noise ratios of several hundred at temperatures above $3,000^O$Kelvin. The radiance falls very rapidly below this temperature, however, and useful optical output would probably not be obtained by the time the temperature has decreased to $2,000^O$ Kelvin. CO_2 emission is, of course, very strong in the infrared in the regions of 4.2

143

RADIOMETER
LINE OF SIGHT

SHOCK WAVE
FRONT

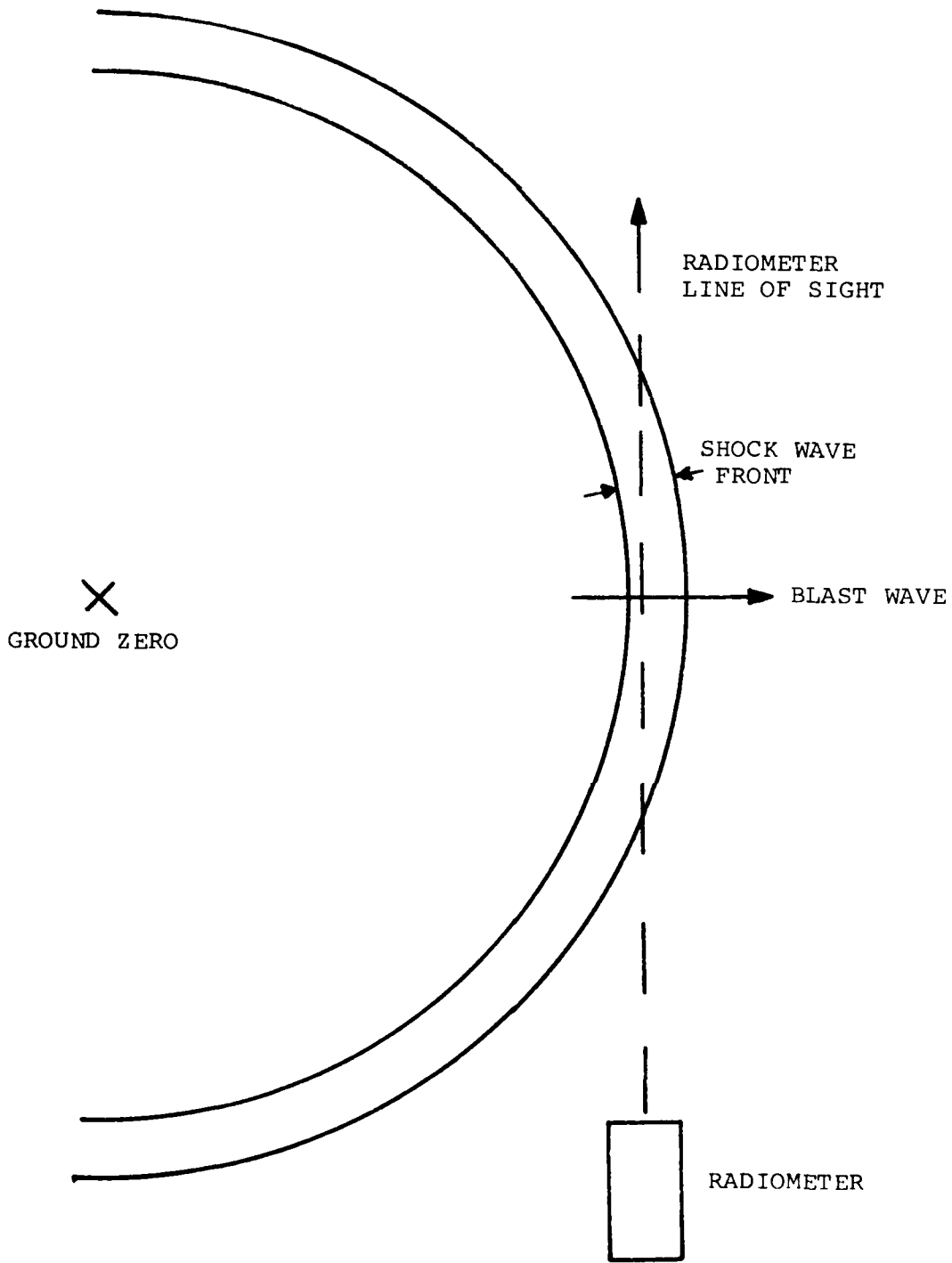BLAST WAVE

GROUND ZERO

RADIOMETER

FIGURE 37   BLAST WAVE GEOMETRY

144

and 2.6 microns. The expressions indicate that good signal-to-noise ratios (of the order of 20-150) would be obtainable using CO_2 in the temperature range from 600° Kelvin upward.

6.6.3 Applicable Sensor Technology

Suitable technology for the telescopes necessary for the radiometers has existed for some time. The nitric oxide radiation is in the visible and the CO_2 radiation is in the shorter wavelength portion of the long wave infrared region. Both reflective and refractive components are available in considerable variety. Multi-layer interference filters are available to establish optical bandwidths of these systems. The major difficulty in the past has been the lack of sufficiently fast detectors. Fortunately, there has been a concerted effort over the last few years to develop very high speed detectors for use in laser radars and laser communication systems. A number of solid state detectors are now available which are suitable for use in both the visible and infrared regions of the spectrum and which have response times of the order of nanoseconds or microseconds. A number of these were described in the recent IRIS Detector Symposium[48]. These references, together with our experience with other workers, makes it apparent that technology is available to permit the development and fabrication of a family of fixed optical bandwidth spectral radiometers which will permit high-speed measurement of the emissivity of shock fronts in certain spectral regions. This information can be used not only to assess the peak temperatures in the shock front (when combined with other data), but can also be useful when assessing the chemical composition of the shock front and/or fireball should this be desired.

The program should begin with a more detailed design study. This would define preferred spectral regions, photon fluxes, signal-to-noise ratios, etc. An important part of

145

this design study will be the engineering of the telescopes to
withstand the rigors of field deployment and blast wave exposure.
Tests of the prototype telescopes would be conducted using narrow-
band emitters such as gaseous discharge tubes. Spectral response,
noise, out-of-band rejection, and environmental responses will
be important parameters. The laboratory qualified prototypes
sould then be fielded to obtain the first actual shock front data.
These data would then be cross-correlated with other measurements
to assess the validity of the measurement.

The measurement concept presented has been developed and in
use for quite some time[49]. It is suggested that the technique
should be upgraded by incorporating the very recent developments
in narrowband detectors with rapid response. This will effec-
tively bring the useful lower temperature limit for such devices
perhaps as low as $300^{o}C$ for fast response measurement of peak
shock wave front temperatures at relatively low peak overpressures.

6.7 Experimental Facilities for Sensor Development

It is evident from the foregoing descriptions of suggested
measurement concepts and sensor developments that a good deal of
exploratory work is required before one could prove the feasibility
of each method. Also, in most cases, this exploratory work
includes testing of the conceptual hardware under dusty flow (or
artificial particle-laden flow) conditions; that is, under
conditions close to those which would obtain in the field. For
this purpose, it is desirable that laboratory facilities be
available where the hardware could be tested and evaluated. If
suitable facilities are not now available in the technical
community*, they would have to be designed and fabricated.

---

*No comprehensive survey of available candidate facilities was
conducted as a part of this study.

146

LIST OF REFERENCES

1. Lederer, Paul S. and Hilten, John S., "A Laser Technique
    for Investigating the Effects of Thermal Transients on
    Pressure Transducer Performance Characteristics," National
    Bureau of Standards, NBS TN 723, May 1972.

2. Hilten, John S., et al, "A Test Method for Determining
    the Effect of Thermal Transients on Pressure-Transducer
    Response," National Bureau of Standards, NBS TN 905,
    March 1976.

3. "Height-of-Burst Blast Effects in High Overpressures,"
    TRW Progress Report, TRW 20453-6004-TO-00, July 1972.

4. Carpenter, H. J., et al, "Blast Wave Boundary Layer Measure-
    ments," Air Force Weapons Laboratory, AFWL-TR-73-211,
    March 1974.

5. Abrahams, Rodney, "Effects of Laser-Generated Thermal
    Transients on Air Blast Transducers," Ballistic Research
    Laboratories, BRL MR 2473, April 1975.

6. Leisher, W. B., "Blast Pressure Transducer Use at Sandia
    Laboratories," Paper G4 Proceedings of 4th International
    Symposium on Military Applications of Blast Simulations,
    AWRE, England, September 1974.

7. Vortman, Luke J., Sandia Laboratories, Private Communication,
    Re: Pre DICE THROW I test.

8. Teel, George D., "Air Blast Measurements," Ballistic
    Research Laboratories, BRL R 1477, February 1970.

9. Teel, George D., "Air Blast Measurements from a 100-Ton
    TNT Detonation Over Granite - Mineral Rock Event, Mine
    Shaft Series," Ballistic Research Laboratories, BRL
    R 1502, October 1970.

10. Jaramillo, E. E. and Pozega, R. E., "Middle Gust Free-Field
    Data Analysis," AFWL-TR-73-251, April 1974.

11. Sachs, Donald C., "High Overpressure Air Blast Loading
    Tests on Cylinders," Kaman Sciences Corporation, KN-72-813/P ,
    (DNA 3062F), December 1972.

12. Glasstone, Samuel, The Effects of Nuclear Weapons, Published
    by USAEC, Revised 1962.

13. Kelso, Jack R., Editor, "Data Reduction Procedures for
    Nuclear Air Blast Instrumentation," Defense Nuclear
    Agency, AFSWP 1084, August 1959.

14. Giglio-Tos, Louis and Petit, Burnett A., "Middle North
    Series, Prairie Flat Event Fundamental Blast Studies,"
    DASA POR-2100 (WT-2100), March 1971.

15. Hoover, C. H., "Design and Calibration of a Large Aspect
    Angle Total head Pressure Gage," Ballistic Research
    Laboratories, BRL MR 2239, October 1972.

16. Gerber, Nathan, et al, "Particle Penetration Into Pitot
    Gages in Supersonic Dusty Flows," Ballistic Research
    Laboratories, BRL R 1677, October 1973.

17. Witherly, T. D., "Instruments for Measurement of Dusty Air
    Blast Effects in High Overpressure Regions," DASA 1433,
    September 1963.

18. Baker, Wilfred E., Explosions in Air, University of Texas
    Press, Austin and London, 1973.

19. Johnson, O. T., Patterson, III, J. D., and Olson, W. C.,
    "A Simple Mechanical Method of Measuring the Reflected
    Impulse of Air Blast Waves," Ballistic Research Labora-
    tories, BRL MR 1088, 1957.

20. Pope, Alan and Goin, Kenneth L., High-Speed Wind Tunnel
    Testing, John Wiley & Sons, Inc., New York, 1965.

21. Nelson, Wallace J., "An Improved Static Pressure Probe-Patent Application," NASA Case LAR-11552-1 (N75-10412), October 1974.

22. Ruetenik, J. Ray and Lewis, S. Dean, "Pressure Probe and System for Measuring Large Blast Waves," Air Force Flight Dynamics Lab, AFFDL-TDR-65-35, June 1965.

23. Jones, Howland B., "Effects of Tubing Connection on Transducer Response," Princeton University, AER No. 595a, January 1962.

24. Millman, Jacob and Taub, Herbert, Pulse, Digital, and Switching Waveforms, McGraw-Hill Book Company, 1965.

25. Bickle, L. W., "A Numerical Technique for Correcting Transient Measurements," Sandia Laboratories, SC-R-72 2601.

26. Swisdak, M. M., Jr., "Explosion Effects and Properties: Part I - Explosion Effects in Air," Naval Surface Weapons Center, NSWC/WOL/TR 75-116, October 1975.

27. Fenrick, W. J. and Campbell, B. R., "Canadian Blast Wave Density-Time Measurements on Event Dial Pack," Suffield Experiment Stations, Memorandum No. 89/71, July 1972.

28. Anderson, J. H. B., "Analysis of Blast Wave Density-Time Data from Event Prairie Flat and Event Dial Pack," Suffield Experiment Station, TN #309 (AD 905122), June 1972.

29. "Development of Air Blast Instrumentation: Vortex-Shedding Anemometer and High-G Accelerometer," DASA 2334, March 1969.

30. Sachs, D. C., "Field Test Particle Velocity Gage, Operation Distant Plain Symposium, Volume II," M. J. Dudash, Editor, DASA 2207, May 1968.

31. Baum, N. P., "A Radar Doppler System for DABS," University of New Mexico (CERF), 1975.

32. Hyzer, W. G., Engineering and Scientific High-Speed Photography, The Macmillan Company, New York, 1962.

33. Hyzer, W. G., Photographic Instrumentation, Science and Engineering, Its Military Equipments, Techniques and and Applications, Prepared Under Navy Contract NOW 63-0524F, October 1965.

34. Coulter, George A. and Peterson, Robert L., "Design of Aircraft Revetments," BRL MR 1440, October 1962.

35. Keefer, John H. and Reisler, Ralph E., "Multiburst Environment-Simultaneous Detonations Project Dipole West," BRL R-1766, March 1975.

36. Dewey, J. M. and Walker, D. K., "Simulation of the Blast Loading on Structures by Analysis of the Particle Trajectories in Two Dimensions," Paper G2 Proceedings of 4th International Symposium on Military Applications of Blast Simulations, AWRE, England, September 1974.

37. Personal communication, Mr. John Wisotski, Denver Research Institute, 1976.

38. Gill, Stephen P. and Gross, Michael B., "Dynamic Calibrator for Air Blast Pressure Gages to 10,000 psi," DNA 3920F, February 1976.

39. Cliff, William C., et al, "Wind Velocity Measurement," NASA Tech Briefs, Volume 1, No. 2, 1976 (pp. 182-183).

40. Coffey, E. W., et al, "Airport Laser Doppler," NASA Tech Briefs, Volume 1, No. 2, 1976 (p. 183).

41. Shapiro, A. H., <u>The Dynamics and Thermodynamics of Compressible Fluid Flow</u>, The Ronald Press Company, New York, 1958.

42. Hoerner, S. F., <u>Fluid Dynamics Drag</u>, Sighard F. Hoerner, 1968.

43. Wolf, Randolf J., (Kaman Sciences Corporation) personal communication.

44. Whitfield, M. L., et al, "An Experimental Drag Facility," DASA 1369, March 1963.

45. Penner, S. S., <u>Quantitative Molecular Spectroscopy and Gas Emissivities</u>, Addison-Wesley, 1959, pp. 393-445.

46. Loudenburg, R. W., Editor, <u>Physical Measurements in Gas Dynamics and Combustion</u>, Princeton University Press, 1954.

47. Valley, S. L., Editor, <u>Handbook of Geophysics and Space Environments</u>, McGraw-Hill Book Company, 1965.

48. "Meeting of the IRIS Specialty Groups on Infrared Detectors," IRIA-IRIS Proceedings, 5-7 March 1974. Office Naval Res. Inst. of Michigan, Report No. 107600-1-X, Paper Numbers 1, 6, and 23.

49. Kottenstette, James P., "Fast-Response Optical Pyrometer," ISA Transactions: 4(270-274) 1965.

50. Wells, P., Bathke, E. and Keeffe, R., "Calculation of Pitot, Dynamic and Reflected Pressures for Blast Tests," Kaman Sciences Corporation Memo, October 1972.

51. Liepmann, H. W. and Roshko, A., <u>Elements of Gas Dynamics</u>, John Wiley and Sons, Inc., New York, 1957.

APPENDIX A

IDEAL GAS RELATIONSHIPS BETWEEN AIR BLAST PARAMETERS

This appendix presents a number of relationships that are frequently used for defining the conditions at the shock wave front as well as the flow parameters as a function of time[50]. Many good references on air blast theory exist with derivations and discussion of the use and applications of the equations presented here[51,18]. The Rankine-Hugoniot equations of state provide the basis from which the unique relationships given are derived. Definitions for symbols used are found in Table A-1.

A.1 PROBLEM #1

Given the incident shock overpressure (Δp_s), calculate the peak Pitot tube pressure (p_{pitot}), the peak free-field dynamic pressure (q_2) and the peak reflected overpressure on a wall (Δp_r). These parameters shown pictorially in Figure A-1.

Assume one-dimensional flow, air behaves as a perfect gas with constant γ, the Pitot tube is aligned parallel to the flow, and the wall is perfectly rigid adiabatic, of semi-infinite extent, and aligned normal to the shock wave.

A.1.2 Analysis

The shock front velocity U_s is expressed by

$$U_s = c_1 \left[1 + \frac{\gamma+1}{2\gamma} \left(\frac{\Delta p_s}{p_1} \right) \right]^{1/2} . \tag{A-1}$$

Note that the quantity

$$\frac{p_2}{p_1} = \frac{\Delta p_s + p_1}{p_1} . \tag{A-2}$$

TABLE A-1 LIST OF SYMBOLS

Symbol	Parameter
c	Speed of sound
U_s	Shock wave front velocity
p	Absolute pressure
Δp_s	Static overpressure immediately behind the shock
Δp_r	Reflected overpressure at the reflecting surface
ρ	Density
T	Absolute temperature
u	Air particle velocity
M'	Pseudo Mach number for computational convenience
M	Mach number
M_s	Shock Mach number
q	Dynamic pressure ($q = 1/2\ \rho u^2$)
γ	Ratio of specific heats

Subscripts	Designation
1	Ambient conditions ahead of shock
2	Peak conditions just behind shock
s	Shock condition
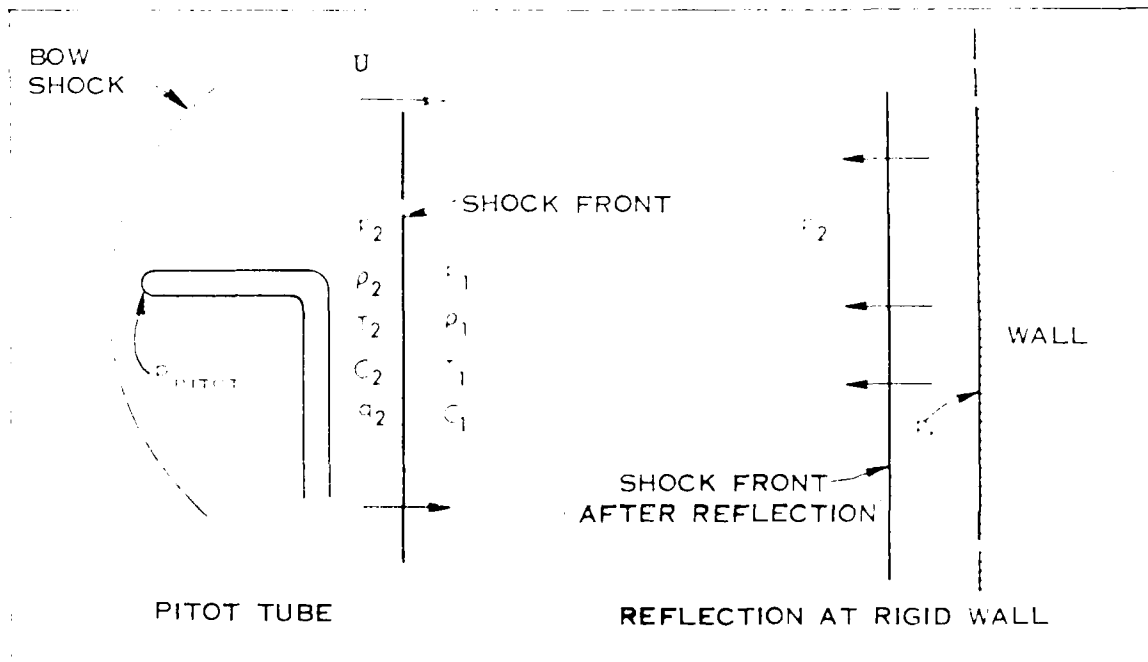
FIGURE A-1   DESCRIPTION OF TERMS, PITOT TUBE AND
            REFLECTED PRESSURES

We can now write the usual shock wave equations in our nomenclature:

$$M_s = \frac{U_s}{c_1} = \left[1 + \frac{\gamma+1}{2\gamma}\left(\frac{p_2}{p_1} - 1\right) \right]^{1/2} \tag{A-3}$$

$$M_2' = \frac{u_2}{c_1} = \frac{2}{\gamma+1}\left(M_s - \frac{1}{M_s}\right) \tag{A-4}$$

$$\frac{\rho_2}{\rho_1} = \frac{\left(\frac{\gamma+1}{\gamma-1}\right)\frac{p_2}{p_1} + 1}{\frac{p_2}{p_1} + \left(\frac{\gamma+1}{\gamma-1}\right)} \tag{A-5}$$

$$\frac{T_2}{T_1} = \frac{\left(\frac{p_2}{p_1}\right)}{\left(\frac{\rho_2}{\rho_1}\right)} \tag{A-6}$$

$$M_2 = \frac{u_2}{c_2} = \frac{M_2'}{\sqrt{\frac{T_2}{T_1}}} \tag{A-7}$$

Now for $M_2 > 1$

$$\frac{p_{pitot}}{p_1} = \left(\frac{p_2}{p_1}\right)\left[\frac{(\gamma+1)M_2^2}{2}\right]^{\frac{\gamma}{\gamma-1}}\left[\frac{\gamma+1}{2\gamma M_2^2 - (\gamma-1)}\right]^{\frac{1}{\gamma-1}} \tag{A-8}$$

156

and for $M_2 \leq 1$

$$\frac{p_{pitot}}{p_1} = \left(\frac{p_2}{p_1}\right)\left[1 + \frac{\gamma-1}{2} M_2^2\right]^{\frac{\gamma}{\gamma-1}} \tag{A-9}$$

$$\frac{q_2}{p_1} = \frac{\frac{1}{2} \rho_2 u_2^2}{p_1} = \frac{\gamma}{2}\left(\frac{p_2}{p_1}\right) M_2^2 \tag{A-10}$$

$$\frac{\Delta p_r}{\Delta p_s} = \left[\frac{\left(\frac{3\gamma-1}{\gamma-1}\right)\frac{p_2}{p_1} + \frac{\gamma+1}{\gamma-1}}{\frac{p_2}{p_1} + \frac{\gamma+1}{\gamma-1}}\right] \tag{A-11}$$

$$\frac{\Delta p_r}{p_1} = \frac{\Delta p_r}{\Delta p_s}\left(\frac{p_2}{p_1} - 1\right) \tag{A-12}$$

These values have been computed for p_2/p_1 values from 1.1 to 100 and for 3 values of γ (1.40, 1.35 and 1.30); the results are plotted and included in this appendix as Figures A-2, A-3, and A-4. Note that all pressures are absolute (except for Δp_r) and that all pressures are divided by the ambient air absolute pressure p_1.

A.2 PROBLEM #2

Given the pitot pressure (p_{pitot}) and static pressure (p_2) as functions of time, calculate the free-field dynamic pressure (q_2) as a function of time. The same assumptions and nomenclature as for Problem 1 apply here.
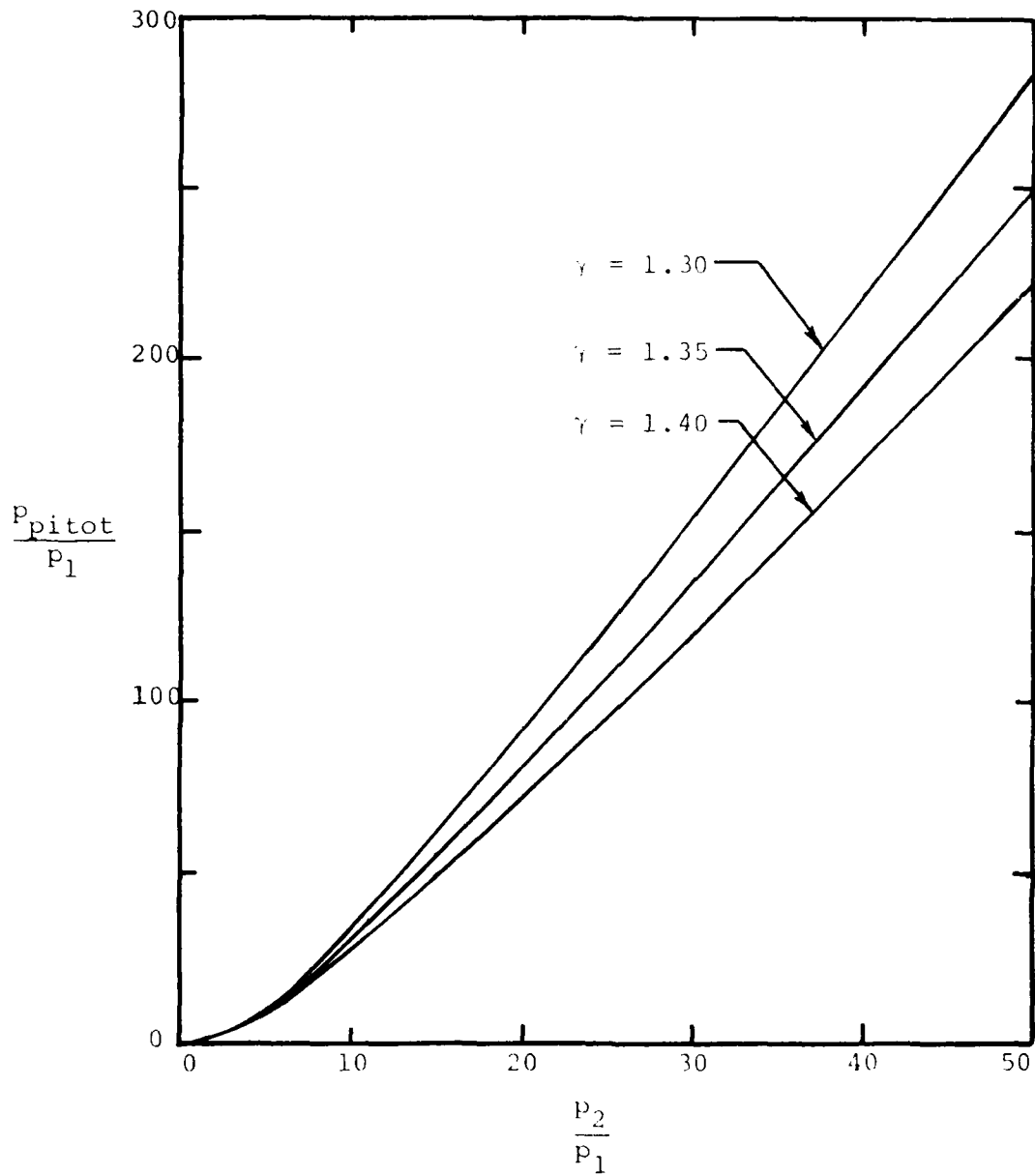
FIGURE A-2   PEAK PITOT TUBE PRESSURE VS. SHOCK STRENGTH
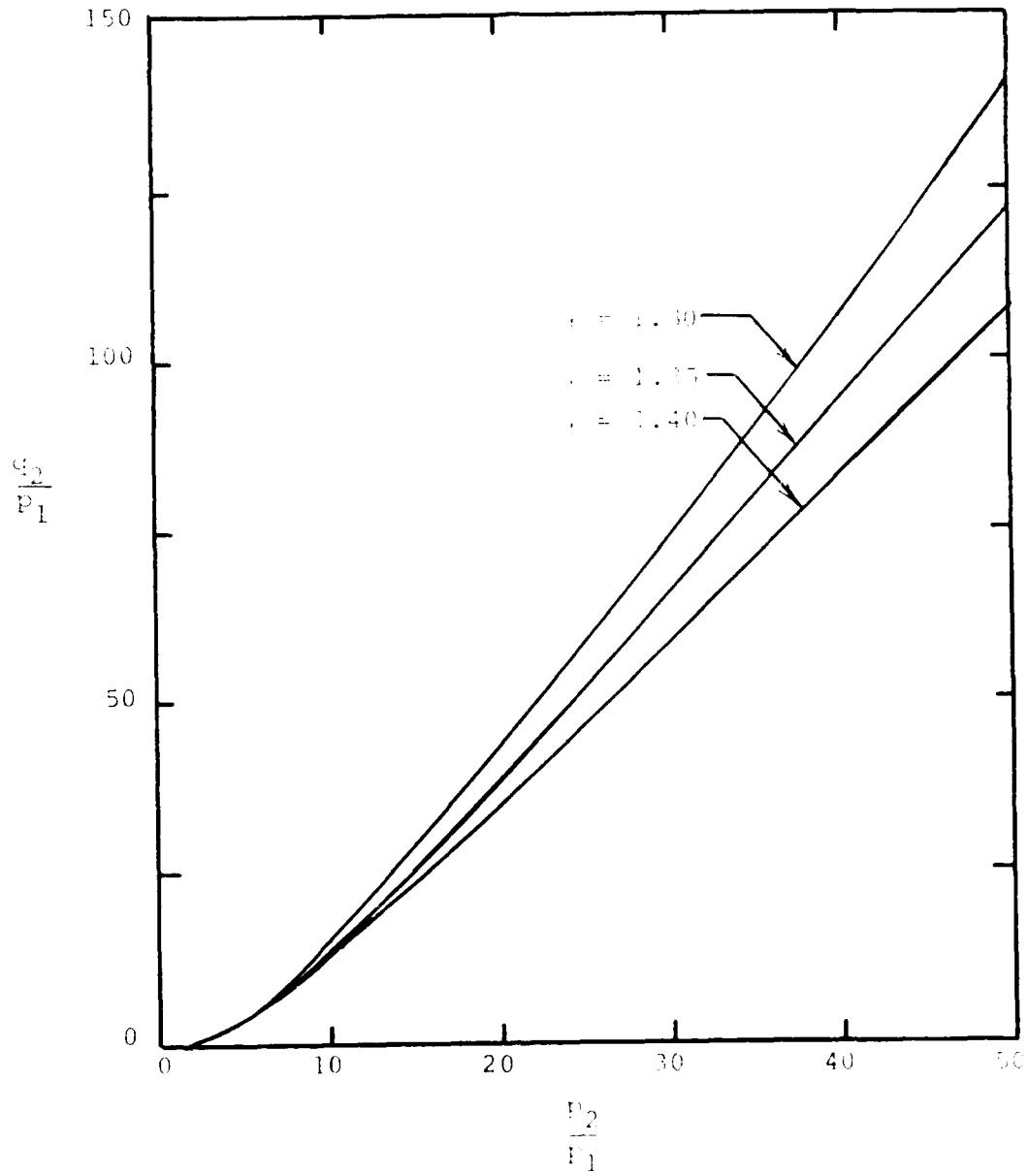
FIGURE A-3 PEAK FREE-FIELD DYNAMIC PRESSURE VS. SHOCK
STRENGTH
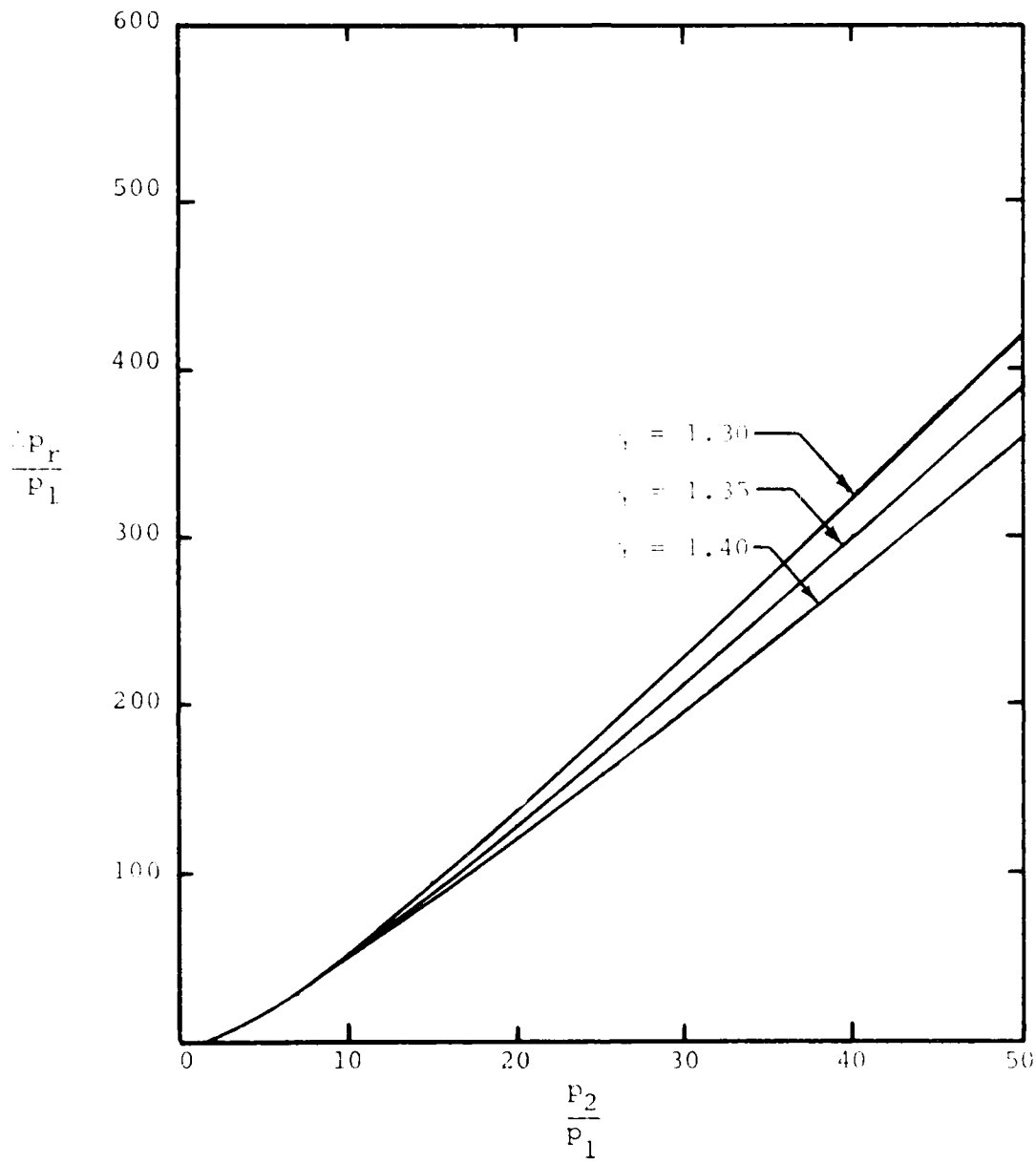
FIGURE A-4   PEAK REFLECTED PRESSURE FOR NORMAL REFLECTION
VS. SHOCK STRENGTH

A.2.1 Analysis

For $M_2 \leq 1$

$$\frac{p_{pitot}}{p_2} = \left(1 + \frac{\gamma-1}{2} M_2{}^2\right)^{\frac{\gamma}{\gamma-1}} \tag{A-13}$$

and if $M_2 > 1$

$$\frac{p_{pitot}}{p_2} = \left[\frac{(\gamma+1)M_2{}^2}{2}\right]^{\frac{\gamma}{\gamma-1}} \left[\frac{(\gamma+1)}{2\gamma M_2{}^2 - (\gamma-1)}\right]^{\frac{\gamma}{\gamma-1}} \tag{A-14}$$

In either case

$$\frac{q_2}{p_2} = \frac{\gamma M_2{}^2}{2} \tag{A-15}$$

21

   Figure A-5 is a plot of the free-field dynamic pressure
versus pitot tube pressure normalized to p_2 while Figure A-6 is
a plot of shock Mach number versus shock strength. Both sets
of curves are computed from the above equations.

   Note that both q_2 and p_{pitot} are divided by p_2, the local
static free-field pressure behind the shock (not the ambient
pressure).

COMMENTS

   The accuracy of these results relative to test situations
is critcally dependent upon how well all the assumptions of this
analysis are reflected in the actual test situation. For example,
if the air is not clean but is heavily dust laden, the pitot
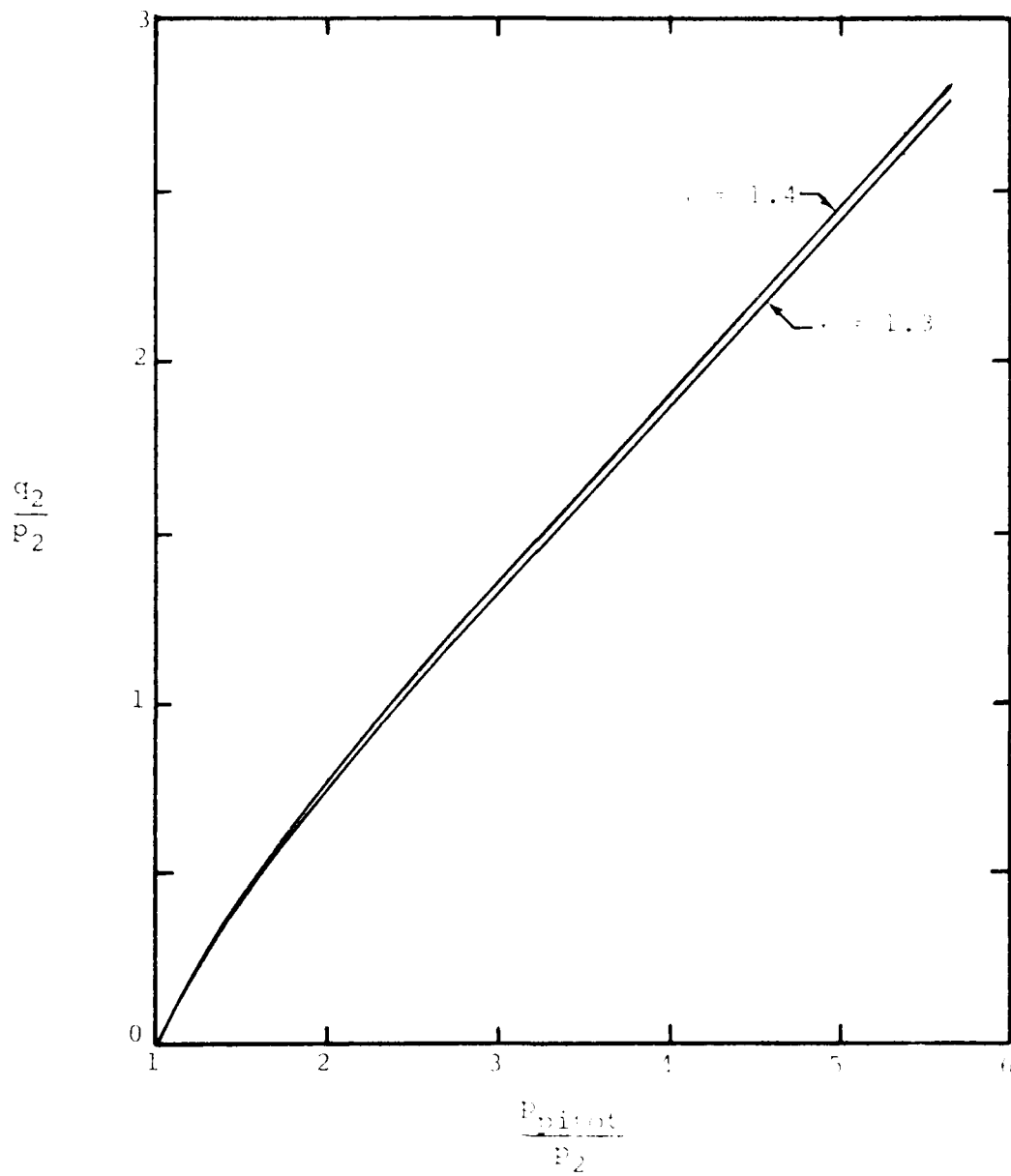
FIGURE A-5   FREE-FIELD DYNAMIC PRESSURE VS. PITOT
TUBE PRESSURE
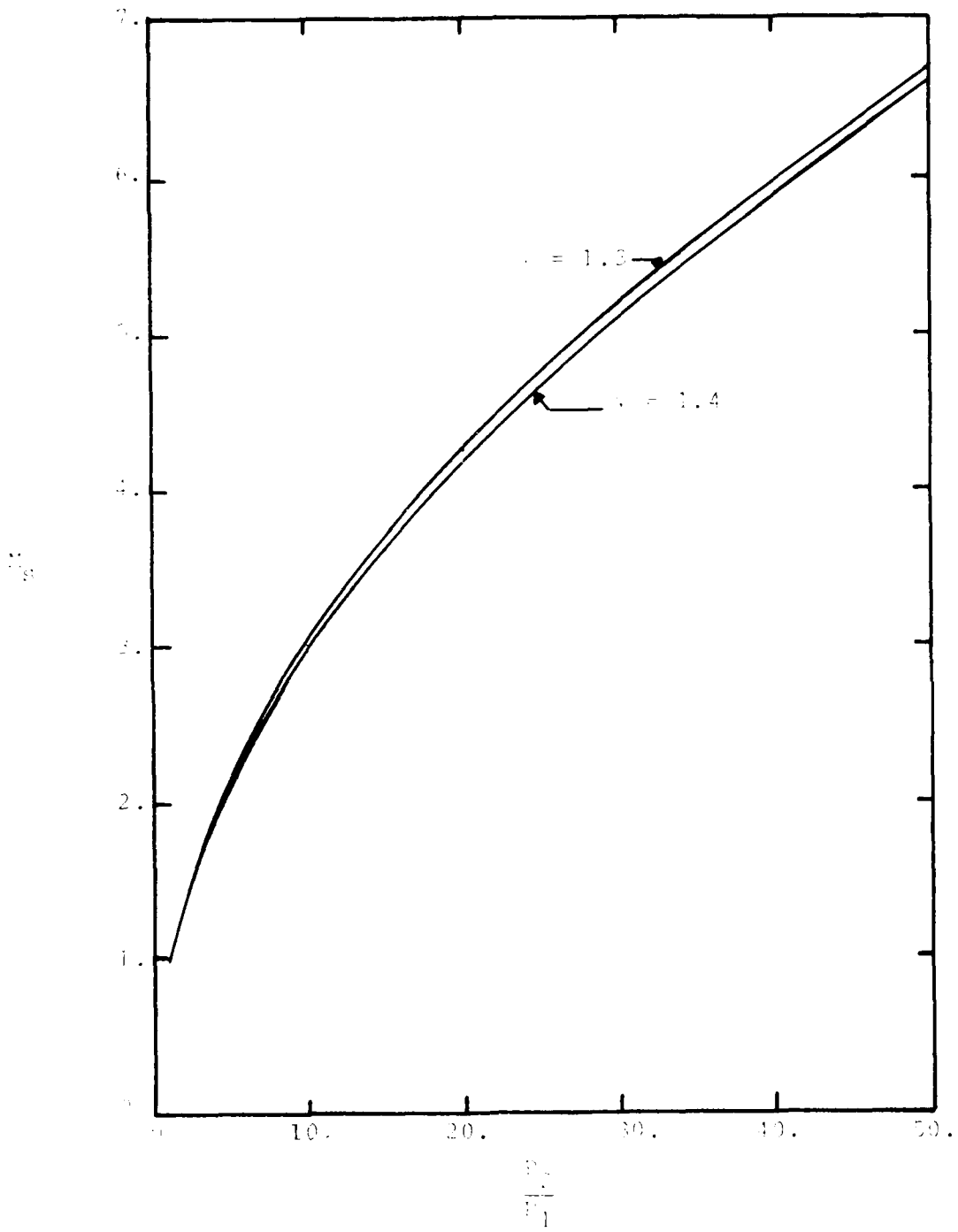
FIGURE A-6   SHOCK WAVE MACH NUMBER VS. SHOCK STRENGTH

163

tube is not properly aligned, the wall is not plane and of
semi-infinite extent, etc., all of these factors introduce
an unknown amount of error into the present results relative
to the real world situation.

A.3 FUNDAMENTAL RANKINE-HUGONIOT RELATIONS[18]

A.3.1 Conservation of Mass

$$\rho_s (U_s - u) = \rho_1 \, U_s \qquad (A-16)$$

A.3.2 Conservation of Momentum

$$\rho_s (U_s - u)^2 + \Delta p_s = \rho_1 U_s^2 + p_1 \qquad (A-17)$$

A.3.3 Conservation of Energy

$$\frac{1}{2} (U_s - u)^2 + e + \Delta p_s / \rho_s = \frac{1}{2} U_s^2 + e_o + p_1 / \rho_1 \qquad (A-18)$$

APPENDIX B

SELECTED TRANSDUCER SPECIFICATIONS

Included in this Appendix are specification sheets from several manufacturers that are representative of commercially-available pressure transducers being used for air blast measurements.

The inclusion or omission of transducers or sources is not intended as endorsement or rejection by the authors or any agency of the U. S. Government.

Contents of Appendix B

TRANSDUCER	DESCRIPTION	DIMENSIONS

LC13
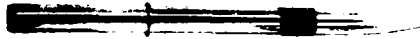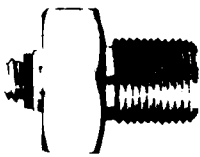
These aerodynamically shaped units can be used to record a variety of dynamic pressure phenomena which typically are found in free field blast measurements and shock tunnel pressure-time profiles. The pointed shape allows the units to measure the side-on pressure of shock fronts with velocities as high as Mach 3 for the LC 13 and Mach 5 for the LC 33. The transducer sensitivity is not seriously affected by misalignments of as much as 25 degrees. In pairs, the units can be used to measure shock front velocity. The units are provided with a four point calibration.

LC33

LD25

The flush-mounting transducer is the economy model for various measurements of dynamic pressure and acoustic phenomena. The low cost makes it ideal for expendable applications or simple triggering of photographic and recording apparatus. The LD-25 has been used in shock tunnels for high pressure transient to low pressure applications including underwater acoustics and flow measurements. The LD-25 is supplied uncalibrated for those utility requirements at a budget price.
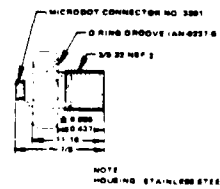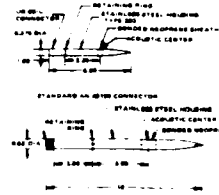
MODEL	CAPACITANCE	VOLTS PSI	CHARGE SENSITIVITY p.c.	SENSITIVITY db re 1V/μb	MAX USEABLE PRESSURE RANGE PSI	RISE TIME FACE ON MICROSECONDS
LC13	1750	.3	610	-107	500	10
LC33	4500	.67	3150	-101	500	15
LD25	240	.15	35	-113	3000	1
					*10,000	

*Special Order
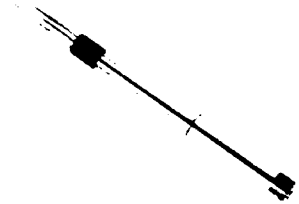
celesco

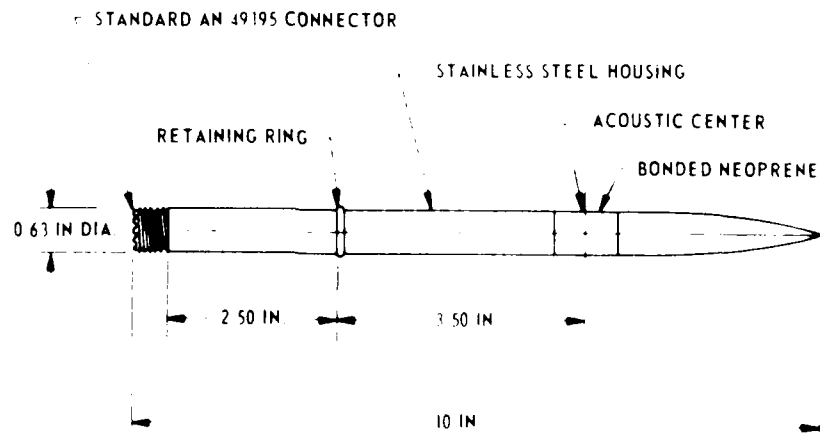Formerly Atlantic Research Systems Division

166

FEATURES

- HIGH SENSITIVITY
- AERODYNAMICALLY-SHAPED
- INDIVIDUALLY CALIBRATED

DESCRIPTION

The LC 33 pencil-type Pressure Transducer can be used to record a variety of dynamic pressure phenomena which typically are found in free field blast measurements, shock tunnel pressure-time profiles. The ogive point allows the LC-33 transducer to penetrate and measure the side on pressure of shock fronts with velocities as high as Mach 5. In shock wave measurements the transducer should be pointed toward the source of the blast wave. However, this alignment can be off as much as 25 without affecting the sensitivity (+2%). The LC 33 piezoelectric transducer is designed for use in air but the sensitive element is sealed in a watertight neoprene covering. The 4500 pF capacitance is extremely high for a transducer of this size and allows it to be used with a minimum amount of associated electronic signal conditioning equipment. In the event that a long cable is required between the transducer and a recording apparatus, a high input impedance, low noise preamplifier should be used. Suitable preamplifiers are available from Celesco Industries. A four point calibration is provided with each transducer.
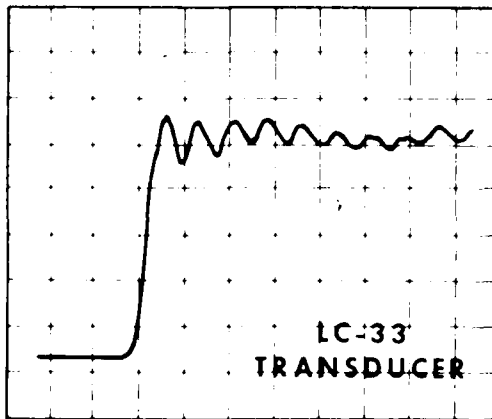
DESIGN DRAWING

STANDARD AN 49195 CONNECTOR

STAINLESS STEEL HOUSING

ACOUSTIC CENTER

RETAINING RING

BONDED NEOPRENE

0 63 IN DIA

2 50 IN   3 50 IN

10 IN

*CONNECTOR NOT WATERPROOF

SPECIFICATIONS

Sensitivity: 0.67 V/psi
Sensitivity: -101 dB
Charge Sensitivity: 3000 pC/Psi
Capacitance: 4500 pF
Maximum Pressure: 500 Psi
Resonant Frequency: >67 kHz
Polarity with Positive Pressure: Positive
D.C. Resistance (MIN): 2500 MΩ
Operating Temperature Range: −40 to +212″ F
Thermal Sensitivity: 0.25%/″F
Overshoot: 20%
Total Weight (MAX): 8.6 oz
Sensing Element: Lead zirconate titanate

Grounding: Case grounded
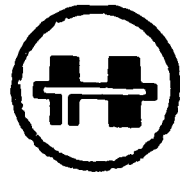**Connector Required:** Standard UHF Coaxial

ORIENTATION . . . . . FACE ON

MEDIUM . . . . . NITROGEN GAS

PRESSURE . . . . 38 PSI

VERTICAL . . . . 5.0 V div

HORIZONTAL . . . . 0.02 ms div

TYPICAL PRESSURE-TIME PROFILE

KULITE SEMICONDUCTOR
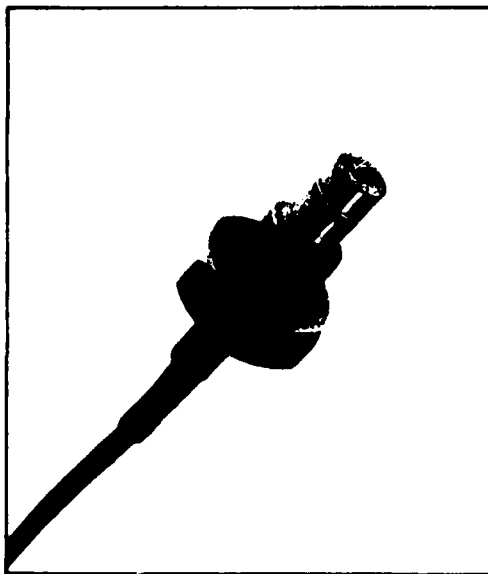
HIGH PRESSURE IS™ TRANSDUCERS

HKM-375 SERIES

- Metal Diaphragm
- Integrated Sensor (IS)
- Easy Installation
- High Natural Frequencies
- ⅜-24 NF Thread

The HKM-375 miniature pressure transducer is a metal diaphragm unit using an Integrated Sensor (IS) as its sensing element.

The ⅜ - 24 NF thread with the hexagonal head and "O" ring seal make the HKM-375 series easy to mount and simple to apply. In addition, the small size, flush diaphragm and robust construction enable installation into pressure container walls and standard AND 10050 fittings, eliminating costly space-consuming hardware.

The heart of the HKM-375 is the Kulite Integrated Sensor. It consists of a miniature silicon member on which a Wheatstone bridge has been atomically bonded using diffusion techniques.

These devices combine the major advantages of microcircuitry: substantial size reduction, excellent repeatability and reliability, low power dissipation, etc. The miniaturization process also yields

a marked increase in the natural frequencies of the transducers making them suitable for shock pressure measurements.

High output and low impedance inherent in piezoresistive sensors make these transducers ideal for use in hostile environments and obviate the requirement for expensive signal conditioning equipment, such as charge amplifiers and impedance matching devices.

The HKM-375 transducer utilizes a 17-4 PH stainless steel diaphragm and threaded body, making it suitable for use in pressure media compatible with stainless steel and the "O" ring used for sealing.
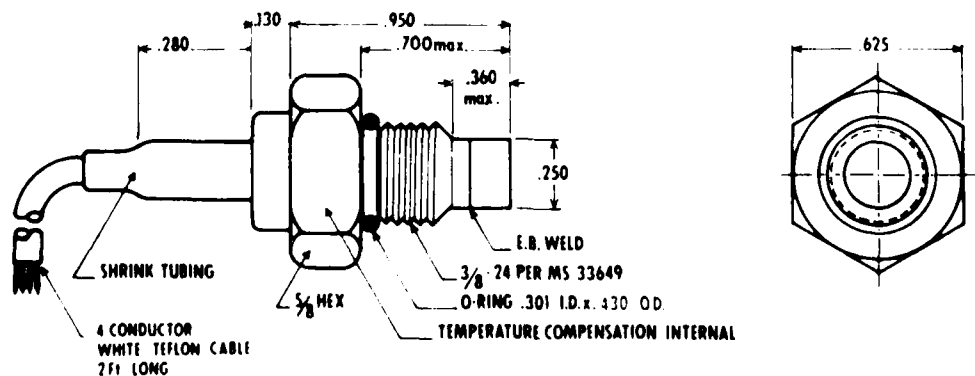
Because the transducer is constructed using electron beam welding techniques, the sensing side of the unit is suitable for immersion in liquids compatible with 17-4 PH stainless steel.
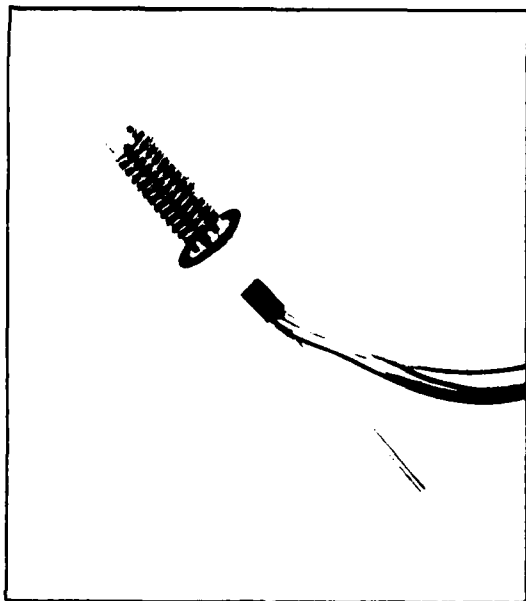
169

HKM-375 Specifications

Model No.	Pressure psi		Output Nom. mV	Acceleration Sensitivity % FS/g		Natural Freqency Min. KHz
	Rated	Maximum		Perpendicular	Transverse	
HKM-375-25	25	50	75	.002	.0004	50
HKM-375-50	50	100	75	.001	.0002	60
HKM-375-100	100	200	75	.0007	.00014	80
HKM-375-250	250	500	75	.0005	.0001	125
HKM-375-500	500	750	75	.0003	.00006	200
HKM-375-1000	1000	1500	75	.0002	.00004	275
HKM-375-2000	2000	3000	75	.00015	.00003	360
HKM-375-5000	5000	7500	75	.0001	.00002	375
HKM-375-10000	10000	15000	75	.00006	.000012	385
HKM-375-20000	20000	30000	75	.00004	.000008	395
HKM-375-30000	30000	35000	110	.00002	.000004	395

Diaphragm .... 17-4 Stainless Steel

Sensing Principle .... Integrated solid state / Wheatstone bridge

Excitation .... 10V DC or AC

Input Impedance .... 1200 ohms min.
Output Impedance .... 650 ohms max.

Zero Balance .... ± 3% FS

Combined Nonlinearity and Hysteresis .... ± 1% FS

Repeatability 0.25%

Operating Temperature Range .... 0 F to 250 F (20 C to 120 C) (Extended temperature range 65 F to 425 F) (55 C to 220 C) available on special order)

Compensated Temperature Range .... 80 F to 180 F (25 C to 80 C) (any 100 F within the operating range on request)

Change of Sensitivity with Temperature .... ± 2% / 100 F

Change of No-Load Output with Temperature .... ± 2% FS / 100 F

Resolution .... Infinite

HKM-375 Series Outline

SHRINK TUBING
4 CONDUCTOR WHITE TEFLON CABLE 2 Ft LONG
5/8 HEX
E.B. WELD
3/8 - 24 PER MS 33649
O-RING .301 I.D. x .430 O.D.
TEMPERATURE COMPENSATION INTERNAL

KULITE SEMICONDUCTOR PRODUCTS, INC. 1039 HOYT AVE. RIDGEFIELD, NEW JERSEY 07657.

170

IS®Pressure Transducers

XT-140 SERIES

- integrated sensor (is)*
- easy installation
- smallest threaded device available
- high natural frequencies
- 6-32 UNF thread

The XT-140 miniature pressure transducer is a new addition to the recently developed Kulite solid state pressure sensors. The 6-32 UNF thread with the hexagonal head and the O ring seal make the XT-140 easy to mount and simple to apply. With a .138″ O.D., the XT-140 is smaller than any other commercially available threaded pressure transducer. The small size and flush diaphragm enable installation of the transducer directly in the wall of pressure containers, tubes, pipes, etc., eliminating costly, space-consuming hardware.

The heart of the XT-140 is the new Kulite integrated circuit sensor. It consists of a miniature silicon diaphragm on which a Wheatstone bridge has been atomically bonded using diffusion techniques.

Microcircuitry techniques and the subminiaturization process employed in the Kulite sensors combine to yield a significant state of the art advance enabling pressure measurement where size and weight have made other devices unsuitable.

The standard XT-140 transducer has a reference tube emerging from its back. The transducer measures gage pressure when this tube is left open to the atmosphere.

For differential pressure measurements, the reference tube may be connected to a pressure source (dry, clean, non-conductive gas). When the reference pressure is a vacuum, the transducer will measure absolute pressure.

In the absolute pressure version, a reference pressure is sealed in the transducer and no reference tube is provided.

Upon request, the XT-140 transducers may be supplied with RTV coating or any other ablative layer on the diaphragm. For long term operation in liquids, complete Kulite form KPS-TO1 and consult the factory. The transducer is also designed to receive a perforated screen whenever diaphragm protection is desired For further detail, see Kulite Application Note AN-01A.

XT-140 Specifications

Model Number	Pressure (Rated)	Pressure (Maximum)	Output (Nom.*)	Bridge Impedance (Nom.)	Acceleration Sensitivity (Perpendicular)	Acceleration Sensitivity (Transverse)	Natural Frequency (Approx.)
XTL-140-25	25 psi	50 psi	75 mv	750 ohms	0.0003% FS/g	0.00006% FS/g	125 kHz
XT-140-50	50 psi	100 psi	90 mv	750 ohms	0.0002% FS/g	0.00004% FS/g	150 kHz
XT-140-100	100 psi	200 psi	100 mv	750 ohms	0.0001% FS/g	0.00002% FS/g	210 kHz
XT-140-200	200 psi	400 psi	100 mv	750 ohms	0.00009% FS/g	0.000018% FS/g	280 kHz
XT-140-500	500 psi	1000 psi	100 mv	750 ohms	0.00005% FS/g	0.00001% FS/g	420 kHz

*With 5v across the bridge.
These units are available with metric threads. Thread size 5mm, pitch .5mm. They are designated XT-2M-140 series.

|	
Bridge Excitation	5v nom. 7.5 max. DC or AC
Zero Balance	3% FS
Combined Non-Linearity and Hysteresis	1.0% FS (max.)
Repeatability	0.5%
Compensated Temperature Range	80°F to 180°F (25°C to 80°C) Any 100°F range within the operating range on request
Operating Temperature Range	0°F to 250°F (−20°C to 120°C) Temperatures to 350°F (175°C) available on special order
Change of Sensitivity with Temperature	0 to −6%/100°F for constant voltage of −2.5%/100°F when excited as in Note 1
Change of No Load Output with Temperature	2.0% FS/100°F (max.)
Resolution	Infinite

Note 1 ... When using a 15v constant voltage source with 1500 ohms in series with the transducer

XT-140 Series Outline

Typical Circuit

172
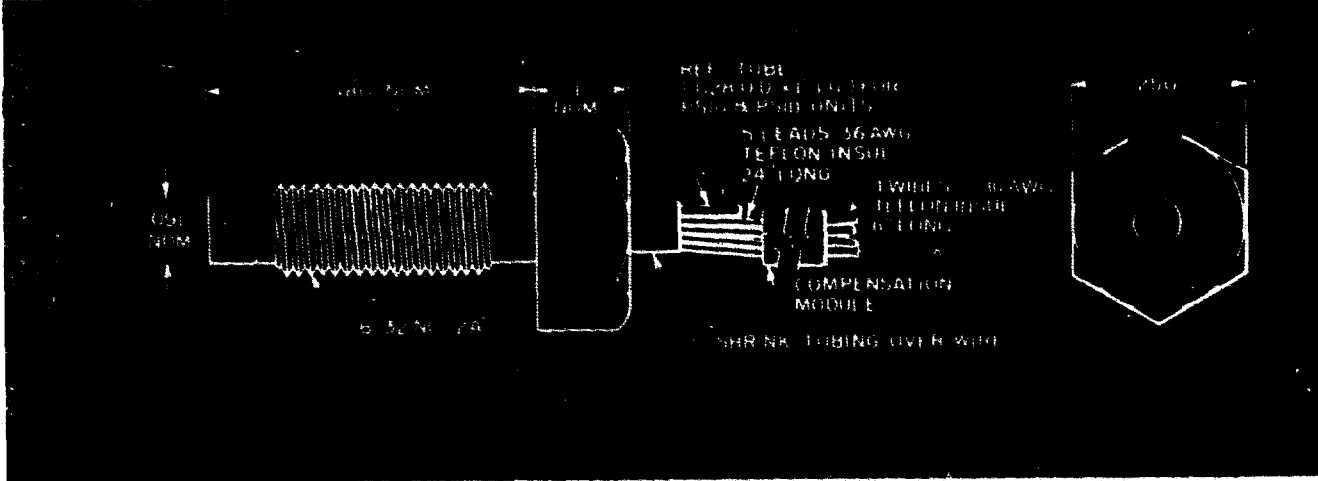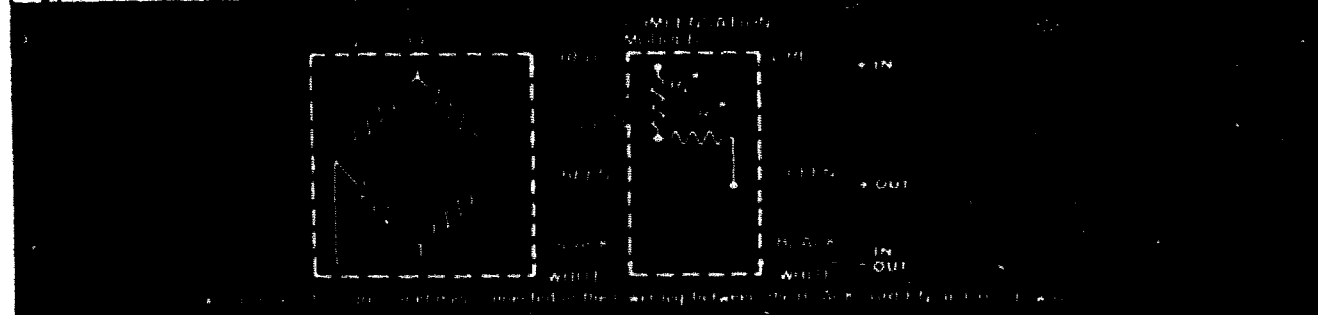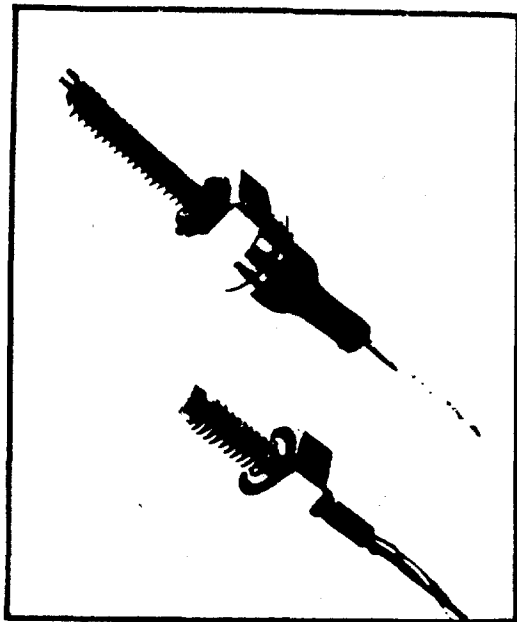
IS Pressure Transducers

XT-190 SERIES

XT-1-190 SERIES
Ruggedized Version

- integrated sensor (IS)
- easy installation
- high natural frequencies
- 10-32 UNF thread

The XT-190 Series are miniature, threaded, general purpose solid state pressure transducers. The 10-32 UNF thread with the hexagonal head and "O" ring seal make them easy to mount and simple to apply. The small size and flush diaphragm enable installation of the transducers directly in the wall of pressure containers, tubes, pipes, etc., eliminating costly space-consuming hardware.

The XT-190 transducer features a 5/16" hexagonal head and a temperature compensation module attached to the leads.

The XT-1-190 transducer features a 3/8" hexagonal head which houses the temperature compensation module. Its external electrical connection is a 4-conductor shielded cable provided with a strain relief.

The heart of the XT-190 series is the new Kulite integrated circuit sensor. It consists of a miniature silicon diaphragm on which a Wheatstone bridge has been atomically bonded using diffusion techniques.

Microcircuitry techniques and the subminiaturization process employed in the Kulite sensors com-

bine to yield a significant state of the art advance enabling pressure measurement where size and weight have made other devices unsuitable.

The standard XT-190 series transducers have a reference tube emerging from the back. The transducers measure gage pressure when this tube is left open to the atmosphere. For differential pressure measurements, the reference tube may be connected to a pressure source (dry, clean, non-conductive gas). In standard units, reference pressure should not exceed 30 psi. Higher pressures can be accommodated upon request. In the sealed version, a reference pressure is sealed in the transducer, and no reference tube is provided.

Upon request, the XT-190 series transducers may be supplied with RTV coating or any other ablative layer on the diaphragm. The transducers are also designed to receive a perforated screen whenever diaphragm protection is desired. For further details, see Kulite Application Note AN-01A.

The XT-190 series transducers should not be used in water or corrosive liquids. The all-welded metal diaphragm version XTM-1-190 series is recommended for these applications (see Bulletin KPS-XTM-1-190).

KULITE SEMICONDUCTOR PRODUCTS, INC.

XT-190 and XT-1-190 Specifications

Model Number	Pressure (Rated)	(Maximum)	Output (Nom.)	Bridge Impedance (Nom.)	Acceleration Sensitivity (Perpendicular)	(Transverse)	Natural Frequency (Approx.)
XTH-190-5 XTH-1-190-5	5 psi	20 psi	50 mv	5,000 ohms	0.002% FS/g	0.0004% FS/g	70 KHz
XTH-190-10 XTH-1-190-10	10 psi	20 psi	100 mv	5,000 ohms	0.001% FS/g	0.0002% FS/g	70 KHz
XTL-190-25 XTL-1-190-25	25 psi	100 psi	75 mv	1,500 ohms	0.0005% FS/g	0.0001% FS/g	100 KHz
XTS-190-50 XTS-1-190-50	50 psi	100 psi	85 mv	500 ohms	0.0004% FS/g	0.00008% FS/g	130 KHz
XTS-190-100 XTS-1-190-100	100 psi	200 psi	100 mv	500 ohms	0.0002% FS/g	0.00004% FS/g	160 KHz
XTS-190-200 XTS-1-190-200	200 psi	400 psi	100 mv	500 ohms	0.00013% FS/g	0.000026% FS/g	200 KHz
XTS-190-300 XTS-1-190-300	300 psi	600 psi	100 mv	500 ohms	0.00012% FS/g	0.000024% FS/g	270 KHz
XTS-190-500 XTS-1-190-500	500 psi	1000 psi	100 mv	500 ohms	0.00009% FS/g	0.000018% FS/g	350 KHz
XTS-190-1000 XTS-1-190-1000	1000 psi	2000 psi	100 mv	500 ohms	0.00006% FS/g	0.000012% FS/g	500 KHz
XTS-190-2000 XTS-1-190-2000	2000 psi	3000 psi	100 mv	500 ohms	0.00005% FS/g	0.00001% FS/g	650 KHz

These units are available with metric size threads. Thread size 5mm pitch 5mm. Designation: XT-190 Series becomes XT2M-190 Series. XT-1-190 Series becomes XT1M-190 Series.

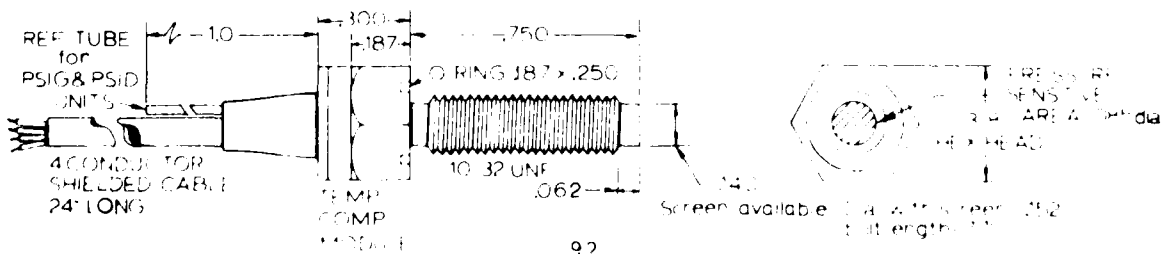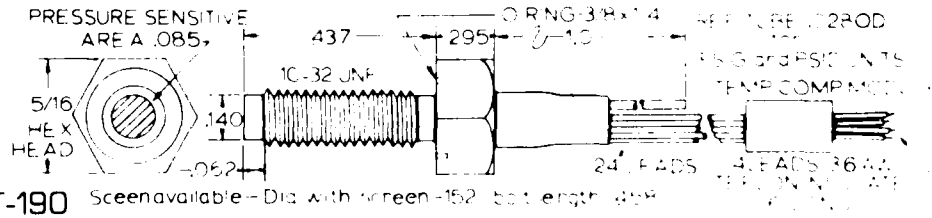|	
Bridge Excitation	XTH units 20v nom. 30v max. DC or AC XTL units 7.5v nom. 15v max. DC or AC XTS units 7.5v nom. 10v max. DC or AC
Zero Balance	±3% FS (±5% FS for 5 psi units)
Combined Non-Linearity and Hysteresis	±0.5% FS (max.)
Repeatability	0.25% (See note)
Compensated Temperature Range	80 F to 180 F (25 C to 80 C) Any 100 F range within the operating range on request
Operating Temperature Range	0 F to 250 F (−20 C to 80 C) Temperatures to 350 F (175 C) available on special order
Change of Sensitivity with Temperature	±2.5%/100 F
Change of No Load Output with Temperature	±1.0% FS/100 F (max.) (±3% FS/100 F for 5 psi units) (±2% FS/100 F for 10 psi units)
Resolution	Infinite

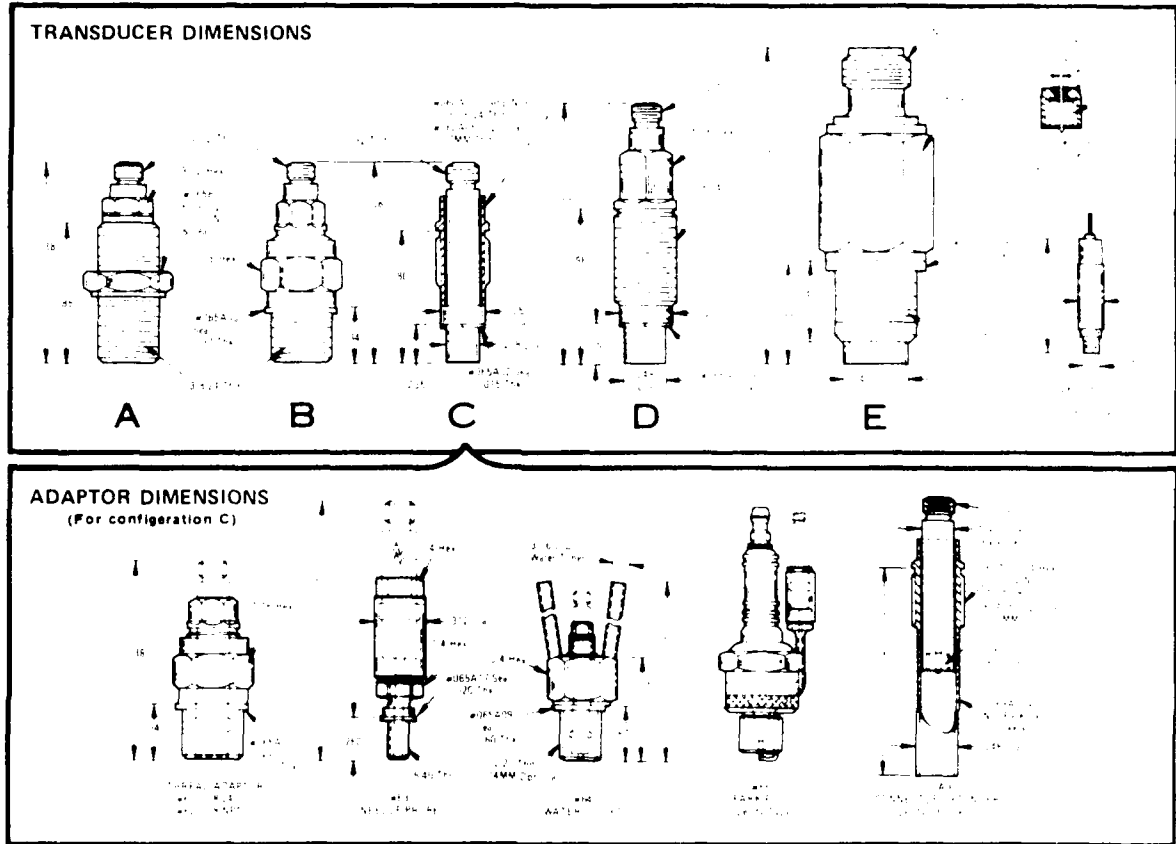Note: For XTH units steady state repeatability is 1%, dynamic repeatability 0.25%.
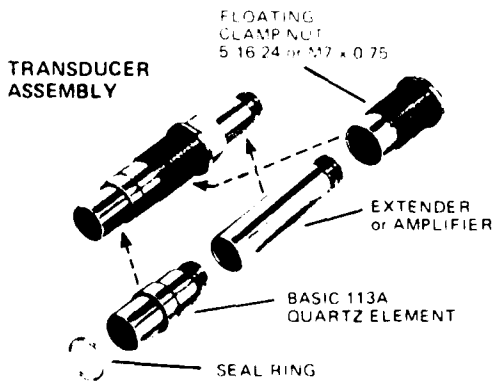

XT Series Outline

XT-190

174

TRANSDUCER DIMENSIONS

A   B   C   D   E

ADAPTOR DIMENSIONS
(For configuration C)

THE 113A QUARTZ ELEMENT . . .

TRANSDUCER ASSEMBLY

FLOATING CLAMP NUT
5 16 24 or M7 x 0.75

EXTENDER or AMPLIFIER

BASIC 113A QUARTZ ELEMENT

SEAL RING

* sensor in many pcb transducers
* acceleration-compensated
* supressed 500,000 Hz resonance
* low strain and transverse motion sensitivity
* floating clamp nut; welded flush diaphragm
* improved, interchangeable, quartz minigage
* with or without built-in amplifier

SHOCK TUBE End-On

2 0 psi div

→1 0 μsec div
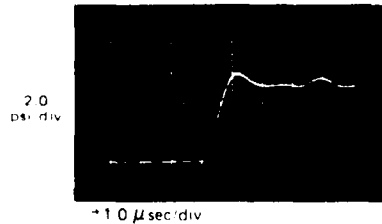
FREQUENCY TAILORED RESPONSE

As illustrated above low-impedance, voltage mode transducers incorporating the 113A element exhibit nearly non-resonant response. The built-in unity gain voltage follower amplifier also enhances the resolution and signal to noise characteristics.

MODULAR CONSTRUCTION

The modular construction illustrated extends the range of application and standardizes production. Over twelve transducers in the PCB line, identified by their 500,000 Hz resonant frequency, incorporate the basic 113A quartz element.

QUARTZ, VOLTAGE MODE, LOW-IMPEDANCE

PRESSURE TRANSDUCERS
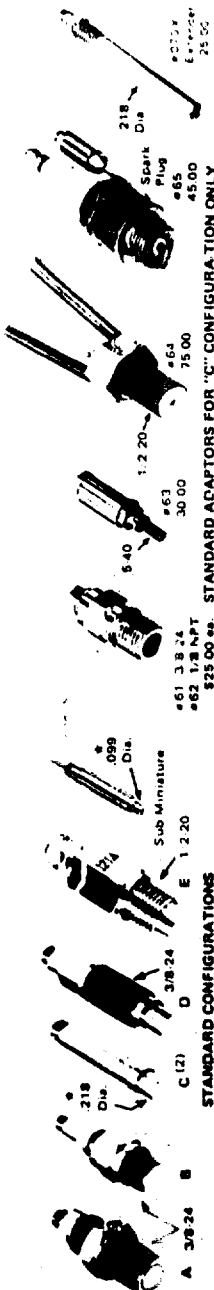
with built-in amplifiers (3) Series 100

LOW-IMPEDANCE, QUARTZ

PRESSURE TRANSDUCERS

with built-in amplifiers (3) Series 100

PCB PIEZOTRONICS

STANDARD CONFIGURATIONS — STANDARD ADAPTORS FOR "C" CONFIGURATION ONLY

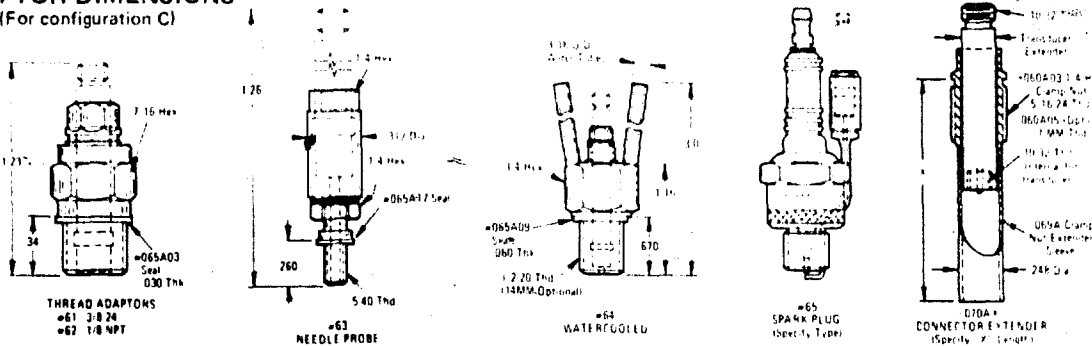| DYNAMIC RANGE (1) — psi	.01 to 100			2 to 1000			1 to 5000		2 to 10,000		10 to 80,000 (Special to 120,000)		
Application	General Purpose	High Resolution	High Frequency	Industrial OEM	General Purpose	High Frequency	General Purpose	High Frequency	General Purpose	High Frequency	Hydraulic Pump	Ballistics	High Frequency
Frequency Tailored (5)			*			*		*		*			*
Acceleration Compensated													
Ground Isolated (A & B Configurations)													
Standardized Sensitivity (±5%)													
Static Calibration													
MODEL NO. Config. A / Price	101A 240.00	102A02 350.00	102A12 430.00		101A04 280.00	102A04 430.00	101A02 280.00	102A 430.00					
MODEL NO. Config B / Price	101A05 240.00	102A05 350.00	102A15 430.00						101A03 300.00	102A03 450.00			
MODEL NO. Config. C (2) / Price	111A21 240.00	112A21 280.00	113A21 410.00		111A24 260.00	113A24 410.00	111A22 260.00	113A22 410.00	111A23 280.00	113A23 430.00			
MODEL NO. Config. D or E / Price				121A (E) 150.00							108A02(D) 350.00	108A(D) 450.00	109A(D) 525.00
SENSITIVITY — mV/psi	40 ±10	50 ±10	20 ±4	40 ±20	5 ±.5	5 ±.25	1 ±.1	1 ±.05	.5 ±.05	.5 ±.03	.5	.1	.1
Resolution — psi (200 μV P-P Elect. Noise)	.005	.004*	.01	.005	.04	.04	.2	.2	.4	.4	.4	2	2
Resonant Frequency — Hz	300,000	250,000	500,000*(5)	200,000	400,000	500,000*(5)	400,000	500,000*(5)	400,000	500,000*(5)	300,000	300,000	500,000*(5)
Rise Time — μsec	2	2	1*	3	1	1*	1	1*	1	1*	2	2	1*
Time Constant (6) — sec	1	1	1	1	100	100	500	500	1000	1000	1000	2000	2000
Low Frequency (5% down)(6) — Hz	.5	.5	.5	.5	.005	.005	.001	.001	.0005	.0005	.0005	.0003	.0003
Linearity (7) — %	1	1	1	2	2	1	2	1	2	1	2	2	2
Range (for 5 volts out)(4) — psi	125	100	250	125(11)	1000	1000	5000	5000	10,000	10,000	10,000	50,000	50,000
Range (for 10 volts out)(4) — psi	250	200	500	250	2000	2000	10,000	10,000	20,000	20,000	20,000	100,000	100,000
Maximum Pressure — psi	1000	1000	1000	1000	10,000	10,000	15,000	15,000	20,000	20,000	20,000	125,000	125,000
Output Impedance — ohms	100*	100*	100*	100*	100*	100*	100*	100*	100*	100*	100*	100*	100*
Vibration/Shock (8) — g	2000/20,000	2000/20,000	2000/20,000	2000/20,000	2000/20,000	2000/20,000	2000/20,000	2000/20,000	2000/20,000	2000/20,000	2000/20,000	2000/20,000	2000/20,000
Acceleration Sensitivity — psi/g	.01	.004*	.002*	.02	.002*	.002*	.001	.001	.0005	.0005	.005	.01	.004
Temperature Range (10) — °F	-100 +275	-100 +275	-100 +275	-100 +275	-100 +275	-100 +275	-100 +275	-100 +275	-100 +275	-100 +275	-100 +275	-100 +275	-100 +275
Temperature Coefficient — %/°F	.03	.03	.03	.04	.03	.03	.03	.03	.03	.03	.03	.03	.03
Flash Temperature — °F	3000	3000	3000	3000	3000	3000	3000	3000	3000	3000	3000	3000	3000
Case Material (12) — SS	17-4PH	17-4PH	17-4PH	303	17-4PH	17-4PH	17-4PH	17-4PH	17-4PH	17-4PH	17-4PH	17-4PH	17-4PH
Diaphragm Material (12)	Invar	Invar	Invar	303(9)	Invar	Invar	Invar	Invar	Invar	Invar	Invar	Invar	Invar
Connector	10-32	10-32	10-32	TNC	10-32	10-32	10-32	10-32	10-32	10-32	10-32	10-32	10-32

NOTES: (* denotes exceptional characteristic)

(1) Measures relative to initial or average level — Measures to full vacuum — Dynamic range 5000:1 independent of cable length.

(2) Installs interchangeably with .218 dia. quartz minigages. 5/16-24 clamp nut is standard. 7 mm installation available.

(3) Power required 2 to 20 ma thru cc diode from +18 to +24V DC supply for ±5 volts output. Higher current drives long cables (>100 ft.).

(4) +24V DC supply required for ±10V DC output.

(5) Near non-resonant response — suppressed ringing.

(6) Measures transients lasting a few % of time constant.

(7) % F.S. any calibrated range — zero based best straight line.

(8) Built-in amplifier withstands 100,000 g shock.

(9) Diaphragms are integral.

(10) Special models operate from -340°F to +325°F

(11) Other ranges available.

(12) Special diaphragm or case material available.

Options include other time constants, sensitivities and calibrations, signal conditioning, conformal diaphragm and welded hermetic sealing.
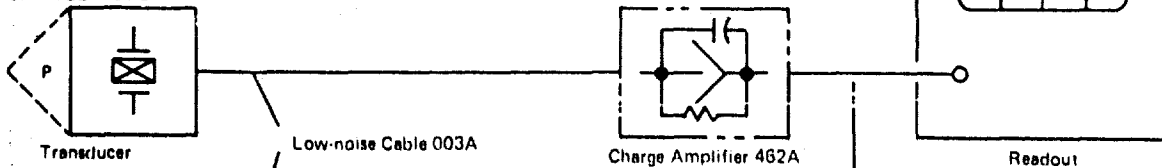
PCB PIEZOTRONICS

TRANSDUCER DIMENSIONS

CONFIGURATION

| C | D | F | G | H |

ADAPTOR DIMENSIONS
(For configuration C)

THREAD ADAPTORS
=61 3-8-24
=62 1/8 NPT

=63
NEEDLE PROBE

=64
WATERCOOLED

=65
SPARK PLUG
(Specify Type)

-070A-
CONNECTOR EXTENDER
(Specify "X" Length)
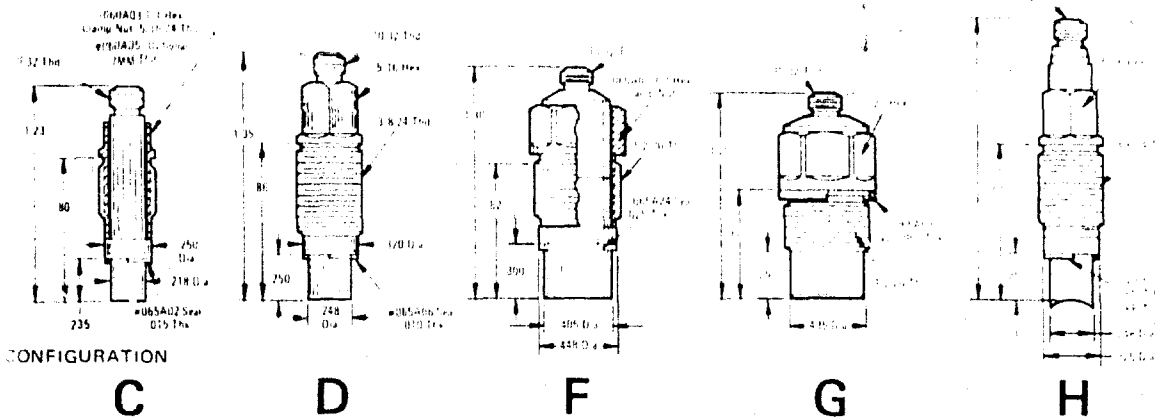
TYPICAL SYSTEMS

CHARGE-MODE

Transducer

Low-noise Cable 003A

Charge Amplifier 462A

Readout

Coaxial Cable 002A

HYBRID

Transducer

In-line Ampl. 402A or 422B

Power Unit 480A, 482A

Output Cable
002A03 (micro)
or 012A03 (BNC)

VOLTAGE-MODE, LOW IMPEDANCE

Transducer

Connector Ampl. 401A
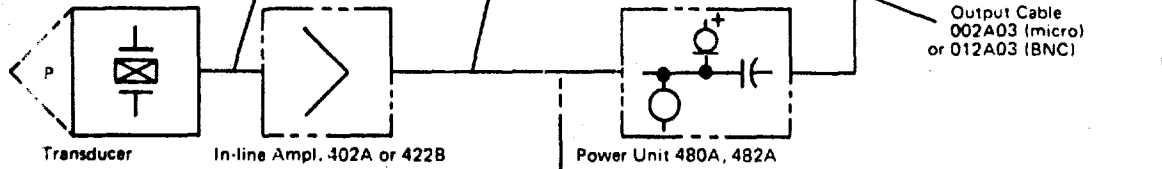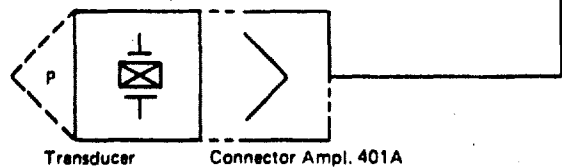
The 100 series charge-mode transducers will operate with any charge amplifier or converter, which usually inverts the signal. For this reason, standard model transducers have a negative charge output, producing a positive going signal at the readout. When operating with voltage-followers, which do not invert the signal, reverse the polarity of the readout or order optional positive-polarity transducers, designated with a suffix "P" after the model number.

QUARTZ CHARGE MODE

PRESSURE TRANSDUCERS

Series 110

PCB PIEZOTRONICS

PRESSURE

STANDARD CONFIGURATIONS / STANDARD ADAPTORS FOR 'C' CONFIGURATION ONLY

DYNAMIC RANGE [1] (psi) [12]		.01 to 100				.1 to 3000			1 to 10,000				2 to 30,000		
MODEL NO.	$ Price	111A02	112A02	113A02	116A5	111A	112A	113A	111A03	112A03	113A03	118A02	118A	117A	119A
Application		General Purpose	High Resolution	High Frequency	High Sensitivity	General Purpose	General Purpose	High Frequency	General Purpose	General Purpose	High Frequency	High Frequency			
Configuration		C	C	C	F	C	C	C	C	C	C	C			
Acceleration – Compensated			Yes	Yes	Yes	Yes	Yes	Yes	Yes	Yes	Yes	Yes			
SENSITIVITY	pC/psi	.35	1.0*	.35	8.0*	.35	1.0*	.35	.35	1.0*	.35	20	20	20	25
Resolution [9]	psi	.005	.004*	.01	.003*	5	1	5	1						
Resonant Frequency	KHz	400	250	500*	130	400	250	500	400		500*			300	
Rise Time	μsec	2	2	1*	5	2	2	1*	2	2			2	2	
Linearity [3]	%FS	1	1	1	1	1	1	1½	1						
Maximum Pressure	psi	3000	3000	3000	3000.5	10,000	10,000	12,500	15,000	15,000	15,000				
Capacitance	pF	5	18	12	100	5	18		5	16	10				
Resistance (75° F)	>ohms	10^{12}	10^{12}	10^{12}	10^{12}	10^{12}	10^{12}		10^{12}	10^{12}	10^{12}				
Output Polarity [8]		Neg	Neg	Neg	Neg	Neg	Neg	Neg	Neg	Neg	Neg		Neg	Neg	
Vibration	g	2000	2000	2000	2000	2000	2000	2000	2000	2000	2000		2000	2000	
Shock	g	20,000	20,000	20,000	20,000	20,000	20,000	20,000	20,000	20,000	20,000		20,000	20,000	
Acceleration Sensitivity [6]	psi/g	.01	.002*	.002*	.002*	.01	.002*	.002*	.01	.002*	.002*		.01	.01	
Temperature Range [6]	°F	400	400	400	400	400	400	400	400	400	400		400	400	
Temperature Coefficient	%/°F	.01	.01	.01	.01	.01	.01	.01	.01	.01	.01		.01	.01	
Flash Temperature	°F	3000	3000	3000	3000	3000	3000	3000	3000	3000	3000		3000	3000	
Case Material [7]		17-4 PH	17-4 PH	17-4 PH	17-4 PH	17-4 PH	17-4 PH	17-4 PH	17-4 PH	17-4 PH	17-4 PH		17-4 PH	17-4 PH	
Diaphragm Material [7]		Invar	Invar	Invar	Invar	Invar	Invar	Invar	Invar	Invar	Invar		Invar	Invar	
Connector		10/32	10/32	10/32	10/32	10/32	10/32	10/32	10/32	10/32	10/32		10/32	10/32	
Weight	grams	5	5	5	2½	5	5	5	5	5	5		11	11	

NOTES: (* denotes exceptional characteristic)
(1) Measures dynamic pressure from full vacuum to rated maximum, relative to initial or average level.
(2) Installs interchangeably with .218 dia. quartz mini gages. 5-16-24 clamp nut is standard. M7x.75 installation available
(3) %F S any calibrated range; zero based best st. line.
(4) Diaphragm integral with housing

(5) Optional ranges: 116A02 to 1000 & 116A03 to 5000 psi.
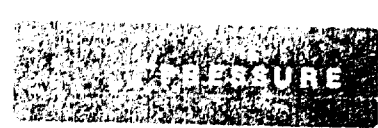(6) HiTemp (550°F) version with ceramic... ranges available
(7) Special case and diaphragm material ...
(8) Add suffix "P" after model no. to spec... tive output
(9) Resolution determined by system noise figures specified ... with 401A Voltage Follower (noise ~2pC ...)
(10) 1% linearity optional

(11) For optional 'C' configuration ...
(12) 1 psi = .0703 kgf/cm² ... .06895 bar, 10³ dynes/cm² ...

Options include various configurations ... the case ... and ... water cooled or welded ...
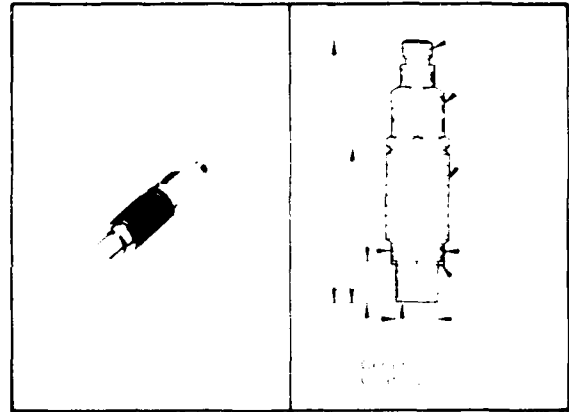
HIGH-PRESSURE TRANSDUCER

with built-in amplifier   Model 109A

PCB
PIEZOTRONICS

- range to 100,000 psi

- acceleration-compensated quartz element

- high resonant frequency: 500,000 Hz

- frequency-tailored — nearly non-resonant response

- high-level (10V), low-impedance output

- static calibration

For shock wave, blast, explosion, detonation and ballistic applications, in shock and vibration environments. Not suited for continuous hydraulic nor rapid-fire ammunition testing.

Model 109A is a high pressure quartz transducer with a built-in unity-gain amplifier for dynamic and short term static pressure measurements to 100,000 psi on shock tubes, detonation chambers, closed bombs, gas guns and explosive metal forming machines. To improve the quality of the signal, an internal compensating accelerometer reduces vibration sensitivity and suppresses resonance effects, which tend to mask the actual pressure signal. An integral diaphragm with a permanent ceramic coating insulates and protects the transducer against damaging temperature effects.

The Model 109A installs flush or recessed directly in the test object and fits many existing ports for older type transducers. The thin shoulder seal illustrated is recommended for new installations. Request a detailed installation drawing.

When connected to a PCB power unit, self amplifying transducers generate a high level low-impedance analog output signal proportional to the measurand and compatible with most readout instruments. The simple power unit circuit powers the transducer over the signal lead (coaxial or 2 wire), eliminates bias on the output and monitors normal or faulty operation. Signal quality is almost independent of cable length, condition and motion.

Model 109A excells in tough applications. If detonation, stress waves, shock, strain, motion or temperature is involved or causing trouble (noisy signals), try this rugged, sophisticated instrument. The thermal, motion and resonance compensating techniques employed within have helped improve the quality of the result in numerous difficult situations.

SPECIFICATIONS: Model No.		109A
Range (8 volt output)	psi	50,000
Overrange (10 volt output)	psi	100,000
Resolution	psi	2
Sensitivity	mV/psi	0.1
Resonant Frequency	Hz	500,000
Rise Time	μ sec	1
Discharge Time Constant	sec	200u
Low Frequency (5)	Hz	0.0003
Linearity (B.S.L., Zero Based)		2
Output Impedance	ohms	100
Excitation (thru C.C. Diodes)	VDC MA	+18 to 24 2 to 20
Acceleration Sensitivity	psi/g	0.004
Temperature Coefficient	%/°F	0.03
Temperature Range	°F	-100 to +275
Shock	g	200 20,000

MODEL NO. (Optional Versions)	109A02
Range to 120,000 psi	

Conventional Charge-Mode No.	119A

(Sensitivity 0.25 pC/psi for charge amplifiers)

TYPICAL SYSTEM:
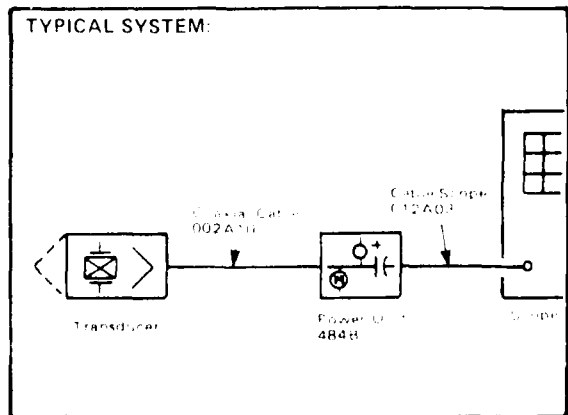
MINIATURE, QUARTZ, LOW IMPEDANCE, VOLTAGE-MODE

HIGH-RESOLUTION PRESSURE TRANSDUCER

with built-in amplifier   Model 112A21

PCB
PIEZOTRONICS

* improved interchangeable quartz minigage
* high-sensitivity, acceleration-compensated element
* built-in low-noise amplifier
* exceptionally low strain and motion sensitivity
* floating metric or American clamp nut
* flush-welded, flat, invar diaphragm
* measures small variations at high static levels

For turbulence, noise, sound, cavitation, pulsation, fluidic, aerodynamic, pneumatic, hydraulic and blast applications, especially in adverse environments.

Model 112A21 quartz minigage measures dynamic and sound pressure from 0.01 to 200 psi at any level from full vacuum to 1,000 psi. An internal integral accelerometer minimizes vibration sensitivity and a discharging resistor automatically eliminates static (D.C.) signal components. This sophisticated instrument contains a high-sensitivity multi-plate quartz element and a selected low-noise amplifier to impart a high signal-to-noise ratio.

A floating clamp nut with either a metric (M7 x .75) or American (5/16-24) thread isolates against strain and facilitates installation and removal of the sealed transducer assembly, which flush or recess mounts directly in the test object or in a variety of threaded mounting adaptors.
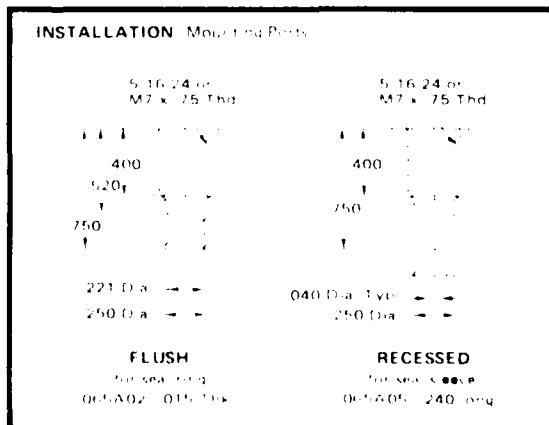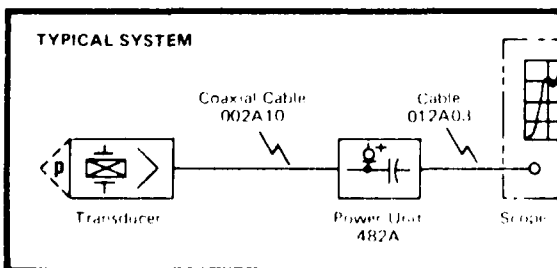
When connected to a PCB power unit, this self-amplifying transducer generates a high level, low-impedance analog output signal proportional to the measurand and compatible with most readout instruments. The simple power unit circuit powers the transducer over the signal lead (coaxial or 2-wire), eliminates bias on the output and monitors normal or faulty operation. Signal quality is almost independent of cable length, condition and motion.

Variations of this transducer incorporating voltage gain can be supplied with sensitivities to 500 mV/psi.
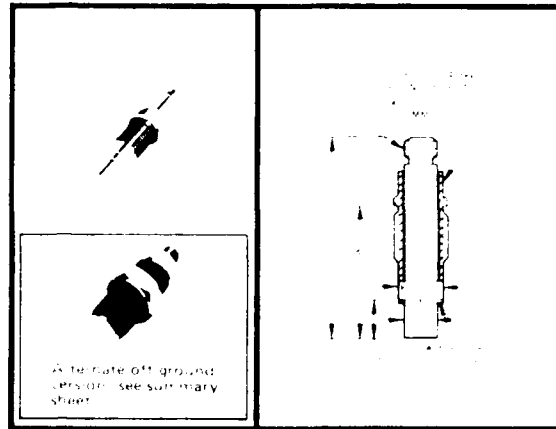
SPECIFICATIONS:

	Model No.	112A21
Range, F.S. (1V output)	psi	20
Range, F.S. (10V output)	psi	200
Maximum Pressure	psi	1,000
Resolution (Noise)	psi	.004
Sensitivity	mV/psi	50 · 10
Resonant Frequency	Hz	250,000
Rise Time	μsec	2
Discharge Time Constant	sec	1
Low Frequency (-5%)	Hz	0.5
Linearity	%	1
Output Impedance	ohms	100
Acceleration Sensitivity	psi/g	0.002
Temperature Coefficient	°/F	0.03
Temperature Range	F	-100 to +275
Flash Temperature	F	3,000
Shock/Vibration	g	20,000/2,000
Excitation (thru C.C. diode)	+VDC/mA	+18 to 24/2 to 20

Note: For clamp-nut with metric (M7 x .75) thread add suffix "M" after model number (ie 112A21M)

TYPICAL SYSTEM

Coaxial Cable 002A10   Cable 012A03

Transducer   Power Unit 482A   Scope

INSTALLATION Mounting Ports

FLUSH   RECESSED

180

HIGH-FREQUENCY PRESSURE TRANSDUCER

for charge amplifiers   **Model 113A**

PCB
PIEZOTRONICS

- **500,000 Hz, one microsecond response**
- **acceleration-compensated quartz element**
- **low strain and motion sensitivity**
- **floating clamp nut; metric or American thread**
- **flush welded, flat diaphragm; static calibration**
- **improved interchangeable quartz minigage**

TRANSDUCER ASSEMBLY
(As Supplied)

For shock wave, blast, explosion, ultrasonic and dynamic combustion pressure measurements requiring ultra-fast response.

Model 113A high-frequency, quartz transducer measures ultra-fast dynamic pressures for full vacuum to 3000 psi (15,000 psi optional). This miniature transducer measures transient or repetitive phenomena relative to the initial or average pressure level; over wide amplitude and frequency ranges under the most adverse environmental conditions. System voltage sensitivities range from 0.01 mV/psi to 300 mV/psi depending upon the amplifier involved. The electrostatic charge signal from this conventional peizoelectric transducer is converted into a voltage signal in a PCB similar charge amplifier.

The structure of this sophisticated instrument contains a super-rigid compression-mode quartz element with an integral compensating accelerometer to reduce vibration sensitivity and partially suppress internal resonance effects. The net result is unmatched dynamic response from a transducer that installs interchangeably in existing systems.

Miniature quartz transducers install flush or recessed in existing or new mini-gage ports directly in the test object or in a variety of threaded mounting adaptors, as illustrated. A floating nut, with either a 5/16-24 or M7 x 0.75 thread clamps the transducer in place, isolates against strain and facilitates installation and removal of the sealed transducer assembly.

To order a typical system, specify: the transducer model number (113A), low-noise transducer cable (003A 10' or other length); laboratory charge amplifier (model 462A); output cable (002A03') and mounting adaptor (60 Series), if required. For the metric threaded version (M7 x .75 clampnut), add the suffix "M" after the model number.
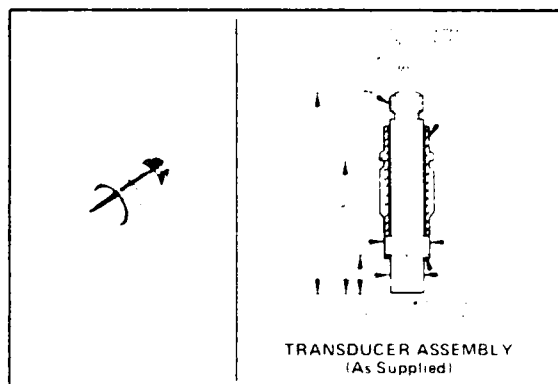
SPECIFICATIONS: Model No.		113A
Range, Full Scale	psi	3000
Maximum Pressure	psi	10,000
Resolution	psi	0.5
Sensitivity	pC/psi	0.35
Resonant Frequency	Hz	500,000
Rise Time	µsec	1
Linearity, B.S.L.	% F.S.	1
Resistance	ohms	10^{12}
Capacitance	pF	12
Acceleration Sensitivity	psi/g	0.002
Temperature Coefficient	%/°F	0.01
Temperature Range	°F	400
Flash Temperature	°F	3,000
Vibration/Shock	g	2000/20,000
Thread, Clamp Nut	UNF	5/16-24
Polarity		Neg

Model No. (Optional Ranges)		
Low-Range	100 psi	113A02
High-Range	10,000 psi	113A03

INSTALLATION: MOUNTING PORTS

181
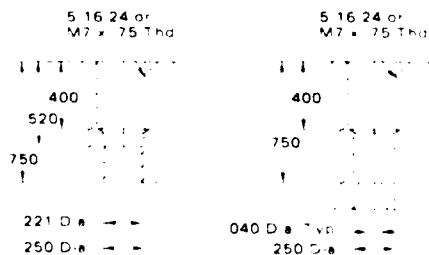
MINIATURE, UNIVERSAL, VOLTAGE-MODE

HIGH-FREQUENCY PRESSURE TRANSDUCER

with built-in amplifier   Series 113A20

PCB
PIEZOTRONICS

- acceleration-compensated ultra-rigid quartz element
- frequency-tailored ~ non-resonant one microsecond response
- high level (10V), low-impedance (100 ohm) analog output
- low strain and transverse motion sensitivity
- floating clamp nut with metric or American thread
- flush welded, flat, invar diaphragm
- improved, interchangeable quartz minigage

For shock wave, blast, explosion, combustion, compression, actuation, pulsation, cavitation, ultrasonic, aerodynamic, hydraulic and fluidic pressure measurements.

To quickly appreciate the advantages and superior performance of the 113A series frequency-tailored quartz minigages, you only need to try one and compare results. Usually it is convincing enough just to install one in your test object and feel the difference. There are no binding or interference problems in the self-aligning floating clamp nut construction. This decoupling feature and the smooth action experienced assure that strains encountered in the object under test don't couple through the threads into the crystals, generating spurious signals that obscure the actual pressure trace. In addition, the transducer seals and you can remove it.

Shock tube results show these frequency-tailored transducers to be almost completely free of ringing and other internal resonance effects that also distort the signal. The rigid structure of these sophisticated instruments contain a compression mode quartz element with an integral compensating accelerometer to reduce vibration sensitivity and supress resonance effects. Nearly non-resonant behavior is primarily achieved by meticulously matching the resonant frequency as well as the acceleration sensitivity of the compensating element to that of the pressure sensing element. A minimum number of quartz plates imparts structural integrity.
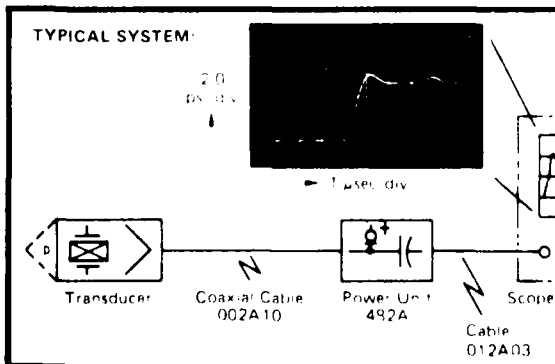
Miniature quartz transducers install flush or recessed in existing or new minigage ports directly in the test object or in a variety of threaded mounting adaptors, which are also available as off-ground factory sealed assemblies. When connected to a PCB power unit, these self amplifying transducers generate a high level, low impedance analog output signal compatible with most readout instruments. The simple power unit circuit powers the transducer over the signal lead (coaxial or 2-wire), eliminates output bias and indicates normal or faulty operation. Signal quality is almost independent of cable length, condition and motion.

These transducers have won many competitions. You can expect and get sharper, cleaner signals!

Alternate off ground version (see summary sheet)
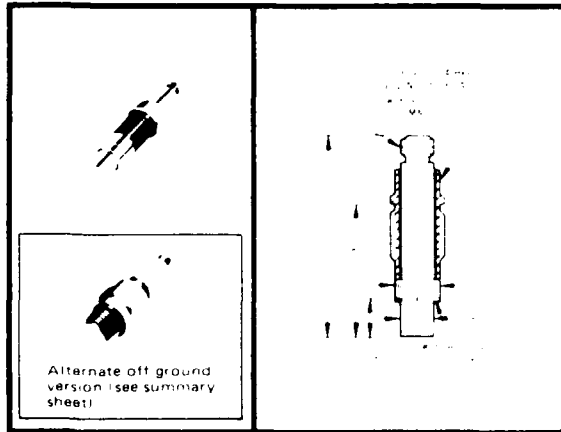
SPECIFICATIONS	Model No	113A21
Range (1 volt output)	psi	50
Range, F.S. (10 volt output)	psi	500
Maximum Pressure	psi	1000
Resolution (Noise 200 μV p-p)	psi	0.01
Sensitivity	mV/psi	20
Resonant Frequency	Hz	500,000
Rise Time/Overshoot (max)	μsec	1/15%
Discharge Time Constant (T.C.)	sec	1
Low Frequency Response (−5%)	Hz	0.5
Linearity (B.S.L.)	%	1
Output Impedance	ohms	100
Acceleration Sensitivity	psi/g	0.002
Temperature Coefficient	%/F	0.03
Temperature Range	F	100 to +275
Shock	g	20,000
Excitation (thru C.C. diode)	VDC.mA	+18 to 24 2 to 20

Model No. (other 10V Ranges)		
2,000 psi; 100 sec T.C.	5 mV/psi	113A24
10,000 psi; 500 sec T.C.	1 mV/psi	113A22
20,000 psi; 1,000 sec T.C	0.5 mV/psi	113A23

Note: For metric (M7 x .75) thread, add suffix "M" after model no.

TYPICAL SYSTEM

2.0
psi/div

1 μsec/div

Transducer   Coaxial Cable   Power Unit   Scope
              002A10   482A
                                          Cable
                                          012A03

SPECIFICATIONS
MODEL 113A51
ICP FREE FIELD BLAST PRESSURE TRANSDUCER

SENSITIVITY (NOM)	mV/psi	20
RESOLUTION ⚠1	Psi	.01
RESONANT FREQUENCY	kHz	500
TIME CONSTANT	Sec	10
LOW FREQUENCY, -5%	Hz	.05
LINEARITY ⚠2	±% FS	1
FULL SCALE RANGE, 5V OUT ⚠3	Psi	250
RANGE FOR 10 VOLTS OUT	Psi	500
MAXIMUM PRESSURE	Psi	1000
OUTPUT IMPEDANCE	Ohms	100
OUTPUT BIAS VOLTAGE, NOM.	Volts	11
VIBRATION, PEAK, MAX.	±G	2000
SHOCK, MAX.	G	2000
ACCELERATION SENSITIVITY	Psi/G	.002
TEMPERATURE RANGE	°F	-100 to +275
TEMPERATURE SENSITIVITY	%/°F	.03
FLASH TEMPERATURE, MAX.	°F	3000
CASE MATERIAL		17-4 Ph Stainless Steel
DIAPHRAGM MATERIAL		Invar
WEIGHT	Grams	
CONNECTOR		BNC, Co-axial
POWER SUPPLY VOLTAGE	Volts	18-24V DC, 30V Max.
POWER SUPPLY CURRENT	mA	2-20 mA thru current limiting diode (or equiv.). Do not exceed 20 mA.

⚠1 200 uV pk-pk broadband electrical noise

⚠2 Any calibrated range, zero-based best fitting straight line

⚠3 Optional range 500 psi (10mV/psi)
1000 psi (5mV/psi)

Sundstrand Data Control, Inc. 🔵
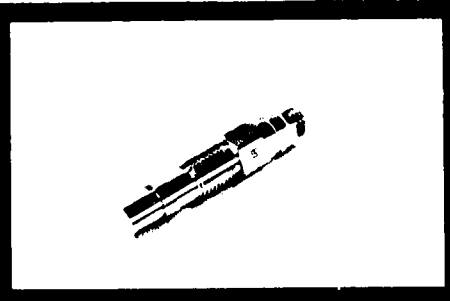
Kstler **Series**

PIEZOTRON® MINIATURE

Pressure Sensors

...WITH INTEGRAL ADAPTORS

Features

- LOW IMPEDANCE OUTPUT
- ACCELERATION COMPENSATED
- HIGH RESOLUTION 10,000 : 1 RANGE
- HIGH RESONANT FREQUENCY
- STABLE QUARTZ SENSORS
- KISTLER QUALITY

The new 201 Series Miniature Pressure Transducers with integral connector/adaptors are the latest development in this field. The 201 design is based on the highly successful 601 type quartz sensor produced for many years. However, the addition of Piezotron low impedance electronics adds important capabilities to this mini-gage. The 201 with its internal impedance converter gives a direct, high level, voltage signal with less than 100 ohms output impedance. Long, moving cables present no problem and special cables are not required. Also, a charge amplifier is no longer necessary. A less expensive coupler may be used, instead. All 201

Mini-Gages are interchangeable with 601 or 603 transducers for present or new uses

The unit construction of the transducer and adaptor eliminates sealing problems and saves installation time.

Four models of the 201 Sensor are offered with full scale ranges from 0 to 100 psi in Model 201B5 and 0 to 5,000 psi in Model 201B1

The 201 is not limited by shock or vibration except in the most extreme environments, and is enclosed in a rugged, sealed, stainless steel case

Dimensions — 201 Series
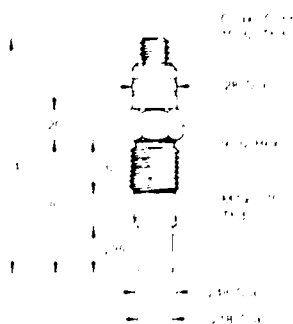
Cavity Dimensions
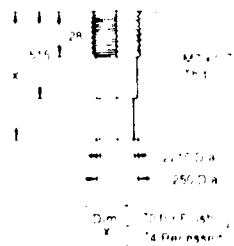
Flush mounting exposes the sensor to the pressure source for maximum fidelity. Recessed mounting affords a measure of protection for the sensor diaphragm, and permits use of ablative coating for maximum protection

Recessed Mounting
(where installation area is restricted)
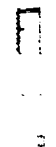
The cavity for the mounting must be carefully machined to match dimensions of individual transducer and seal. The optimum space between diaphragm and bottom of cavity is .010 in. High frequency response is somewhat impaired by this method of installation

Typical **PIEZOTRON®** Pressure Sensing System

COUPLER

128M (x) CABLE

201 TRANSDUCER   READOUT
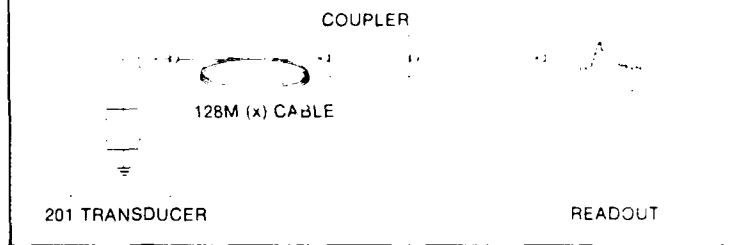
Couplers

To complete the system a wide choice of couplers is offered in the 548 and 549 series. Optional filters and several types of power inputs are available. Model 587D Coupler provides increased capability. Please refer to our Coupler Data Sheet for details.

In addition Models 583, 503D and 504D Laboratory Amplifiers are offered with extensive versatility and many options for more complete pressure studies

Specifications

PERFORMANCE	UNITS	201B1	201B2	201B4	201B5
Pressure Range, 5V out	psi	5,000	500	200	100
Overrange	psi	7,500	750	300	150
Resolution (noise)	psi rms	0.05	0.005	0.002	0.001
Maximum Pressure	psi	15,000	5,000	2,000	1 000
Sensitivity	mV/psi	1	10	25	50
Linearity, B.F.S.L.	%	+1	±1	·1	·1
Resonant Frequency, nom.	kHz	500	500	500	250
Rise Time, 10-90%	μ sec	1	1	1	2
Time Constant, R.T.	sec	1,500	400	200	100
Low Frequency Response, −5%	Hz	0.0003	0.001	0.0025	0 005
High Frequency Response, +5%	Hz	100,000	100,000	100.000	50.000
ENVIRONMENTAL		**Common Specs**			
Vibration Sensitivity, max.	psi/g	0.002	0.002	0.002	0 002
Shock, 1 ms	g	5,000	5,000	5,000	5 000
Vibration Limit	g	500	500	500	500
Temperature Range	F	−65 to 280	−65 to 280	−65 to 280	−65 to 280
Temperature Sensitivity Shift	/ F	0.03%	0.03%	0.03%	0 03%
ELECTRICAL					
Output Current, min.	mA	2	2	2	2
Polarity, pressure increase		Negative	Negative	Negative	Negative
Bias Voltage	V	11 ±2	11 ±2	11 ±2	11 ±2
Circuit Return		Case	Case	Case	Case
Output Impedance, max.	ohms	100	100	100	100
MECHANICAL					
Weight	gms	< 10	< 10	< 10	< 10
Case and Diaphragm Material		Stainless St.	Stainless St.	Stainless St.	Stainless St
Mounting Torque	in-lb	24	24	24	24
Sealing		All Welded	All Welded	All Welded	All Welded
POWER SUPPLY					
Constant Current Source	mA	4 ±1	4 ±1	4 ±1	4 ±1
Supply Ripple, max.	mV rms	25	25	25	25
Supply Voltage, no load	VDC	20-30	20-30	20-30	20-30
Source Impedance, nom.	ohms	250 k	250 k	250 k	250 k

Model Variation

To order, Specify:

[ ] Model 201B1, 201B2, 201B4, 201B5 (includes one each Model 600A3, Stainless Steel Sleeve 248 long, 600A6, Brass Seal 060 long, and 600A11, Teflon Seal 060 long)

[ ] Tap, Model 600A13 (M7 x 0 75) if required to thread mounting cavity

[ ] Model 128M (x) Cable, length (x) ft Standard length, 10 ft

[ ] Extension Cables see Data Sheet

[ ] Model 623B Ruggedized Adaptor 3/8 24 thd, 7/16" hex

Choose:

·· 548 Series Coupler

·· 549 Series Coupler

· 587D Coupler

· 503D Dual-Mode Amplifier

· 504D Dual-Mode Amplifier

See data sheets on above electronics for choice of models & filters

Sundstrand Data Control, Inc.

Subsidiary of Sundstrand Corporation

Sundstrand Data Control, Inc.

KISTLER **Model**

ACCELERATION COMPENSATED, MINIATURE

Pressure Sensor

One Instrument Covers All Ranges 0 - 15,000 psi

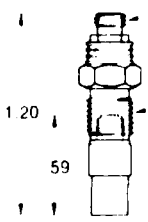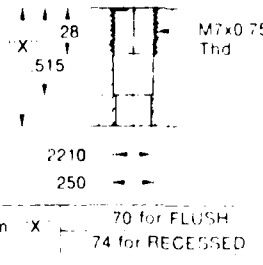### FEATURES

- Acceleration Compensated
- High Resolution--w/Wide Dynamic Range
- Miniature, w/Higher Resonant Frequency
- Rugged, Hardened Stainless Steel Case

ALSO AVAILABLE!
Advanced, Low Impedance 201B Series

601B Dimensions

The 601B is our most advanced design of the widely used miniature quartz pressure transducers. To satisfy today's more demanding needs several major improvements have been made. The 601B is acceleration compensated. This reduces vibration sensitivity by a factor of five. The resonant frequency has been greatly increased, and transient temperature effect, or thermal zero shift, is reduced. Temperature sensitivity shift is also improved.

The 601B is the direct replacement for the 601A, 601A1, 601L1 and 601H. All previous advantages are retained and the size and configuration are identical. The superb linearity exhibited by quartz allows multi-range, full scale calibrations. A fraction of a psi as well as full scale can be measured with one sensor. Calibration from 0 to 5,000 and 0 to 15,000, both with better than 1% linearity, is provided with each sensor. When required lower range calibrations can be supplied.

Typical Thermal Sensitivity Shift of Model 601B

Dimensions 601B/105A Assembly	Cavity Dimensions	Recessed Mount (where instalation area is restricted)

10-32 Thd
Coax. Recpt

M7x0 75
Thd

1.20

59

28
"X"
.515

M7x0 75
Thd

2210
250

Dim "X" ... 70 for FLUSH
74 for RECESSED

Flush mounting exposes the sensor to the pressure source for maximum fidelity, recessed mounting affords a measure of protection for the sensing diaphragm and permits use of ablative coating for maximum protection.

Specifications:

Range full scale	0 - 15 000 psi
Resolution	*0 01 psi
Maximum pressure	18 000 psi
Sensitivity nominal	1 0 pCb psi
Resonant frequency nom	300 kHz
Linearity zero based best straight line of cal range	± 1%
Capacitance nominal	17 pF
Insulation resistance min at R T	10 ohms
Acceleration sensitivity through sensitive axis	0 002 psi g
Thermal sensitivity shift	0 02% F
Temperature range	320 to + 400 F
Shock 1 ms width	20 000 g
Vibration limit	1000 g
Material Case Diaph	Stainless Steel
Weight	2 5 grams

* Limited by noise in signal conditioning equipment

Typical Pressure Calibration Curve Quartz Pressure Sensor Mod. 601B

Model 601B Acceleration Sensitivity thru pressure sensitive axis at 30g:
.0016 psi/g over comp.
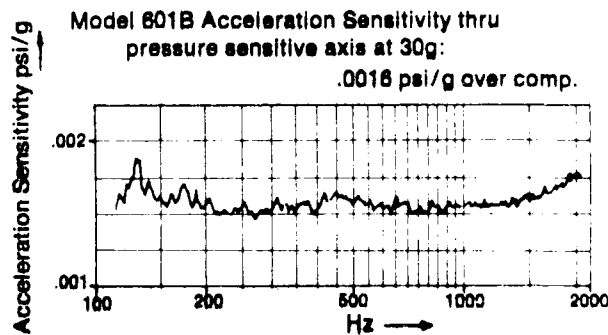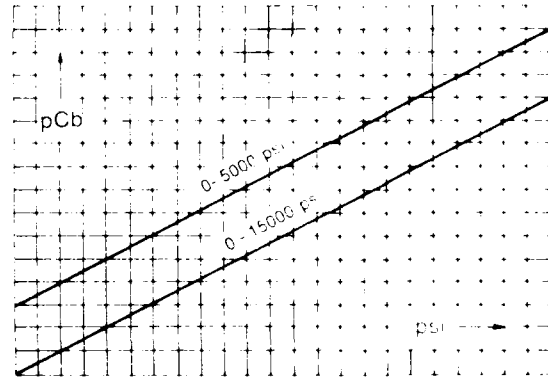
Typical Measurement System

121M(X) LOW NOISE CABLE
MAX 15 FT RECOMMENDED

131A(X) CABLE

102 ADAPTOR

601B TRANSDUCER

SIGNAL CONDITIONING EQUIPMENT

READOUT EQUIPMENT
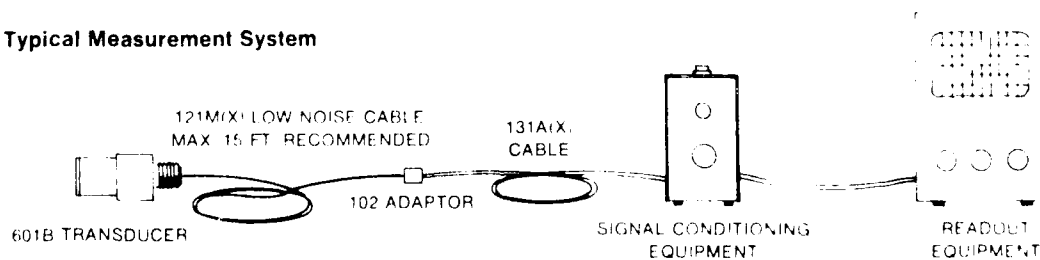
To Order—Specify:

Model 601B Sensor incl 105A Conn Adapt & 1 ea seals 600A3 (5 5 sleeve 248 long) 2 ea 600A (brass seal 060 long) & 4 each 600A11 (teflon seal 060 long))

Tap 600A13 (M7x0 75 if req to thread mounting cavity

Model 121M (X) Low Noise Cable X ft lg (1 2 5 10 15 ft stkd)

Model 101 Cable Adaptor 10 32 to BNC receptacle if req at sig cond)

Model 102 Cable Adaptor 10 32 to BNC plug (w ext cable)

Model 131A (X) Low Noise Cable X ft lg (5 15 25 ft stkd)

Signal Conditioning Equipment Recommended:

Model 504E Dual Mode Amplifier with Model 03A3 plug in for for   charge operation

Sundstrand Data Control, Inc.

HIGH SENSITIVITY

Pressure Transducer

Kistler Models
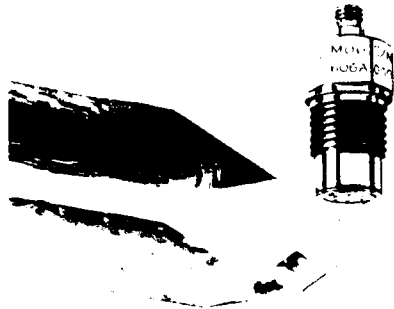
ALL-WELDED, HERMETICALLY SEALED QUARTZ PRESSURE TRANSDUCER

Model 606 features high sensitivity to pressure inputs with minimal sensitivity to acceleration and measures dynamic and short term static pressures under severe conditions. It is primarily recommended for use in high temperature and radiation environments and for high intensity sound measurements. Excellent performance is also achieved in hydraulic applications (with the exception of fuel injection). In blast or shock wave applications, optimum performance requires the use of a 20kHz or 50kHz low-pass filter in conjunction with the transducer.

SPECIFICATIONS	MODEL 606A*
Pressure range, full scale	to 3000 psi
Resolution	0.005 psi rms
Maximum pressure	5000 psi
Sensitivity (nominal)	5.5 picocoulomb psi
Resonant frequency (nominal)	130 kHz
Rise time	3.0 microseconds
Linearity, zero based best straight line	1%
Capacitance (nominal)	50 picofarads
Insulation resistance (at room temp.)	10 ohms
Acceleration sensitivity – thru press. sens. axis	.005 psi g. .001 psi g special selection
Temperature effect on sensitivity	0.03% F
Temperature range	350 to 450 F
Shock, 1 ms pulse width	1000 g
Cable connector	coaxial, 10-32
Case material	Stainless steel
Weight	22 grams

Sundstrand Data Control, Inc.

MODEL ST-2

Sensor	Lead metaniobate
Sensitive surface	.210" diameter
Natural frequency	250 kc
Pressure range	.1 - 500 psi
Charge sensitivity	20 pcmbs/psi
Transducer capacitance	150 pico farads
Resistance	10^{10} ohms or better
Linearity	Within 2% full scale
Ambient temperature range	0 - 50°C
Temperature stability	1% per 10°C change
Dimensions	.50" od x 9/16" length
Mounting thread	1/2 - 20 NF
Body material	Stainless steel construction with nylon pressure plate

A high sensitivity shock tube transducer designed to measure incident pressure. This transducer has a very low cross axis sensitivity and modes of vibration other than its principal mode are difficult to stimulate.

EG

6/73

Susquehanna Instruments

MODEL ST-4, 10000

Sensor	Tourmaline
Range	10 - 10 k psi
Sensitivity	.1 pcmbs/psi
Transducer capacitance	10 pico farads
Overload	Maximum pressure 15000 psi
Maximum temperature	150°F gauge, intermittent gas 5000°F
Linearity	Within $\pm 2\%$ full scale
Dimensions	1/2" diameter x 2" length
Natural frequency	1.5 megacycles
Mounting thread	1/2 - 20 NF
Resistance	10^{13} ohms or better

A high frequency tourmaline probe. An aperiodic pressure transducer designed so that high speed reflected shocks can be accurately measured in one microsecond or better. Natural resonance of the crystal element is dissipated in an acoustic wave guide within the transducer.

Calibrations up to 10,000 psi are obtained by means of a hydraulic drop testing device. Dynamic evaluations are made with the aid of a helium driven shock tube.

EG

11/70

MODEL ST-7

Sensor	Lead metaniobate
Sensitive surface	.210" diameter
Natural frequency	250 kc
Charge sensitivity	20 pc/psi
Transducer capacitance	150 pico farads
Resistance	10^{10} ohms or better
Linearity	Within ±2% full scale
Pressure range	.1 - 500 psi
Ambient temperature range	0 - 50°C
Temperature stability	+1%/+10°F change
Dimensions	7/8" od x 16" length
Body material	303 stainless steel

    The Model ST-7, a free field incident pressure probe, is virtually free from mechanical noises usually produced by shock, flying missiles, or resonance of the transducer element. The probe consists of four basic parts, each of these parts is replaceable in case of severe damage. All units are shock tube tested.

    All ST-7 pressure probes are designed to accommodate new pressure sensors and in lin amplifiers, if desired.

EG

2/76
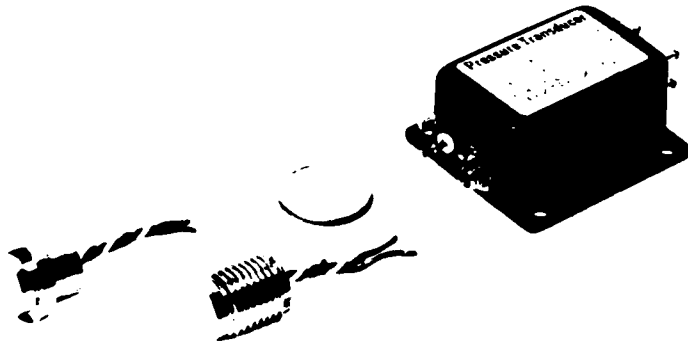
HFA, HFH, and Compensating Module

FEATURES

- Rugged Construction
- High Frequency Response
- Static or Dynamic Measurements
- Low Acceleration Sensitivity
- Small Size
- Accurate
- Low Impedance — No Charge Amplifier Required
- Signal can be Transmitted over Long Cables
- Low Thermal Gradient Sensitivity
- Radiation Hardened
- Shunt Calibration Data Supplied

APPLICATIONS

These miniature transducers are used in applications requiring one or more of the following characteristics:

1. Small size.

2. Superior dynamic performance.

3. Rugged construction.

Some of the principal uses have been in measuring blast effects, in open field testing, in shock tubes, in underground explosions and in aerial tests. They have also been used to measure blast effects under water.

The ability to measure both static and dynamic pressures makes these transducers particularly useful in evaluating and controlling hydraulic systems. A special version of the HFH performs an operational function in the landing gear hydraulic system of the Air Force's most advanced fighter. Other types have also been used to investigate "water hammer" in submarine piping systems, measure blast effects on rocket sleds, and provide feedback signals in hydraulic servo systems.

The Bytrex Models HFA and HFH are miniature pressure transducers particularly suited to rugged environments. Their case and diaphragm are integrally machined from a single piece of stainless steel, thus eliminating all joints which may degrade performance. The unique construction utilizes a force member supporting the diaphragm at its center. The deflection of this force member at rated pressure is typically only 150 micro-inches. As a result, the diaphragms can be made quite thick without absorbing excessive force from the force member. This thick diaphragm is very resistant to handling damage and puncture by flying particles encountered in blast tests.

Semiconductor strain gages bonded to the force member change their resistances proportional to pressure applied to the diaphragm. These strain gages are wired into a half-Wheatstone bridge which is connected to a three-conductor cable on the transducer. A separate compensation module, supplied with each transducer, completes the bridge and provides temperature compensation and a trimming potentiometer for setting electrical zero. The use of a patented circuit (U. S. Pat. 3,245,252) allows temperature compensation to be achieved with temperature-insensitive components. Thus, the compensation module need not be at the same temperature as the transducer and may be located in a convenient remote location. This circuitry also allows the use of shunt calibration techniques without large temperature errors.

The location of the strain gages on the force member provides thermal isolation from temperature inputs through the diaphragm or case. As a result these transducers are quite insensitive to thermal gradients. Also, since all temperature compensation is done with temperature-insensitive components, thermal transients have little effect.

Field and laboratory tests performed by users indicate that the highly-doped semiconductor strain gages used in these transducers are little-affected by nuclear radiation.

SPECIFICATIONS

Ranges:	HFA: 0-100, 0-200, 0-300, 0-500 and 0-1000 PSIS (sealed reference pressure). Other ranges available. HFH: 0-100, 0-200, 0-300, 0-500, 0-1000, 0-2000, 0-5000 and 0-10,000 PSIS (sealed reference pressure).
Case and Diaphragm Material:	Stainless steel.
Maximum Pressure Without Damage:	150% of rated pressure.
Maximum Pressure Without Diaphragm Rupture:	300% for ranges 2000 PSI and below. 200% for 5,000 and 10,000 PSI ranges.
Combined Non-Linearity and Hysteresis:	Less than 0.5% of F.S. deviation from best fit straight line through zero.
Repeatability:	Within 0.2% of F.S.
Resolution:	Infinite.
Shock:	Will withstand 5000 G's, any axis, with no damage (except compensation module).
Bridge Resistance:	Input: 200-700 ohms. Output: 650 ohms $\pm$ 20%.
Bridge Balance:	Adjustable to within 0.1% F.S.
Excitation:	12 VDC or AC rms.
Signal Output:	100 mv nominal, reported to 0.25% for each unit.
Shunt Calibration:	Shunt resistor to simulate 70% signal specified with each unit.
Insulation Resistance:	Greater than 5000 megohms at 50 VDC, measured between any terminal and case.
Storage and Operating Temperature:	$-$ 65° to $+$ 300°F (165°F maximum for compensation module).
Compensated Temperature Range:	$+$ 80°F to $+$ 180°F (tested with compensation module at room temperature).
Thermal Effect on Zero:	Changes less than 1% F.S. over compensated range.
Thermal Effect On Sensitivity:	Changes less than 1% of reading over compensated range.
Weight:	Approx. 0.2 oz. for sensor section. Approx. 1.5 oz. for compensation module.
Electrical Connections:	2 ft. of 3-conductor cable attached to transducer, plus 3 ft. of 4-conductor cable for attachment to compensation module.

Dynamic Characteristics

Range (PSI)	50	100	200	300	500	1000	2000	5000	10000
Acceleration Sensitivity % FS/G	.005	.001	.001	.0008	.0007	.0005	.0005	.0002	.0001
Natural Frequency, KC	30	40	60	70	75	75	100	130	160

PURCHASE INFORMATION

The following pressure ranges are stocked for rapid delivery:

HFA: 0-200, 0-500 PSI.

HFH: 0-100, 0-300, 0-1000, 0-2000, 0-10,000 PSI.

Ranges not in stock can be delivered in approximately 8 weeks.

Several optional features and versions of these transducers are available on special order:

1. Ablative coating on diaphragm to provide short term protection from flash temperatures to 5000°F.

2. Other compensated temperature ranges.

3. Elimination of module for applications not requiring temperature compensation (Orders of five or more).

4. Installation wrench for Model HFH.

5. Model HFL. Special version of HFH with hex flange and O-ring to facilitate sealing against pressure. Case thread is ⁷⁄₁₆-18 and mates with threaded boss per MS 33649-6.

OUTLINE DIMENSION
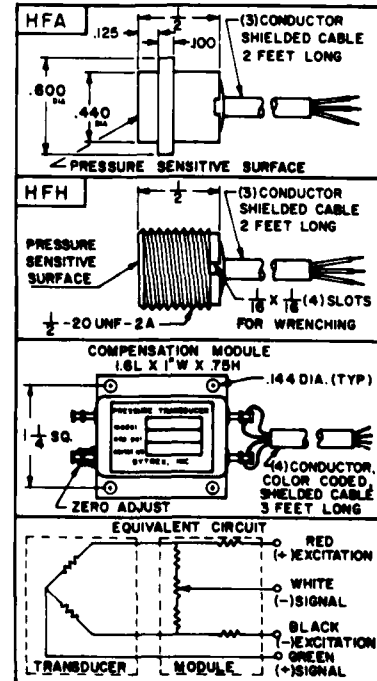
TYCO INSTRUMENT DIVISION

PRODUCT SPECIFICATION SHEET

HFG BLAST PRESSURE TRANSDUCERS
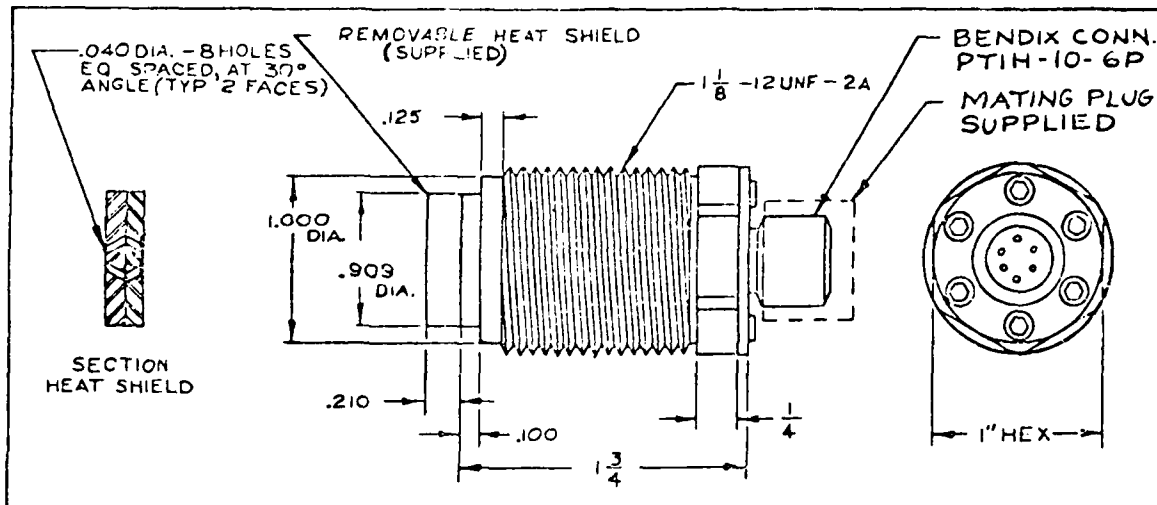
The HFG is a unique pressure transducer specifically designed for the measurement of dynamic pressures and blast phenomena. The semiconductor strain gage sensors suit it for both static and dynamic applications.

Proven in field tests, these transducers incorporate features of significant advantage in the investigation of blast effects.

1) High output

2) Excellent dynamic characteristics

3) Can be statically calibrated

4) Rugged construction suitable for field service

5) Heat shield protects diaphragm from radiant heat inputs, hot gases, and flying particles

6) May be used with AC or DC excitation, tape recorders, oscillographs and oscilloscopes

7) Temperature compensated over normal field temperature range

8) Low acceleration sensitivity

TYCO INSTRUMENT DIVISION

Ranges: 2, 5, 15, 25, 50, 150, 500, 1,000, 2,000 and 6,000 psi

Output: 100 mv minimum

Excitation: 20 VDC or AC rms

Operating Temperature Range: -65°F to +200°F

Compensated Temperature Range: +20°F to +120°F

Temperature Effect on Zero: Less than 2% of F.S. for 50°F
        excursion from 70°F

Temperature Effect on Sensitivity: Less than 1% of reading
        for 50°F excursion from 70°F

Input Impedance: 1000 to 1400 ohms (2 psi through 25 psi)
        and 750 to 1000 ohms (50 psi through 6000 psi)

Output Impedance: 1400 ohms, maximum

Combined Linearity and Hysteresis: 2% of F.S.

Resistance to Ground: 5000 megohms minimum, any terminal
        to case at 50 VDC

Shock Capability: 500G's minimum, all axes

Acceleration Response: see table below

Natural Frequency: see table below

CAPACITY	ACCELERATION RESPONSE % F.S./G	NATURAL FREQUENCY
2 psi	0.04	10 Kc.
5 psi	0.04	10 Kc.
15 psi	0.006	20 Kc.
25 psi	0.005	20 Kc.
50 psi	0.005	30 Kc.
150 psi	0.002	40 Kc.
500 psi	0.002	75 Kc.
1000 psi	0.001	75 Kc.
2000 psi	0.001	100 Kc.
6000 psi	0.001	130 Kc.

APPENDIX C

GLOSSARY

The glossary contains terms that are commonly encoun-
tered in study of air blast with special effort to include
those terms which are used ambiguously or loosely both in
conversation and in the literature. Not all of the terms
will be found in the main text of this report but are in-
cluded for the convenience and reference of the reader.

The definitions or interpretations of meanings are
given in the context of the subject of air blast. Many of
the words and terms (e.g. probe) are commonly known to have
a more general definition in every day usage.

Five major references have been used as sources to
provide definitions or verify the author's own understand-
ing and to assure the technical accuracy of the terms in-
cluded. These sources are listed at the end of the glossary
and have been identified with numbers in parenthesis at the
end of each definition. Cross-references are given where
another term is felt to provide the user with additional
information and insight regarding a specific term.

ADIABATIC PROCESS: A process in which no heat is transferred
to or from the system. An adiabatic process may be
either reversible or irreversible (see ISENTROPIC). (4)

AERODYNAMIC HEATING: The transfer of heat to a solid body
immersed within a fluid with relative motion between
the body and the fluid (air). (1)

AIR BLAST: The disturbance (shock wave) propagated through
the air arising from a source of suddenly expanding gases,
as from explosions (see SHOCK WAVE).

AIR BURST: The explosion of a charge at a height such that
the expanding fireball does not touch the earth's surface
when the luminosity is a maximum. (2)

BLAST LOADING: The force on an object caused by the air blast
from an explosion striking and flowing around the object.
It is equal to the net pressure in excess of the ambient
value multiplied by the area of the loaded object. (2)

BLAST WAVE: A pulse of air in which the pressure increases
sharply at the front accompanied by flow propagated
continuously from an explosion (see SHOCK WAVE). (2)

BURST: An explosion or detonation. (2)

CONTACT SURFACE: The interface surface between gas that is
expanding outward from an explosion and the gas that has
been compressed by the shock wave. Across the contact
surface the velocities are the same but densities,
chemical composition and temperatures will be different.

DETONATION: The fast chemical (or nuclear) reaction accom-
panied by rapidly expanding shock waves driven by the
release of chemical (or nuclear) energy.

DRAG LOADING: The force on an object due to the transient flow around that object during passage of a blast wave. (2)

DYNAMIC HEAD: DYNAMIC PRESSURE

DYNAMIC PRESSURE: The pressure associated with a moving fluid resulting from the mass flow. It is equal to one-half the fluid density times the square of the fluid velocity. (2)

FACE-ON PRESSURE: REFLECTED PRESSURE

FIREBALL: The luminous sphere of hot gases which forms immediately after detonation of an explosive as a result of the absorption of the surrounding medium by thermal energy of the explosion. (2)

FLOW VELOCITY: PARTICLE VELOCITY

FREE AIR OVERPRESSURE: FREE FIELD OVERPRESSURE

FREE AIR SHOCK: A shock moving through the atmosphere with no chemical or physical outside influences affecting it.

FREE FIELD OVERPRESSURE: The unreflected pressure, in excess of the ambient atmospheric pressure, created in the air by a blast wave. (2)

GAMMA: The ratio of specific heats for a gas. Gamma (λ) is defined by the equation $\lambda = C_p/C_v$ (see SPECIFIC HEAT). (4)

HEAD PRESSURE: TOTAL PRESSURE

IDEAL GAS: By definition, an ideal gas obeys the ideal gas law which states that the pressure times the volume is equal to the temperature times the gas constant (pv = RT). An ideal gas behaves as an assembly of perfectly elastic spherical point masses in random motion which exert no forces on each other except during collisions. (1)

IMPACT PRESSURE: PITOT PRESSURE

IMPULSE: The integral, with respect to time, of the overpressure-time history (see POSITIVE IMPULSE).

INCIDENT OVERPRESSURE: FREE FIELD OVERPRESSURE

IRREVERSIBLE PROCESS: A physical process at the conclusion of which it cannot be returned to its original thermodynamic state (reversed) without supplying outside energy to the system. By the second law of thermodynamics, all natural physical processes are irreversible. (1)

ISENTROPIC PROCESS: A process that results in no change of entropy, that is to say, the internal energy is conserved. Note that a reversible adiabatic process is isentropic, but an isentropic process is not necessarily reversible adiabatic. (1)

LOADING: The force on an object (see BLAST LOADING). (2)

MACH FRONT: MACH STEM

MACH NUMBER: The ratio of speed of an object to the speed of sound in the undisturbed medium ahead of the object. (1)

MACH REGION: The region on the ground surface at which the Mach Stem has formed as a result of an explosion in the air. (2)

MACH STEM: The shock front formed by the fusion or coalescence of the incident and reflected shock fronts from an explosion in air. (2)

MACH WAVE: The shock wave created by an object moving with a Mach number greater than unity. (1)

MOUNT: The supporting structure required for physical support and placement of a probe in the blast field to measure an air blast parameter. Mount and probe are sometimes an integral unit but the terms have different connotation (see PROBE).

NEGATIVE PHASE: See SHOCK WAVE

NON-IDEAL GAS: A gas that does not obey the ideal gas laws (see IDEAL GAS).

NORMALLY REFLECTED PRESSURE: Pressure created on a rigid surface oriented normal to the shock wave velocity vector.

OVERPRESSURE: The transient pressure exceeding the ambient value manifested in the shock (or blast) wave (see PEAK OVERPRESSURE).

PARTICLE VELOCITY: As the shock wave propagates through the fluid, the pressure disturbance sets the fluid in motion, giving it a velocity which is called the particle velocity. This should not be confused with the shock wave front velocity (see SHOCK WAVE FRONT VELOCITY). (4)

PEAK OVERPRESSURE: The maximum value of the overpressure. It is a function of the distance from the blast source and generally occurs at the instant of shock arrival at any given location; but is not necessarily identical with the shock front overpressure. The term is ambiguous unless its meaning is clearly stated by the user (see PEAK SHOCK OVERPRESSURE and OVERPRESSURE).

PEAK SHOCK OVERPRESSURE: The maximum value of overpressure at the shock wave front.

PERFECT GAS: IDEAL GAS

PITOT PRESSURE: For subsonic flow (Mach number M < 1.0), the
pitot pressure is equal to the stagnation pressure. For
supersonic flow conditions (M > 1.0), it is the stagnation
pressure behind a stationary normal shock. Note that this
is not the free-stream stagnation pressure for M > 1.0.
In both cases it is the pressure that will be measured
with a pitot-probe (see TOTAL PRESSURE). (3,5)

POSITIVE PHASE: See SHOCK WAVE

PROBE: The adapter or fixture designed to introduce a sensing
element (transducer) into the environment to be measured.
The function of a probe is to expose the active sensing
element or sensitive area of the transducer to the desired
parameter with minimum perturbation of the environment
(see MOUNT).

REAL GAS: A gas which assumes a variable value of gamma, the
ratio of specific heats (see SPECIFIC HEAT). (5)

REFELECTED PRESSURE: Total pressure that results at the
interface when a shock wave traveling in one medium
encounters a discontinuity such as a rigid surface or
another shock wave front (see NORMALLY REFLECTED PRESSURE).
(2)

REFLECTION FACTOR: The ratio of reflected pressure to the
incident pressure when a shock wave traveling in one medium
strikes another medium. (2)

REVERSIBLE PROCESS: A physical process whose effects can be
reversed, so as to return the system involved to its
original thermodynamic state.

SHOCK: A pressure discontinuity in a compressible fluid. (1)

SHOCK WAVE: A pressure wave characterized by a very steep,
     almost discontinuous, rise in pressure which occurs when
     a region of high pressure overtakes a region of low
     pressure, with a consequent rapid compression of the
     medium. A shock wave in air is commonly referred to as
     an air blast wave. The duration of a shock (or blast)
     wave is distinguished by two phases. First there is the
     positive (or compression) phase during which the pressure
     rises very sharply to a value that is higher than
     ambient and then decreases rapidly to the ambient pres-
     sure. The positive phase for the dynamic pressure is
     somewhat longer than for overpressure, due to the momentum
     of the moving air behind the shock front. The duration
     of the positive phase increases and the maximum (peak)
     pressure decreases with increasing distance from an
     explosion of given energy yield. In the second phase,
     the negative (or suction) phase, the pressure falls below
     ambient and then returns to the ambient value. The duration
     of the negative phase is approximately constant throughout
     the blast wave history and may be several times the
     duration of the positive phase. Deviations from the
     ambient pressure during the negative phase are never
     large and they decrease with increasing distance from
     the explosion.

SHOCK WAVE FRONT: The region of compression propagated through
     the medium (gas, liquid, or solid) ahead of which the
     pressure change is nearly discontinuous to the ambient
     level (see SHOCK WAVE). (2)

SHOCK WAVE FRONT VELOCITY: The velocity or speed of the shock
     wave front relative to the velocity of the ambient medium.

SIDE-ON OVERPRESSURE: FREE FIELD OVERPRESSURE

SPECIFIC HEAT: The specific heat is defined as the heat
    needed to raise the temperature of unit mass of the system
    by one degree. The value depends upon the process by
    which the heat is added. For an ideal gas, if we know
    the specific heat for two different processes, we know it
    for all processes. One usually chooses the specific heat
    at constant volume C_v and the specific heat at constant
    pressure C_p (see GAMMA). (4)

STAGNATION POINT: In fluid flow, a point where the velocity
    of the fluid is zero i.e. the fluid is brought to rest
    (usually relative to a solid body) and where a stream-
    line divides into two or more streamlines continuing
    downstream. Stagnation conditions are also called total
    conditions, e.g., total pressure, total temperature,
    etc. (1)

STAGNATION PRESSURE: TOTAL PRESSURE

STAGNATION TEMPERATURE: TOTAL TEMPERATURE

STATIC OVERPRESSURE: In a moving fluid, static overpressure
    refers to the pressure, in excess of ambient, that would
    be measured by an infinitesmally small instrument at
    rest relative to the fluid. (See FREE FIELD OVERPRESSURE).

TOTAL CONDITIONS: The local total conditions at a point in
    fluid flow are the conditions that would be attained if
    the flow were brought to rest (stagnated) isentropically. (4)

TOTAL PRESSURE: The pressure of a flowing fluid that exists
    under stagnation or total conditions (see STAGNATION POINT,
    also TOTAL CONDITIONS). (4)

TOTAL TEMPERATURE: The temperature of a flowing fluid that
    exists under stagnation or total conditions (see STAGNATION
    POINT, also TOTAL CONDITIONS). (4)

TRANSDUCER: An instrument that expresses the magnitude of one
    physical quantity in terms of another. It is commonly
    used for remote measurement when the related quantity is
    more suitable for recording than the quantity of interest.
    A device for conversion of energy in one form to another
    e.g. pressure to voltage. (1)

TRIPLE POINT: The intersection of the incident, reflected, and
    fused (or Mach) shock fronts accompanying an air burst.
    The height of the triple point above the surface, i.e., the
    height of the Mach stem, increases with increasing
    distance from a given explosion (see MACH STEM). (2)

YIELD: The total effective energy released in an explosion. It
    is usually expressed in terms of the equivalent tonnage
    of TNT required to produce the same energy release in an
    explosion. (2)

REFERENCES FOR GLOSSARY

1.   Thewlis, James, <u>Concise Dictionary of Physics and Related Subjects</u>, Pergamon Press, 1973.

2.   Glasstone, Samuel, <u>The Effects of Nuclear Weapons</u>, Published by USAEC, Revised, 1962.

3.   Shapiro, Ascher, H., <u>The Dynamics and Thermodynamics of Compressible Fluid Flow</u>, The Ronald Press Company, 1953.

4.   Liepmann, H. W. and Roshko, A., <u>Elements of Gasdynamics</u>, John Wiley and Sons, 1957.

5.   Pope, Alan and Goin, Kenneth L., <u>High-Speed Wind Tunnel Testing</u>, John Wiley and Sons, 1965.

APPENDIX D

ABBREVIATIONS AND SYMBOLS

TABLE D-1 ABBREVIATIONS

AFWL	Air Force Weapons Laboratory
BRL	Ballistic Research Laboratories
DABS	Dynamic Air Blast Simulator
DNA	Defense Nuclear Agency
DRI	Denver Research Institute
EMP	Electromagnetic Pulse
EMSI	Electro-Mechanical Systems, Inc.
FCP	Fluid Couple Plate
HE	High Explosive
ISA	Instrument Society of America
LDA	Laser Doppler Anemometer
NBS	National Bureau of Standards
NWC	Naval Weapons Center
PCB	PCB Piezotronics, Inc.
RDA	R&D Associates
SLA	Sandia Laboratories, Albuquerque
SRI	Stanford Research Institute
TDD	Time Domain Deconvolution
TRW	TRW Systems Group
UNM/CERF	University of New Mexico/Eric H. Wang Civil Engine-ering Research Facility
VSA	Vortex Shedding Anemometer

TABLE D-2   SYMBOLS

α	–	Attenuation per unit
β	–	Phase shift per unit
δ	–	Thickness of shock wave front
γ	–	Ratio of specific heats for gas (C_p/C_v)
	–	Propagation constant for EM waves
θ	–	Angle of incidence
λ	–	Wavelength
ρ	–	Density
τ	–	Time constant
ϕ_d	–	Dust momentum flux
Φ	–	Oscillator strength
ψ	–	Molecular concentration
ω	–	Angular frequency
a	–	Acceleration
A	–	Area
c	–	Velocity of light
C_D	–	Drag coefficient
d	–	diameter
E	–	Electromagnetic field strength
E_{eff}	–	Effective emissivity
E_o	–	Dissociation energy of molecule
f	–	Frequency
f_2	–	Upper 3-db frequency
F	–	Force
G	–	Antenna design constants
h	–	Planck's constant
i	–	Unit vector along x
I	–	Impulse
	–	Electric current
j	–	Mathematical operator $\equiv \sqrt{-1}$
	–	Unit vector along y

TABLE D-2 SYMBOLS (CONT'D)

k	-	Acoustic propagation constant
	-	Gladstone-Dale constant
K	-	Boltzmann's constant
m	-	Mass
L	-	Length
M	-	Mach number
n	-	Index of refraction
ΔN	-	Number of fringe shifts
p	-	Absolute pressure
p_o	-	Total pressure ($M<1$)
Δp	-	Overpressure
Δp_r	-	Reflected overpressure
Δp_s	-	Static overpressure
q	-	Gas dynamic pressure
q_p	-	Particle dynamic pressure
r	-	Path length
R	-	Resistance in electric circuit
R_e	-	Reynolds number
S	-	Strouhal number
t	-	Time
t_r	-	rise time
T	-	Temperature
u	-	Gas particle velocity (x-component)
u_p	-	Particle velocity
U_s	-	Shock wave front velocity
v	-	Gas particle velocity (y-component)
v_c	-	Sonic velocity
v_q	-	Gas particle velocity
x,y	-	Rectilinear spatial coordinates
X,Y	-	Functions

APPENDIX E
METRIC (SI) CONVERSION FACTORS

This appendix presents factors for conversion of quantities in various systems of measurement to the International System of Units, which is officially abbreviated as SI. The information given is taken from the Metric Practice Guide (ANSI Z210.1-1973). The list of abbreviations has been abridged to delete units that are not commonly encountered in air blast work.

The SI units and symbols are included in Table E-1 as a convenience to the reader who is unfamiliar with some of the newer terms. Table E-2 is an alphabetical list of units and conversion factors. Relationships that are exact in terms of the base unit are followed by an asterisk. Relationships that are not followed by an an asterisk are either the result of physical measurements or are approximate.

Preceding page blank

TABLE E-1   SI UNITS AND SYMBOLS

BASE UNITS:

Quantity	Unit	SI Symbol	Formula
length	metre	m	---
mass	kilogram	kg	---
time	second	s	---
electric current	ampere	A	---
thermodynamic temperature	kelvin	K	---
amount of substance	mole	mol	---
luminous intensity	candela	cd	---

SUPPLEMENTARY UNITS:

plane angle	radian	rad	---
solid angle	steradian	sr	---

DERIVED UNITS:

Quantity	Unit	SI Symbol	Formula
acceleration	metre per second squared	---	m/s^2
activity (of a radioactive source)	disintegration per second	---	(disintegration)/s
angular acceleration	radian per second squared	---	rad/s^2
angular velocity	radian per second	---	rad/s
area	square metre	---	m^2
density	kilogram per cubic metre	---	kg/m^3
electric capacitance	farad	F	$A \cdot s/V$
electrical conductance	siemens	S	A/V
electric field strength	volt per metre	---	V/m
electric inductance	henry	H	$V \cdot s/A$
electric potential difference	volt	V	W/A
electric resistance	ohm	Ω	V/A
electromotive force	volt	V	W/A
energy	joule	J	$N \cdot m$
entropy	joule per kelvin	---	J/K
force	newton	N	$kg \cdot m/s^2$
frequency	hertz	Hz	(cycle)/s
illuminance	lux	lx	lm/m^2
luminance	candela per square metre	---	cd/m^2
luminous flux	lumen	lm	$cd \cdot sr$
magnetic field strength	ampere per metre	---	A/m
magnetic flux	weber	Wb	$V \cdot s$
magnetic flux density	tesla	T	Wb/m^2
magnetomotive force	ampere	A	---
power	watt	W	J/s
pressure	pascal	Pa	N/m^2
quantity of electricity	coulomb	C	$A \cdot s$
quantity of heat	joule	J	$N \cdot m$
radiant intensity	watt per steradian	---	W/sr
specific heat	joule per kilogram-kelvin	---	$J/kg \cdot K$
stress	pascal	Pa	N/m^2
thermal conductivity	watt per metre-kelvin	---	$W/m \cdot K$
velocity	metre per second	---	m/s
viscosity, dynamic	pascal-second	---	$Pa \cdot s$
viscosity, kinematic	square metre per second	---	m^2/s
voltage	volt	V	W/A
volume	cubic metre	---	m^3
wavenumber	reciprocal metre	---	(wave)/m
work	joule	J	$N \cdot m$

SI PREFIXES:

Multiplication Factors	Prefix	SI Symbol
1 000 000 000 000 = 10^{12}	tera	T
1 000 000 000 = 10^9	giga	G
1 000 000 = 10^6	mega	M
1 000 = 10^3	kilo	k
100 = 10^2	hecto	h
10 = 10^1	deka	da
0.1 = 10^{-1}	deci	d
0.01 = 10^{-2}	centi	c
0.001 = 10^{-3}	milli	m
0.000 001 = 10^{-6}	micro	μ
0.000 000 001 = 10^{-9}	nano	n
0.000 000 000 001 = 10^{-12}	pico	p
0.000 000 000 000 001 = 10^{-15}	femto	f
0.000 000 000 000 000 001 = 10^{-18}	atto	a

TABLE E-2

ALPHABETICAL LIST OF UNITS

(Symbols of SI units given in parentheses)

To Convert From	To	Multiply By
angstrom	meter (m)	1.000 000*E-10
atmosphere (normal)	pascal (Pa)	1.013 25 E+05
bar	pascal (Pa)	1.000 000*E+05
British thermal unit (thermochemical)	joule (J)	1.054 350 E+03
Btu (thermochemical)/foot²-second	watt/metre² (W/m²)	1.134 893 E+04
cal (thermochemical)/cm²·s	watt/metre² (W/m²)	4.184 000*E+04
centimeter of mecury (0 C)	pascal (Pa)	1.333 22 E+03
centimeter of water (4 C)	pascal (Pa)	9.806 38 E+01
decibar	pascal (Pa)	1.000 000*E+04
degree Celsius	kelvin (K)	$t_k = t_c + 273.15$
degree Fahrenheit	degree Celsius	$t_c = (t_f - 32)/1.8$
dyne	newton (N)	1.000 000*E-05
dyne-centimetre	newton-metre (N·m)	1.000 000*E-07
dyne/centimetre²	pascal (Pa)	1.000 000*E-01
erg	joule (J)	1.000 000*E-07
foot	metre (m)	3.048 000*E-01
foot of water (39.2 F)	pascal (Pa)	2.988 98 E+03
gram/centimetre³	kilogram/metre³ (kg/m³)	1.000 000*E+03
gram-force/centimetre²	pascal (Pa)	9.806 650*E+01
inch	metre (m)	2.540 000*E-02
inch of mecury (32 F)	pascal (Pa)	3.386 389 E+03
inch of water (39.2 F)	pascal (Pa)	2.490 82 E+02
kilocalorie (International Table)	joule (J)	4.186 800*E+03
kilocalorie (thermochemical)/second	watt (W)	4.184 000*E+03
kilogram-force (kgf)	newton (N)	9.806 650*E+00
kilogram-force-second²/metre (mass)	kilogram (kg)	9.806 650*E+00
kip (1000 lbf)	newton (N)	4.448 222 E+03
kip/inch² (ksi)	pascal (Pa)	6.894 757 E+06
mile (U.S. statute)	metre (m)	1.609 344*E+03
millibar	pascal (Pa)	1.000 000*E+02
millimetre of mecury (0 C)	pascal (Pa)	1.333 224 E+02
pound-force/inch² (psi)	pascal (Pa)	6.894 757 E+03
ton (nuclear equivalent of TNT)	joule (J)	4.20 E+09

DISTRIBUTION LIST

DEPARTMENT OF DEFENSE

Director
Defense Advanced Rsch. Proj. Agency
    ATTN: NMRO
    ATTN: PMO
    ATTN: STO
    ATTN: Tech. Lib.

Defense Documentation Center
12 cy ATTN: TC

Director
Defense Nuclear Agency
    ATTN: STSI, Archives
    ATTN: DDST
2 cy ATTN: SPSS
3 cy ATTN: STTL, Tech. Lib.

Commander
Field Command
Defense Nuclear Agency
    ATTN: FCTMOF
    ATTN: FCPR
    ATTN: FCT

Chief
Livermore Division, Fld. Command DNA
    ATTN: FCPRL

DEPARTMENT OF THE ARMY

Dep. Chief of Staff for Rsch., Dev. & Acq.
    ATTN: Tech. Lib.

Commander
Harry Diamond Laboratories
    ATTN: DRXDO-NP
    ATTN: DRXDO-TI, Tech. Lib.

Director
U.S. Army Ballistic Research Labs.
    ATTN: DRXBR-X, Julius J. Meszaros
    ATTN: DRXBR-TL-IR, J. H. Keefer
    ATTN: Tech. Lib., Edward Baicy

Director
U.S. Army Engr. Waterways Exper. Sta.
    ATTN: J. K. Ingram
    ATTN: F. Hanes
    ATTN: William Flathau
    ATTN: Technical Library
    ATTN: Leo Ingram

Commander
U.S. Army Materiel Dev. & Readiness Cmd.
    ATTN: Tech. Lib.

DEPARTMENT OF THE NAVY

Chief of Naval Research
    ATTN: Technical Library

Officer-in-Charge
Civil Engineering Laboratory
Naval Construction Battalion Center
    ATTN: Technical Library
    ATTN: R. J. Odello

DEPARTMENT OF THE NAVY (Continued)

Commander
Naval Facilities Engineering Command
    ATTN: Technical Library

Commander
Naval Ship Engineering Center
    ATTN: Technical Library

Commander
Naval Ship Rsch. and Development Ctr.
    ATTN: Code L42-3, Library

Commander
Naval Ship Rsch. and Development Ctr.
    ATTN: Technical Library

Commander
Naval Surface Weapons Center
    ATTN: Code WX21, Tech. Lib.
    ATTN: Code WA501, Navy Nuc. Prgms. Off.

DEPARTMENT OF THE AIR FORCE

AF Geophysics Laboratory, AFSC
    ATTN: SUOL, AFCRL Rsch. Lib.

AF Institute of Technology, Au
    ATTN: Library, AFIT, Bldg. 640, Area B

AF Weapons Laboratory, AFSC
    ATTN: SUL
    ATTN: DES-S, M. A. Plamondon
    ATTN: DEX
    ATTN: DEX, J. Renick

HQ USAF/IN
    ATTN: INATA

ENERGY RESEARCH AND DEVELOPMENT ADMINISTRATION

University of California
Lawrence Livermore Laboratory
    ATTN: Tech. Info., Dept. L-3

Sandia Laboratories
Livermore Laboratory
    ATTN: Doc. Con. for Tech. Lib.

Sandia Laboratories
    ATTN: Doc. Con. for Luke J. Vortman
    ATTN: Doc. Con. for A. J. Chaban
    ATTN: Doc. Con. for Org. 3422-1,
        Sandia Rpt. Coll.

U.S. Energy Rsch. & Dev. Admin.
Albuquerque Operations Office
    ATTN: Doc. Con. for Tech. Library

U.S. Energy Rsch. & Dev. Admin.
Division of Headquarters Services
    ATTN: Doc. Con. for Class. Tech. Lib.

U.S. Energy Rsch. & Dev. Admin.
Nevada Operations Office
    ATTN: Doc. Con. for Tech. Lib.

ENERGY RESEARCH AND DEVELOPMENT ADMINISTRATION
(Continued)

Union Carbide Corporation
Holifield National Laboratory
    ATTN: Civ. Def. Res. Proj., Mr. Kearny

DEPARTMENT OF DEFENSE CONTRACTORS

Aerospace Corporation
    ATTN: Tech. Info. Services
    ATTN: Prem N. Mathur

Agbabian Associates
    ATTN: M. Agbabian

Artec Associates, Inc.
    ATTN: D. W. Baum

Civil/Nuclear Systems Corp.
    ATTN: Robert Crawford

EG&G, Inc.
Albuquerque Division
    ATTN: Tech. Lib.

General Electric Company
TEMPO-Center for Advanced Studies
    ATTN: DASIAC

IIT Research Institute
    ATTN: Technical Library

Kaman Sciences Corporation
    ATTN: Donald C. Sachs
    ATTN: Lib.
2 cy ATTN: Eldine Cole

Merritt Cases, Incorporated
    ATTN: Tech. Lib.
    ATTN: J. L. Merritt

The Mitre Corporation
    ATTN: Lib.

Nathan M. Newmark
Consulting Engineering Services
    ATTN: W. Hall
    ATTN: Nathan M. Newmark

Physics International Company
    ATTN: Doc. Con. for Coye Vincent
    ATTN: Doc. Con. for Fred M. Sauer
    ATTN: Doc. Con. for Charles Godfrey
    ATTN: Doc. Con. for Tech. Lib.

DEPARTMENT OF DEFENSE CONTRACTORS (Continued)

R & D Associates
    ATTN: Tech. Lib.
    ATTN: J. G. Lewis

Science Applications, Inc.
    ATTN: Tech. Lib.

Southwest Research Institute
    ATTN: Wilfred E. Baker
    ATTN: A. B. Wenzel

Stanford Research Institute
    ATTN: George R. Abrahamson
    ATTN: Burt R. Gasten
    ATTN: P. De Carli

Systems, Science and Software, Inc.
    ATTN: Tech. Lib.
    ATTN: Donald R. Grine

TRW Systems Group
    ATTN: Tech. Info. Center, S-1930
    ATTN: Peter K. Dai, R1 2170
    ATTN: Paul Lieberman

TRW Systems Group
San Bernardino Operations
    ATTN: E. Y. Wong, 527/712

The Eric H. Wang
Civil Engineering Rsch. Fac.
    ATTN: Neal Baum

Weidlinger Assoc. Consulting Engineers
    ATTN: Melvin L. Baron

Weidlinger Assoc. Consulting Engineers
    ATTN: J. Isenberg

Electromechanical Sys. of New Mexico
    ATTN: R. A. Shunk

H-Tech. Laboratories
    ATTN: Bruce Hartenbaum